University of Zagreb

FACULTY OF SCIENCE
Department of Biology

Antonija Matek

ISLAND TRAPPED WAVES AS DRIVERS OF PRIMARY PRODUCTION

DOCTORAL DISSERTATION

Mentor:
Zrinka Ljubešić, Full Professor

Zagreb, 2026.

Sveučilište u Zagrebu

PRIRODOSLOVNO MATEMATIČKI FAKULTET
Biološki odsjek

Antonija Matek

UTJECAJ VALOVA VEZANIH UZ OTOK NA PRIMARNU PROIZVODNJU

DOKTORSKI RAD

Mentor:
Prof. dr. sc. Zrinka Ljubešić

Zagreb, 2026.

This doctoral thesis was prepared within the Postgraduate Doctoral Programme in Biology at the University of Zagreb, Faculty of Science, Department of Biology, under the supervision of prof. dr. sc. Zrinka Ljubešić. The research was performed in the framework of the project “Island trapped waves as driver of primary production - ISLAND” (project number IP-2020-02-9524, principal investigator prof. dr. sc. Zrinka Ljubešić) funded by the Croatian Science Foundation (HRZZ).

.

Information about Mentor

Dr. Zrinka Ljubešić was born in 1975 in Zagreb. She has graduated from the Faculty of Science of the University of Zagreb with a degree in biology-ecology in 1997, and has obtained a master's degree in 2003 and a PhD in 2007. She has been working at the Faculty of Science, University of Zagreb, since 1997 and is now employed as a full professor. She is actively involved in teaching various undergraduate and graduate courses in the field of biological oceanography, marine ecology, pelagic microbiology, taxonomy and ecology of protists and cyanobacteria. She mentored 20 master's students, 12 bachelor's students and two doctoral students.

The field of her research is biological oceanography, with a focus on taxonomy and ecology of marine phytoplankton and biophysical coupling. She has attended several scientific trainings at reputable international institutions and has participated in four international scientific expeditions. In 2014 she obtained funding and became a principal investigator in an installation research project “Biotracers of Adriatic water masses, BIOTA”, and in 2021 in research project “Island trapped waves as driver of primary production, ISLAND”. Both projects were funded by the Croatian Science Foundation. She participated in three COST actions, seven international research projects, and one additional Croatian Science Foundation project.

Currently, she is an author or a co-author of 77 scientific publications, 132 conference abstracts and 10 popular science publications. She is the Croatian representative in the international association Federation of European Phycology Societies, and was the president of the Croatian Botanical Society. She is the winner of "For Women in Science" award, and Ambassador Award in the category of client for meetings of more than 150 participants. She has organized one national and four international scientific conferences and was a member of the organizing and scientific committees of numerous congresses and symposia. She is actively involved in popularisation of science through public media, by organizing numerous popular scientific lectures and science-meets-art exhibitions.

Acknowledgements

Four years have passed in what feels like a blink of a moment, and when I rewind, I can only feel amazement at everything this period has brought. There were challenges along the way, but facing them allowed me to grow intellectually, emotionally and personally. Above all, this journey has been defined by people - some who have been present from beginning to end, and others who crossed my path more briefly, yet left a lasting impact.

First, I wish to express my sincere gratitude to my mentor, Zrinka Ljubešić, for giving me the space to learn at my own pace, to explore and to discover my passion. Even more importantly, thank you for encouraging me through tight deadlines and moments of chaos, and for giving me the push I needed to keep moving forward. You helped me to become more confident, and for that I am profoundly grateful. Adventures at Lastovo, sharing the gifts from the garden, conversations on the train, and travelling together will remain beautiful memories I will always cherish.

I extend my heartfelt thanks to my colleague and friend, Maja Mucko, for her support throughout the ups and downs of this journey. Your dedication and curiosity continue to inspire me, and I am grateful to learn from such an exceptional scientist and amazing person.

I am also thankful to the entire Algology Group, whom I have known since my master's studies. You have always made me feel at home. Thank you for the stimulating discussions and ever-flowing ideas for new projects. In particular, I want to thank Sunčica Bosak for our always insightful conversations, and my fellow past and present PhD colleagues - Antonija Kulaš, Lucija Kanjer, Klara Filek, and Dunja Jurina - whose companionship I truly appreciate, as it made this journey truly more enjoyable.

I also wish to thank Žarko Kovač and Ivona Cetinić for helping me seize opportunities for scientific training abroad, which allowed me to acquire new skills and meet new people. My sincere appreciation goes to Melissa Omand, Hrvoje Mihanović, Zoran Pasarić and Mirko Orlić for their guidance in developing new skills in data analysis and modeling.

I am grateful to all members of the ISLAND research project. A PhD student could not hope for a more supportive, constructive and friendly environment - you made this experience truly rewarding.

Field research at our beautiful Cape Struga on the Lastovo Island would not have been possible without collective effort. I would first like to thank our cook and uplifter, Pagi, for bringing cheer to every field campaign and for always welcoming us at the Biological Station Čavoglave. My sincere thanks also go to the Marine Explorers Society 20.000 leagues team, particularly Hrvoje Čižmek and Barbara Čolić, without whom I would not have the dataset at the core of this thesis. I am also grateful to the captain and crew of the R/V Baldo Kosić II for their help during intense sampling campaigns. Lastly, I gratefully acknowledge the Croatian Science Foundation for funding the ISLAND project.

Completing a PhD research is far from easy, and I owe my gratitude to all who shaped me - both in the past and today. To my family, my sisters, mum, and dad, whom I can always seek support from. To my friends, for offering comfort and making me laugh - especially those who have been with me since my student days: Ana, Ivana, Meić, and Anika. Thank you. And to my Dora, who always brings a fresh perspective. And finally, to my partner and best friend, Tihomir, for being my rock, my safe harbour, and my constant source of strength throughout every journey.

Doctoral dissertation

University of Zagreb

Faculty of Science

Department of Biology

Division of Botany

ISLAND TRAPPED WAVES AS DRIVERS OF PRIMARY PRODUCTION

ANTONIJA MATEK

Division of Botany, Department of Biology, Faculty of Science,

Horvatovac 102a, 10000 Zagreb

Net primary production (NPP) is essential in global ocean ecosystems, forming the foundation of the marine food web and driving biogeochemical cycles. Climate change-driven ocean warming is causing a decline in global NPP, expanding stratified oligotrophic areas, and making local productivity hotspots increasingly important. This thesis investigates the effects of internal island-trapped waves (ITWs) on biological processes at the Lastovo Island in the southern Adriatic Sea, focusing on phytoplankton community structure and NPP in the stratified water column. Results show a phytoplankton community typical for oligotrophic seas, dominated by pico- and nanophytoplankton, with vertical distribution constrained by stratified layers: pico- and nano-fractions in surface and thermocline layers, and microphytoplankton in deeper layers. While ITWs do not affect phytoplankton temporal succession, indirect effects are observed in shifts in bacterial activity and functions, and zooplankton grazing. Nutrient dynamics suggest possible transport to the thermocline due to ITWs, however it is potentially modulated by plankton activity as well. Light availability increases in the thermocline when ITWs and light cycle are in phase, shaping the NPP at the Lastovo Island. Although daily NPP increases in the thermocline during ITWs, this effect is less pronounced in total water column production, with no significant correlation between ITWs and NPP. This thesis demonstrates bio-physical interactions at comparable scales, showing that ITWs can temporarily transform nutrient-poor stratified ecosystems into more favorable ones for primary producers, highlighting the importance of understanding such dynamics for monitoring changes in global ocean productivity.

(111 pages, 19 figures, 9 tables, 288 references, original in English)

Keywords: primary production, Adriatic Sea, internal island-trapped waves, phytoplankton, light, nutrients

Supervisor: Dr Zrinka Ljubešić, Full Professor

Reviewers: Dr Marija Gligora Udovič, Full Professor

Dr Žarko Kovač, Associate Professor

Dr Mirko Orlić, Full Professor, F. C. A.

Doktorski rad

Sveučilište u Zagrebu

Prirodoslovno-matematički fakultet

Biološki odsjek

Botanički zavod

UTJECAJ VALOVA VEZANIH UZ OTOK NA PRIMARNU PROIZVODNJU

ANTONIJA MATEK

Botanički zavod, Biološki odsjek, Prirodoslovno-matematički fakultet

Horvatovac 102a, 10000 Zagreb

Neto primarna proizvodnja ključna je za morske ekosustave jer čini temelj hranidbenog lanca i ima važnu ulogu u regulaciji biogeokemijskih ciklusa. Zbog globalnog zagrijavanja oceana uzrokovanog klimatskim promjenama, dolazi do širenja područja veće raslojenosti oceana i siromašnosti hranjivim solima, te posljedično i do smanjenja neto primarne proizvodnje. Stoga, područja lokalno povećane neto primarne proizvodnje u navedenim uvjetima dobivaju na sve većoj važnosti. Ovaj doktorski rad istražuje utjecaj valova vezanih uz otok na biološke procese kod otoka Lastova u južnom Jadranskom moru, s naglaskom na strukturu fitoplanktonske zajednice i neto primarnu proizvodnju. Rezultati pokazuju fitoplanktonsku zajednicu tipičnu za raslojena oligotrofna mora gdje prevladava piko- i nanofitoplankton. Vertikalna raspodjela uvjetovana je raslojenošću vodenog stupca: piko- i nanofitoplankton prevladava u površinskom sloju i sloju termokline, dok je mikrofitoplankton najbrojniji u dubokom sloju. Iako valovi vezani uz otok ne utječu na vremensku sukcesiju fitoplanktona, zabilježeni su neizravni učinci kroz promjene u aktivnosti i funkciji bakterija, te zooplanktona. Dinamika hranjivih soli upućuje na mogući donos u sloj termokline za vrijeme valova, no također moguće je da je regulirana aktivnošću planktona. Dostupnost svjetlosti u sloju termokline raste kada su ciklusi valova i svjetlosti usklađeni, čime se oblikuje prostorna raspodjela neto primarne proizvodnje na području Lastova. Iako dnevna neto primarna proizvodnja raste u sloju termokline tijekom valova vezanih uz otok, taj učinak je slabije izražen u ukupnoj proizvodnji vodenog stupca i nije doveden u značajnu vezu s prisutnošću valova. Ova disertacija pokazuje biofizičke interakcije na usporedivim skalama, otkrivajući da valovi vezani uz otok mogu privremeno preobraziti raslojene ekosustave siromašne hranjivim solima u područja povoljna za primarne proizvođače, te naglašava važnost razumijevanja takvih dinamika u svrhu praćenja globalnih promjena u produktivnosti oceana.

(111 stranica, 19 slika, 9 tablica, 288 literaturnih navoda, jezik izvornika: engleski)

Ključne riječi: primarna proizvodnja, Jadransko more, valovi vezani uz otok, fitoplankton, svjetlost, hranjive soli

Mentorica: prof. dr. sc. Zrinka Ljubešić

Ocjenjivači: prof. dr. sc. Marija Gligora Udovič

izv. prof. dr. sc. Žarko Kovač

prof. dr. sc. Mirko Orlić, akademik

LIST OF ABBREVIATIONS

Abbreviation	Full name	Unit
α^B	Initial slope	mg C (mg Chl)$^{-1}$ (W m^{-2})$^{-1}$
ANOSIM	Analysis of similarities	
ANOVA	Analysis of variance	
AOPs	Apparent optical properties	
BiOS	Bimodal Adriatic-Ionian Oscillation	
CCA	Canonical correspondence analysis	
Chl *a*	Chlorophyll *a*	mg m^{-3}
Chl F	Chlorophyll *a* fluorescence	
DCM	Deep chlorophyll maximum	
DPM	Disintegrations per minute	min^{-1}
IME	Island Mass Effect	
IOPs	Inherent optical properties	
I(z, t)	Light model (irradiance as a function of depth and time)	W m^{-2}
I_0	Surface irradiance	W m^{-2}
I_0^m	Surface irradiance at noon	W m^{-2}
ITWs	Internal island-trapped waves	
K_{PAR}	Attenuation coefficient of PAR	m^{-1}
NIG	Northern Ionian Gyre	
NO_2^-	NO_2; nitrite	μmol L^{-1}
NO_3^-	NO_3; nitrate	μmol L^{-1}
NPP	Net primary production	mg C m^{-3}
PAR	Photosynthetically active radiation	μmol m^{-2} s^{-1}

$P^{B}_{Z,T}$	Daily normalized depth-integrated primary production	mg C m^{-2}
P^{B}_{m}	Assimilation number	mg C (mg Chl)$^{-1}$ h^{-1}
$P^{B}_{T}(z)$	Normalized daily net primary production at depth	mg C (mg Chl)$^{-1}$
PCA	Principal component analysis	
PPEs	Photosynthetic picoeukaryotes	cells mL^{-1}
$P_{T}(z)$	Daily net primary production at depth	mg C m^{-3}
$P_{Z,T}$	Daily depth-integrated primary production	mg C m^{-2}
PO_4^{3-}	PO_4, phosphate	μmol L^{-1}
SiO_4^{4-}	SiO_4, silicic acid	μmol L^{-1}
Tukey HSD	Tukey Honest Significance Difference	
VIFs	Variance inflation factors	
~Chl *a*	Copernicus L4 chlorophyll a (gap-free, 1 km)	mg m^{-3}
$\sim P_{Z,T}$	Integrated Copernicus daily 4-km resolution primary production reanalysis model	mg C m^{-2}
$\sim P_{T}(z)$	Daily net primary production profile (output of inverse model)	mg C m^{-3}

TABLE OF CONTENTS

1 INTRODUCTION

Primary producers form the basis of the marine food web. In the global ocean, primary production is driven by autotrophic organisms that use photosynthesis to convert inorganic carbon into organic matter (Chavez et al., 2011). Through this process, phytoplankton play a central role in global biogeochemical cycles, particularly the carbon cycle. Although they comprise about 1% of the biomass of primary producers, phytoplankton are responsible for roughly half of global annual primary production (Field et al., 1998). They contribute to the export of atmospheric CO_2 into the ocean surface through the biological pump, where part of the organic carbon produced in the euphotic zone is transported to deeper layers and can be sequestered, thus removed from the short-term carbon cycle (De La Rocha & Passow, 2007). The efficiency of carbon export below the euphotic zone is influenced by phytoplankton cell size, taxonomic composition, and incorporation into aggregates, fecal pellets, or detrital material (Durkin et al., 2021, 2022). The fraction of particulate organic carbon (POC) that is not exported is remineralized, supporting regenerated primary production in the euphotic zone or returning to the atmosphere (Henson et al., 2012).

The availability of light and nutrients regulates primary production in the ocean, and these limiting factors vary not only across climatic zones but also at much smaller spatial and temporal scales (Kirk, 2010). Phytoplankton depend on a delicate balance between light and nutrient availability to maintain efficient photosynthesis, adapting physiologically to changes in their vertical position within the water column (Behrenfeld et al., 2008, Marzetz et al., 2020). Their efficiency as primary producers is further modulated by physical processes that shape the oceanic environment (Mahadevan, 2016). From a biological perspective, physical processes serve as an auxiliary energy source, influencing the boundary layer surrounding plankton, transporting nutrients, and facilitating vertical or horizontal migrations. Stratification traps plankton in the upper ocean layer, while temperature regulates the metabolic rates that drive biological activity (Mann & Lazier, 2005a).

As passive, free-floating organisms, phytoplankton are inherently linked to water mass movements driven by physical processes operating across a range of spatial and temporal scales (Williams & Follows, 2003). Vertical and horizontal circulation patterns determine both nutrient availability and the underwater light environment (Freilich & Mahadevan, 2019, Simoes-Sousa et al., 2022), thus shaping the habitats that phytoplankton occupy. Because they cannot actively migrate to more favorable conditions, physical forcing plays a critical role in

transporting them to regions with enhanced light or nutrient supply, thereby promoting localized increases in primary production (Sverdrup et al., 1942, Mann & Lazier, 2005b).

Physical processes in the ocean operate over a broad spectrum of scales, from basin-scale thermohaline circulation spanning thousands of kilometers to mesoscale (10–100 km) and submesoscale (0.1–10 km) processes such as upwelling, downwelling, eddies, tidal mixing, internal waves, and fronts (Mann & Lazier, 2005b, Mahadevan, 2016). Their temporal scales vary accordingly, from a thousand-year overturning global circulation belt to gyres persisting for several years, mesoscale eddies lasting weeks to months, and submesoscale processes fluctuating over hours to days (Mann & Lazier, 2005a, Mahadevan, 2016). The biological relevance of these physical processes depends on the correspondence between their spatio-temporal scales and those of the organisms affected (Denman, 1994). Phytoplankton, with doubling times ranging from hours to days, respond to physical variability on similar time scales (Mann & Lazier, 2005a). For a physical process to directly influence primary production, its spatio-temporal scales must align with those of phytoplankton growth and turnover (Harris & Trimbee, 1986). Therefore, physical drivers operating at scales comparable to phytoplankton-mediated biological processes are relevant for understanding localized variations in primary production (Harris, 1987, Freilich et al., 2022).

Such scale matching has been observed particularly around oceanic islands, where unique biological and physical interactions can enhance primary production, a phenomenon known as the Island Mass Effect (IME) (De Falco et al., 2024). Among the processes contributing to IME are internal island-trapped waves (ITWs) (Doty & Oguri, 1956, De Falco et al., 2022), which can enhance primary production through nutrient transport to the euphotic zone (Pan et al., 2012), changes in light properties (Evans et al., 2008, Holloway & Denman, 1989, Gaxiola-Castro et al., 2002) and phytoplankton vertical displacement (Orr & Mignerey, 2003). ITWs have been observed at only a few locations worldwide, including the Lastovo Island in the southern Adriatic Sea (Mihanović et al., 2009).

In the Adriatic Sea, areas of elevated primary production have historically been associated with upwelling, a process that transports deep, nutrient-rich water masses to the euphotic zone (Zore-Armanda, 1984, Marasović et al., 1999). One well-documented example is the Palagruža Sill, where upwelling has been shown to influence primary production (Turchetto et al., 2000). However, another productivity hotspot may exist in the southern oligotrophic Adriatic Sea, at the Lastovo Island, driven by ITWs during the stratified summer period. The Adriatic Sea, a

semi-enclosed basin in the northeastern Mediterranean Sea, exhibits a pronounced north-south gradient in productivity. The northern Adriatic is eutrophic and highly productive, the middle Adriatic is characterized by eutrophic and highly productive coastal areas and contrasting open sea, while the southern Adriatic is oligotrophic and least productive (Matek & Ljubešić, 2024).

At the Lastovo Island, ITWs propagate clockwise around the island with a 24-hour period. Their excitation depends on island geometry, water-column stratification, and the strength of physical forcing (Mihanović et al., 2014). The largest observed thermocline oscillations, reaching up to 30 m, are driven by strong diurnal wind (Orlić et al., 2011). Such oscillations could enhance primary production by transporting nutrients upward or vertically redistributing phytoplankton into more favorable light conditions. In this oligotrophic region, where primary production is constrained by stratification during summer, understanding the influence of localized physical processes such as ITWs in sustaining productivity hotspots is essential. These processes play a key role in providing ecological refuges and supporting ecosystem regeneration, particularly in the context of ongoing climate change.

The ocean's response to climate change is reflected in increased stratification (Li et al., 2020), the expansion of oligotrophic areas (Polovina et al., 2008), and a global decline in primary production (Silsbe et al., 2025). Due to the vast size of the oceans, studying these changes remains challenging, and even with intensive sampling efforts, some biogeochemical processes may go undetected (Parasyris et al., 2025). As an enclosed basin, the Adriatic Sea serves as a natural laboratory for investigating ecosystem responses under different future climate scenarios. Following global trends, the Mediterranean Sea, including the Adriatic, is undergoing more frequent heatwaves due to climate change, leading to a rising sea surface temperature and extended seasonal stratification (Coma et al., 2009, Denamiel, 2025). Climate projections under the RCP8.5 scenario suggest 35% decrease in river discharge, which may destabilize stratification in the northern Adriatic, while the southern Adriatic will likely be influenced by altered water-mass exchanges with the Mediterranean (Verri et al., 2024). Stratification stability influences primary production, especially in nutrient-limited ecosystems (Chen et al., 2021). In the phosphate-limited Adriatic (Pojed & Kveder, 1977), prolonged stratification may inhibit nutrient transport to the euphotic zone, further reducing ecosystem productivity. These dynamics highlight the importance of studying primary production hotspots in the oligotrophic ecosystems such as the southern Adriatic Sea.

This doctoral thesis presents a multidisciplinary research that includes both ship-based and moored measurements, as well as the application of ocean colour remote sensing to reveal the

influence of physical phenomena on biology, specifically plankton communities and primary production. This research aims to explore the connectivity between ITWs and primary production in the southern Adriatic Sea. Optimizing the sampling method, generating spatial and temporal databases of high resolution, understanding the coupling of physics and biology at small spatio-temporal scales, and testing the effects of ITWs on primary production at fine spatial scales represent a significant contribution to the understanding of basic bio-physical processes in marine ecosystems. The implementation of different platforms, including *in situ* measurements, models, and ocean colour remote sensing, contributes to developing a broader understanding of ITWs effects on net primary production (NPP) and improves the scientific approach to the research of marine ecosystems.

Therefore, the objectives of this doctoral dissertation are as follows:

O1: Describe taxonomic composition of phytoplankton in the stratified oligotrophic ecosystem influenced by rare oceanographic phenomena - island trapped waves (ITWs).

O2: Describe succession and correlation between plankton communities, and their response to changes in the physico-chemical conditions of the oligotrophic stratified water column.

O3: Determine *in situ* daily net primary production in the oligotrophic stratified ecosystem off the Lastovo Island influenced by ITWs.

O4: Implement inverse numerical model to determine daily net primary production profile, and daily and yearly water column production in the stratified island ecosystem of the Southern Adriatic Sea.

The hypotheses that this doctoral dissertation investigates are as follows:

H1: Nano- and pico-fraction dominate the phytoplankton community in the stratified oligotrophic water column of the Lastovo Island in the Southern Adriatic Sea.

H2: Changes in physico-chemical conditions of the water column due to vertical thermocline oscillations define plankton succession and correlations between plankton communities.

H3: Island trapped waves influence daily net phytoplankton primary production in the oligotrophic ecosystem off the Lastovo Island.

H4: Inverse numerical model defines daily net primary production profile, and daily and yearly water column production off the Lastovo Island.

2 LITERATURE OVERVIEW

2.1 Primary production in global oceans

Primary production is a globally significant biogeochemical process supported by photosynthetic and chemosynthetic organisms that can utilize sunlight and water to assimilate inorganic carbon into organic form (Chavez et al., 2011). Phytoplankton are the main primary producers in marine ecosystems (Falkowski et al., 2004), although phytobenthos also contributes to some extent (Goto et al., 1999). Marine phytoplankton are a group of free-floating autotrophic prokaryotic and eukaryotic organisms that form the basis of the pelagic food web and are responsible for a large amount of carbon fixation in the planet's biosphere (Harrison, 1980, Falkowski et al., 2004). Their size fractions are defined as nano- and picophytoplankton (2–10 μm, and <2 μm, respectively), and as microphytoplankton (>10 μm) (Sieburth et al., 1978). Marine phytobenthos are a group of autotrophic prokaryotic and eukaryotic organisms that live on various surfaces (seabed, other organisms, etc.), and can be categorized as macrophytobenthos or microphytobenthos, depending on size fraction.

In the oceans, primary production significantly affects biogeochemical cycles and is restricted to the euphotic layer where light is available. Factors limiting primary productivity include light availability and nutrient concentrations, both of which vary across climate zones and geographical regions (Kirk, 2010, Chavez et al., 2011). These limiting factors are inherently interlinked (Holloway & Denman, 1989), and their combined effect on primary production is further modulated by the depth of the mixed layer, particularly in pelagic systems of the open ocean. The Critical Depth Theory, first introduced by Gran & Braarud (1935) and later formalized by Sverdrup (1953), proposes that phytoplankton blooms occur when depth-integrated primary production from the surface to the critical depth exceeds respiratory losses. When the mixed layer is deeper than the critical depth, phytoplankton are exposed to less light, and losses dominate. Conversely, a shallower mixed layer favors greater biomass. The theoretical framework has been expanded to include phytoplankton-light feedbacks, recognizing that phytoplankton biomass itself modifies the underwater light field and influences the critical depth (Kovač & Sathyendranath, 2025). Consequently, variability in primary production cannot be explained by individual limiting factors alone. Instead, it arises from the interactions among light attenuation, nutrient availability, mixed-layer dynamics, and biological feedbacks.

Regarding the amount of energy produced and available to the food web, primary production is defined as photosynthetically fixed carbon available to the first heterotrophic level

(Lindeman, 1942), and rates can be calculated. Gross primary production equals the total amount of energy absorbed by light into the cell, which is then available for its growth and division. After accounting for carbon lost through respiration during metabolic pathways, we can calculate NPP. The rate of carbon production within a microbial population after accounting for energy losses and carbon respiration is called net community production (Balch et al., 2022). All of these values are essential for monitoring the flow of energy within the ecosystem, while NPP specifically allows the estimation of the carbon biomass available to the food web (Chavez et al., 2011). Global annual NPP is estimated at about 100 Gt C y^{-1}, being equally split between terrestrial and marine ecosystems (Field et al., 1998). However, a recent study highlights the need to improve global assessments of NPP by accounting for photoacclimation under cloud cover, which has so far been neglected and possibly has led to underestimations (Begouen Demeaux et al., 2025).

2.2 Primary production in the Adriatic Sea

2.2.1 Adriatic Sea hydrography and oceanography

The Adriatic Sea is a semi-enclosed basin in the northeast of the Eastern Mediterranean. It is 800 km long, 200 km wide and covers 139 000 km^2. Its bathymetry divides it into three regions: the northern, middle and southern Adriatic Sea. The northern Adriatic Sea ranges from the 30 to 40 m depths, with a maximum depth of 70 m. The middle Adriatic Sea includes the 270 m deep Jabuka Pit and ends at the Palagruža Sill. The southern Adriatic Sea is the deepest, with the 1200 m South Adriatic Pit between the Palagruža Sill and Otranto Strait, which connects the Adriatic Sea with the Eastern Mediterranean.

The Adriatic Sea exhibits a cyclonic upper circulation, driven by the intrusion of oligotrophic, saline water masses from the Eastern Mediterranean along its eastern coastline. This process forms the Eastern Adriatic Current, while along the western coastline, the outflow of eutrophic and fresher water masses forms the Western Adriatic Current. The properties of Adriatic Sea water masses - such as temperature, salinity, and nutrient concentration - are also influenced by atmospheric and circulation changes in the Mediterranean Sea. For example, decadal shifts in the internal dynamics of the Northern Ionian Gyre (NIG) from cyclonic to anticyclonic (and vice versa), known as the Bimodal Adriatic-Ionian Oscillation (BiOS), influence the inflow of distinct water masses into the Adriatic Sea (Civitarese et al., 2010).

During cyclonic NIG periods, Levantine Intermediate Water intrudes into the southern Adriatic Sea, increasing its salinity, temperature and density. Conversely, anticyclonic NIG favors a

stronger inflow of Modified Atlantic Water, which originates in the Western Mediterranean and is fresher and more eutrophic (Civitarese et al., 2010). Thus, both the cyclonic upper circulation and large-scale Mediterranean circulation patterns shape the water masses of the southern Adriatic Sea. The Middle Adriatic water mass properties are also influenced by upper circulation patterns (Zore-Armanda, 1969, Marasović et al., 1999). In contrast, the northern Adriatic Sea is most affected by river discharge, particularly from the Po River (Degobbis et al., 1986). While historical studies identified this region as the most eutrophic (Degobbis et al., 1986, Granéli et al., 1999), more recent research has established a correlation between increased climate change-induced drought and decreasing Po River discharge (Grilli et al., 2020). Consequently, the phosphate-to-nitrogen ratio in the northern Adriatic Sea, which historically favored nitrogen (Granéli et al., 1999), has now shifted toward phosphate (Cozzi & Giani, 2011, Cozzi et al., 2019).

2.2.2 Regional patterns of primary production

Compared to the middle and southern Adriatic Sea, the northern Adriatic Sea is historically recognized as the most eutrophic region, exhibiting the highest productivity (Kveder et al., 1971, Gilmartin & Revelante, 1983). This northern ecosystem has also been the most frequently investigated compared to other regions of the Adriatic (Matek & Ljubešić, 2024). Among the highly productive areas are the Gulf of Trieste, with annual water column production ranging between 60.2 and 87.4 g C m^{-2} (Talaber et al., 2018), the Po River delta with 130 g C m^{-2} (Gilmartin & Revelante, 1983) and the Istrian coast with 80–100 g C m^{-2} (Kveder & Kečkeš, 1969). The Middle Adriatic coastal area is also eutrophic and characterized by high productivity, with annual water column production in Kaštela Bay estimated between 70 and 150 g C m^{-2} (Gilmartin & Revelante, 1983). In contrast, oligotrophic open waters of the Middle Adriatic exhibit lower productivity. At the Stončica station near Vis Island, annual water column production range from 40 g C m^{-2} to 90 g C m^{-2} (Pucher-Petković & Zore-Armanda, 1973). Data on primary production in the southern Adriatic Sea remain scarce, but comparisons of daily water column production rate with those of the middle and northern regions indicate that it is the least productive part of the basin (Matek & Ljubešić, 2024). Microphytoplankton are the main contributors to the eutrophic coastal ecosystem production, while the pico- and nanophytoplankton are the main producers in the oligotrophic open sea (Ninčević & Marasović, 1998, Mangoni et al., 2008, Talaber et al., 2018). In addition, a shift to small-scale phytoplankton during ocean heat waves was observed in the oligotrophic open Adriatic Sea

(Malej et al., 1995, Pugnetti et al., 2003, Marasović et al., 2005), elucidating a possible trend in future climate scenarios where sea surface temperature is increasing.

Physico-chemical parameters have a direct effect on the productivity of the Adriatic Sea. Thus, the circulation patterns and trophic states of the Adriatic Sea regions should be considered when describing the productivity of the ecosystems. Phosphate is limiting primary production in the Adriatic Sea (Pojed & Kveder, 1977), and the distribution of nutrients is controlled by stratification (Giordani et al., 1997, Vadrucci et al., 2005), river discharges (Cantoni et al., 2003), and circulation dynamics (Marasović et al., 1995). Productivity of the northern regions is influenced by the river discharge rates (Ingrosso et al., 2016, Brush et al., 2020, Grilli et al., 2020) compared to middle and southern Adriatic where circulation patterns, such as dynamics of Mediterranean water mass ingression tightly connected to BiOS (Grbec et al., 2009, Civitarese et al., 2010) and North Atlantic Oscillation (Grbec et al., 2009, Ninčević Gladan et al., 2010), drive interannual variability in primary production (Marasović et al., 1995, Marasović et al., 1999, Matić et al., 2011, 2017). Besides nutrient distribution and water-mass circulation patterns, atmospheric mineral dust deposition is another important environmental factor influencing primary production in the Adriatic Sea (Mifka et al., 2022).

2.3 History of primary production research in the Adriatic Sea

Primary production in the Adriatic Sea was discussed as a very general term in early papers by Ercegović (1938) and Buljan (1964). The first public conference on the primary production in the Adriatic Sea was held in 1938 at the Institute of Oceanography in Split (at that time Yugoslavia, now Croatia), where Ante Ercegović held a public lecture on the limiting parameters, eutrophication effects, and importance of monitoring primary production in relation to fisheries (Ercegović, 1938). Later on, Buljan (1964) divided the Adriatic Sea into four production zones (**Figure 1**). According to historical records, 57% of the Adriatic surface was characterized by low production, which included open sea, while coastal regions influenced by river discharges exhibited higher production (Buljan, 1964, Pucher-Petković, 1974).

Monitoring primary production is of high importance, as it allows observation of interannual variability and examination of trends that can shift due to climate change. This was recognized early, with primary production experiments in the Adriatic Sea starting in the 60s (summary provided in Matek & Ljubešić, 2024) and the ongoing monitoring starting in 1962 in the middle Adriatic Sea at coastal station Kaštela Bay and open sea station Stončica near Vis Island (Pucher-Petković, 1971). Adriatic Sea exhibits one of the longest monitoring programs (Kovač et al., 2018) when compared to global ones such as Bermuda Atlantic Time-Series Study

(BATS) at the Bermuda Station in the North Atlantic (Lohrenz et al., 1992) and Hawaii Ocean Time-Seris (HOT) program at Aloha Station, Hawaii in North Pacific (Karl & Lukas, 1996) that were founded in 1988.

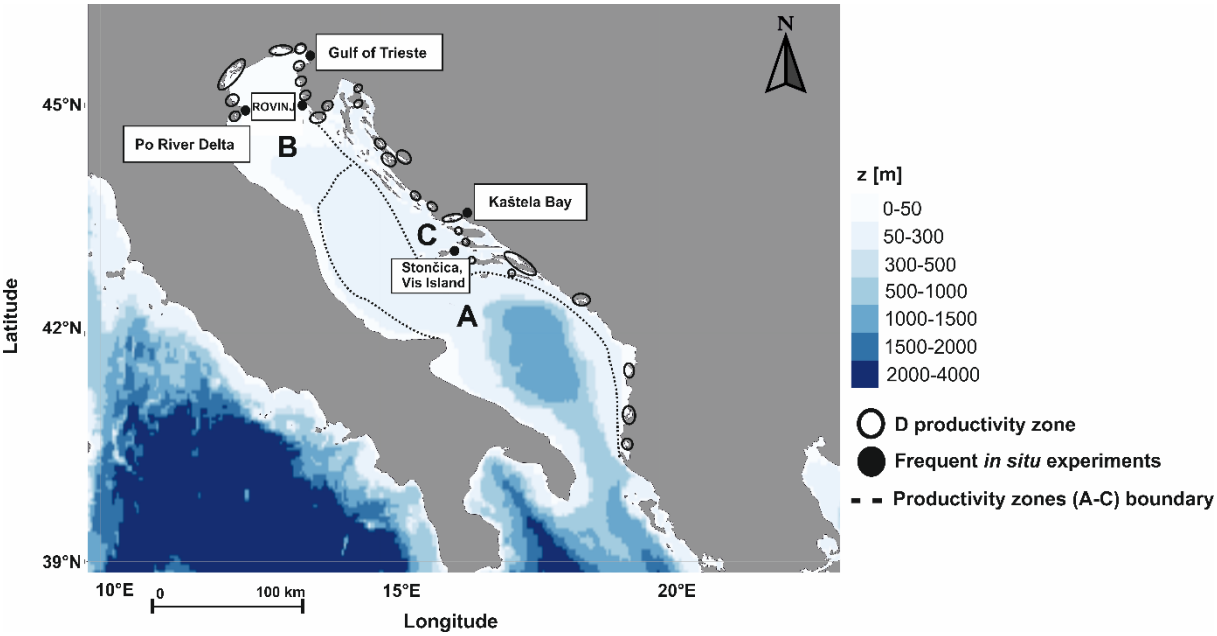

Figure 1. Primary production zones (A-D) in the Adriatic Sea indicated by dashed line and open circles. Sites with frequent *in situ* measurements are marked by black circles. Zone A (57% of the Adriatic Sea surface) represents the open Adriatic Sea and is characterized by low primary production. Zone B (23%) is influenced by the riverine eutrophication and exhibits elevated primary production. Zone C (18%) comprises the coastal areas up to 70 m depth, with pronounced interannual variability driven by both river discharges and circulation dynamics. Zone D (2%) includes very shallow coastal regions affected by river inputs and terrestrial erosion, and is characterized by high primary production (adapted from Buljan, 1964).

2.4 Primary production measurements: methodology

Primary production can be directly measured with high accuracy using carbon assimilation (^{13}C or ^{14}C uptake) and oxygen-based methods (O_2 concentration and isotope ratios), applied across different experimental incubation setups (*in situ*, *in vitro* and *on-deck*) (**Figure 2**). In addition to these direct approaches, primary production can be estimated indirectly through modelling approaches based on photosynthesis-irradiance (P-E) curves or derived from ocean colour remote sensing using Chl *a* as a proxy (**Figure 2**). Collectively, these complementary methodologies enable the assessment of primary production across a wide range of spatial and temporal scales. The following sections provide a detailed description of each approach.

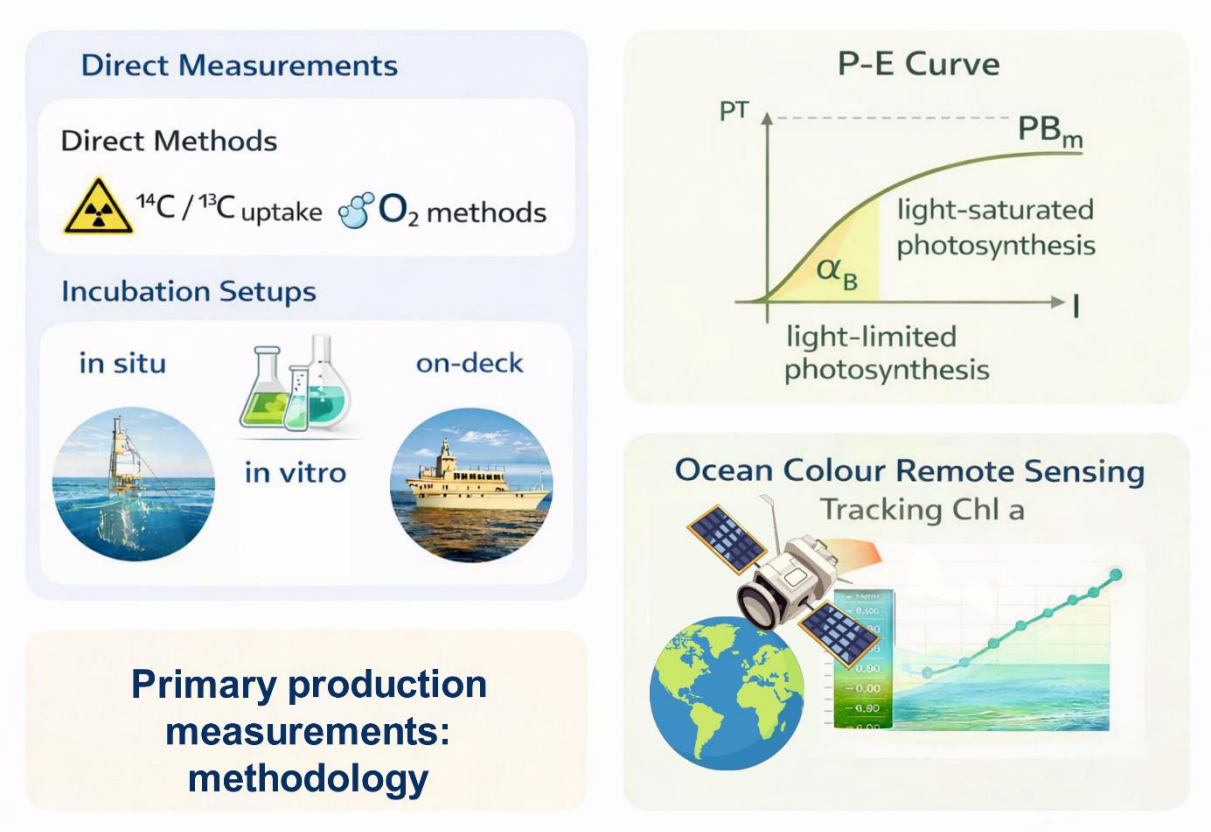

Figure 2. Overview of primary production measurement methods, including direct measurements (^{14}C, ^{13}C, O_2) using different experimental setups, or indirect estimates using modeling approaches (photosynthesis-irradiance curves) or ocean colour remote sensing.

2.4.1 Incubation modes

Depending on the light conditions, primary production experiments can be incubated *in vitro* and *on-deck* (simulated *in situ*) using various methods, such as measuring the rate of carbon assimilation through ^{13}C or ^{14}C isotopes, measuring oxygen concentration through isotope ratio or optode and indirect estimates based on biogeochemical parameters measured by different optical sensors (Balch et al., 2022).

Historically, *in situ* ^{14}C methodology by E. Steemann Nielsen (Nielsen, 1952) is the most commonly used in the Adriatic Sea (Matek & Ljubešić, 2024). It is the most precise method for primary production measurements, and thus a widely used method for estimating ocean productivity (Marra et al., 2021). Besides *in situ* measurements, *in vitro* and *on-deck* experiments were also implemented to estimate primary production in the Adriatic Sea (Matek & Ljubešić, 2024), and globally, they are more frequently done during ship cruises since the method is more feasible (Platt et al., 2017). *In vitro* incubation experiments in the Adriatic are mostly implemented in the laboratory under standard light (2400 lux) and temperature (20 °C),

or in the incubators under constant light (70 W m^{-2}) or light gradient (80–1200 μmol photon m^{-2} s^{-1}, 20–500 μE m^{-2} s^{-1}) and simulated sea surface temperature. *On-deck* incubations are done in the thermostatic bath where the flow-through system maintains the sea surface temperature, and under sunlight or *in situ* light gradient that is reproduced by the nickel screens (Matek & Ljubešić, 2024).

Discrepancy between the values measured using different incubation modes are significant. For instance, *in vitro* incubations revealed 40% higher primary production in the Krka River estuary compared to the *in situ* (Gržetić et al., 1991). In addition, incubation time strongly influences the measured productivity rate. Short incubations primarily capture gross primary production, whereas longer incubations provide a more accurate estimate of NPP. The effect of incubation time on data interpretation is clearly demonstrated in the study by Kovač et al. (2018), where a 55-year time series was corrected for overestimations. In the Middle Adriatic, primary production had originally been estimated based on the incubation period rather than the full photoperiod from sunrise to sunset, leading to inflated values. To address this, a non-linear production model was applied, which revealed new insights into inter-decadal variability with distinguishable trends: 1962–1979 (118 mg C m^{-2}), 1979–1997 (300 mg C m^{-2}), 1997–2008 (128 mg C m^{-2}), 2008–2013 (251 mg C m^{-2}), and 2013–2017 (154 mg C m^{-2}) (Kovač et al., 2018).

Since there is no standardized protocol for primary production measurements in the Adriatic Sea, comparisons across data sources are subject to methodological bias. Many studies in the Adriatic Sea lacked information on the incubation time or the aimed rate of primary production (Matek & Ljubešić, 2024). Therefore, it is highly recommended to introduce standardized protocols, such as those developed by the International Ocean Colour Coordinating Group (Balch et al., 2022), in the future research of primary production in the Adriatic Sea.

2.4.2 Photosynthesis-irradiance curves

Based on *in vitro* or *on-deck* experiments, photosynthesis-irradiance (P-E) curves are constructed to derive photosynthesis parameters such as the initial slope (α_B [mg C (mg Chl)$^{-1}$ (W m^{-2})]) and assimilation number (P^B_m [mg C (mg Chl)$^{-1}$ h^{-1}]) (Platt et al., 1980). These parameters are normalized to chlorophyll *a* (Chl *a* [mg m^{-3}]), and therefore represent fundamental bio-optical properties of phytoplankton and provide insights into the physiological adaptation of primary producers to light conditions (Platt et al., 1983). Specifically, α^B is the photosynthetic rate under light levels close to zero, while P^B_m represents photosynthetic efficiency at light saturation (Jassby & Platt, 1976, Platt et al., 1980, Sakshaug et al., 1997).

Although they are not direct estimates of primary production, they are incorporated into mathematical models to quantify water column production (Platt et al., 1977, Sathyendranath & Platt, 1989, Sathyendranath et al., 1989, Morel, 1991, Morel et al., 1996). Historically photosynthesis parameters in the Adriatic Sea were retrieved from *in vitro* ^{14}C experiments (Vadrucci et al., 2002, Mangoni et al., 2008, Talaber et al., 2014, Mangoni et al., 2020). Recently, inverse methods were developed to estimate *in situ* primary production from primary production profiles (Kovač et al., 2016a, 2016b). The inverse model was successfully validated using a 55-year *in situ* time-series of monthly primary production measurements at the Stončica station in the Middle Adriatic (Kovač et al., 2018), and it will be applied in this thesis.

Photosynthesis parameters reflect the photosynthetic performance of marine phytoplankton and are therefore indirectly shaped by environmental conditions and community composition (Richardson et al., 2016). Global datasets show that pico- and nanophytoplankton generally exhibit higher parameter values than microphytoplankton (Richardson et al., 2016). In the Adriatic Sea, a linear relationship between P^B_m and nutrient availability has been observed (Mangoni et al., 2008, 2020), indicating that photosynthetic efficiency increases under nutrient-rich conditions. Temperature also modulates phytoplankton photophysiology, as revealed during stratification periods in the Adriatic Sea by variability in α^B but relative stability in P^B_m (Talaber et al., 2014). Beyond stratified conditions, physical turbulence can further influence these adaptations. For example, in the Gulf of California, internal waves form during stratification and displace low-light-adapted phytoplankton from deeper layers to the surface, reducing P^B_m (Gaxiola-Castro et al., 2002). Understanding photophysiological adaptation of size-fractionated phytoplankton communities to variable enviornmental drivers is essential for improving regional algorithms used in remote sensing, thereby enabling more accurate assessment of spatio-temporal patterns of global primary production (Bouman et al., 2018).

2.4.3 Ocean colour remote sensing

Light irradiance is of great significance to primary production, which is restricted to the euphotic layer (Kirk, 2010). Specifically, primary producers for photosynthesis utilize wavelengths from 400 nm to 700 nm, a spectral range of visible light defined as photosynthetically active radiation (PAR [μmol m^{-2} s^{-1}]) (Kirk, 2010). Thus, research on the underwater light field is crucial for understanding photophysiological adaptations in cells and the efficiency of primary production. Optics research in the Adriatic Sea has historically used Secchi disk depth (Justić, 1988) and, more recently, profiling radiometers (Morović et al., 2008) and PAR sensors (Umer & Malačič, 2022).

Inherent and apparent optical properties (IOPs and AOPs, respectively) influence light behaviour in the water column (Mobley, 1994). IOPs (absorption and scattering of light) are intrinsic to the medium, and they mainly depend on the physical and chemical properties of the particles comprising the medium, while AOPs (downwelling irradiance, diffuse attenuation coefficient, remote sensing reflectance) are affected by the medium and conditions under which the measurements are made (Mobley, 1994). Accordingly, there is a variety of optical water types in the Adriatic Sea, specifically defined by PAR attenuation (Jerlov, 1964, Morović et al., 2008). The open sea, where the euphotic zone is defined as the 1% of surface PAR that reaches below 80 m, is classified as Type I waters. Open and coastal seas that are more eutrophic are defined between Type I and Type II waters, while Type III waters are very turbid and eutrophic (Jerlov, 1964, Morović et al., 2008).

Radiative transfer theory describes how light interacts with the optical properties of the water column and how this interaction influences the reflected signal (Mobley, 2022). Based on this principle, ocean colour remote sensing is applied to monitor various environmental parameters, including primary production, which is commonly estimated from remotely sensed Chl *a* (Sathyendranath et al., 1989, Balch et al., 2022, Mobley, 2022). The efficiency of those retrievals depends directly on the optical complexity, making it more challenging to accurately derive primary production in coastal and eutrophic areas of the Adriatic Sea. Coastal ocean colour remote sensing presents unique challenges, particularly in achieving precise atmospheric correction to accurately estimate water-leaving remote sensing reflectance (Frouin et al., 2019, Hieronymi et al., 2023). Various atmospheric and near-surface processes influence remote sensing reflectance, and coastal areas such as the Adriatic Sea, which are classified as Type II and Type III waters, are optically complex due to absorbing aerosols, intricate water optical properties, and land adjacency effects (Frouin et al., 2019). Therefore, continuous *in situ* data collection is crucial for refining atmospheric corrections and improving regional algorithms to retrieve accurate spatio-temporal trends in primary production.

Although primary production experiments yield highly valuable data, their high cost, logistical complexity and the constraints of ship time significantly limit their feasibility. Ocean colour remote sensing is essential for addressing this gap and enabling the monitoring of primary production at large spatio-temporal scales (Balch et al., 2022). NASA's Plankton, Aerosol, Cloud, Ocean Ecosystem (PACE) mission, launched in February 2024, now delivers daily global hyperspectral observations of ocean color (Werdell et al., 2024). These hyperspectral products are promising in improving the differentiation of phytoplankton groups (Cetinić et al.,

2024, Kramer et al., 2024). The rapid advancement of ocean colour remote sensing products, including those for primary production, relies on accurate models (Kong et al., 2019, Cervantes-Duarte et al., 2021, Shih et al., 2021) and *in situ* fiducial reference measurements, which are essential for accurate algorithm validation (Goryl et al., 2023).

2.5 Internal waves in the stratified ecosystems

The factors controlling primary production are inherently interlinked, encompassing the underwater light field, nutrient availability, and mixed layer depth. Holloway & Denman (1989) have shown that internal waves can deepen the compensation depth, thereby increasing primary production. This concept has been expanded in recent work by Kovač & Sathyendranath (2025). When the light field remains constant, the relationship between the mixed layer depth and critical depth (the boundary where phytoplankton growth and mortality are in equilibrium) becomes a key determinant of bloom development (Kovač & Sathyendranath, 2025). Internal waves can influence this balance by enhancing vertical mixing. For example, in the northern South China Sea, internal wave dissipation in deep layers drives the upward advection of nutrient-rich, cooler water into the mixing layer, enhancing primary production by 37% (Pan et al., 2012). Similar mechanisms of increase in primary production have been observed in the Angolan upwelling ecosystem (Körner et al., 2024).

Island Mass Effect (IME) is an unique phenomenon occuring around islands in the oligotrophic open oceans, where certain physical processes can enhance biomass and primary production (Doty & Oguri, 1956, Messié et al., 2020, 2022), and it is typically observed as an increase in Chl *a* concentration detectable through ocean colour remote sensing (Bourdin et al., 2024). Distinct physical drivers can generate IME (De Falco et al., 2022). For instance, at the Canary Islands, IME observed in July is linked to eddy shedding, upwelling and downwelling, and a shallower mixed layer. In Hawaii, atmospheric-oceanic wake eddies dominate in March, while in August, IME results from the combined influence of wake eddies, oceanic eddies, and reduced mixed-layer depth. In the Maldives, IME in February is primarily driven by wake-lee upwelling, whereas in April, vertical mixing plays the most significant role. Similarly, vertical mixing is responsible for annual IME episodes at Saint Brandon (De Falco et al., 2022). Among the physical processes categorized under vertical mixing, ITWs represent a unique phenomenon that may influence biological processes.

ITWs are a specific type of coastal trapped waves (Hogg, 1980). These waves occur when wave energy is confined along a coastline (Huthnance, 1978, Brink, 1991). They have been documented at only a few sites globally. Examples include Bermuda (Brink, 1999), Gotland

(Pizarro & Shaffer, 1998), Mallorca (Jordi et al., 2009), Hawaii (Luther, 1985), the Saint Pierre and Miquelon archipelago (Lazure et al., 2018), and the Lastovo Island in the Southern Adriatic Sea (Mihanović et al., 2009). At the Lastovo Island, ITWs are resonantly excited by physical forcing such as diurnal tides and wind (Mihanović et al., 2006, 2009, 2014). They are generated within a stratified water column. These waves induce diurnal thermocline oscillations with amplitudes reaching up to 30 m when the dominant forcing is diurnal wind (Orlić et al., 2011). Less intense but more prolonged oscillations are also present. These are driven by diurnal barotropic tidal flow (Novosel et al., 2004, Mihanović et al., 2006, 2009).

ITWs propagate around the Lastovo Island in a clockwise direction with a 24-hour period. Their excitation depends on island geometry, water-column stratification and the intensity of physical forcing (Mihanović et al., 2014). Island shape and size determine the resonance period; for instance, the geometry of Lastovo yields a 24-hour period (Mihanović et al., 2014), whereas Bermuda exhibits a 26.1-hour period (Brink, 1999) and the less circular, larger Hawaii Island yields a longer 59-hour period (Luther, 1985). The range of thermocline oscillations increases with thermocline depth and is larger when driven by strong forcing (Mihanović et al., 2014). ITWs resonance also depends on density gradients between surface and deep layers; for instance, smaller density differences at the Lastovo Island favour stronger vertical thermocline oscillations (Mihanović et al., 2014). Pronounced ITW episodes occur when strong diurnal tides or intense land-sea breezes coincide with optimal stratification conditions (Mihanović et al., 2014).

Regions affected by ITWs have been reported as productivity hotspots (Luther, 1985, Pizarro & Shaffer, 1998, Brink, 1999, Jordi et al., 2009, Lazure et al., 2018). Therefore, ITWs at the Lastovo Island may similarly influence NPP, which is particularly important in this oligotrophic ecosystem, given its high biodiversity and protected status within the Lastovo Archipelago Nature Park (Getzner et al., 2017). ITWs can support an increase in NPP through several mechanisms, including transport of the nutrients to the euphotic zone (Pan et al., 2012), changes in the underwater light properties (Holloway & Denman, 1989, Gaxiola-Castro et al., 2002, Evans et al., 2008) and vertical displacements of phytoplankton to more favorable light conditions (Orr & Mignerey, 2003). Despite several studies investigating such processes (Sangrà et al., 2001, Wang et al., 2007, Evans et al., 2008, Pan et al., 2012, Muacho et al., 2013, Ma et al., 2020, Guan et al., 2023, Ma et al., 2023, Körner et al., 2024, Zhong et al., 2024), the underlying mechanisms remain poorly understood, particularly at the Lastovo Island, where potential ITW-related effects have yet to be examined.

3 MATERIALS AND METHODS

3.1 Study area and sampling design

Lastovo Archipelago is a Nature Park, an area in the oligotrophic southern Adriatic Sea protected for its biodiversity (**Figure 3A**). Field experiments were conducted on the research vessel (RV) during the summer months from 2021 to 2023 at the Lastovo Island, when the water column was stratified and ITWs were expected. Sampling and measurements were conducted at the northern station near the cliff Maslovnjak (M1), stations near the southern cliff Struga (S1 and S0) and at the control station Prižba at the Korčula Island (P4) (**Figure 3B**, **Table 1**).

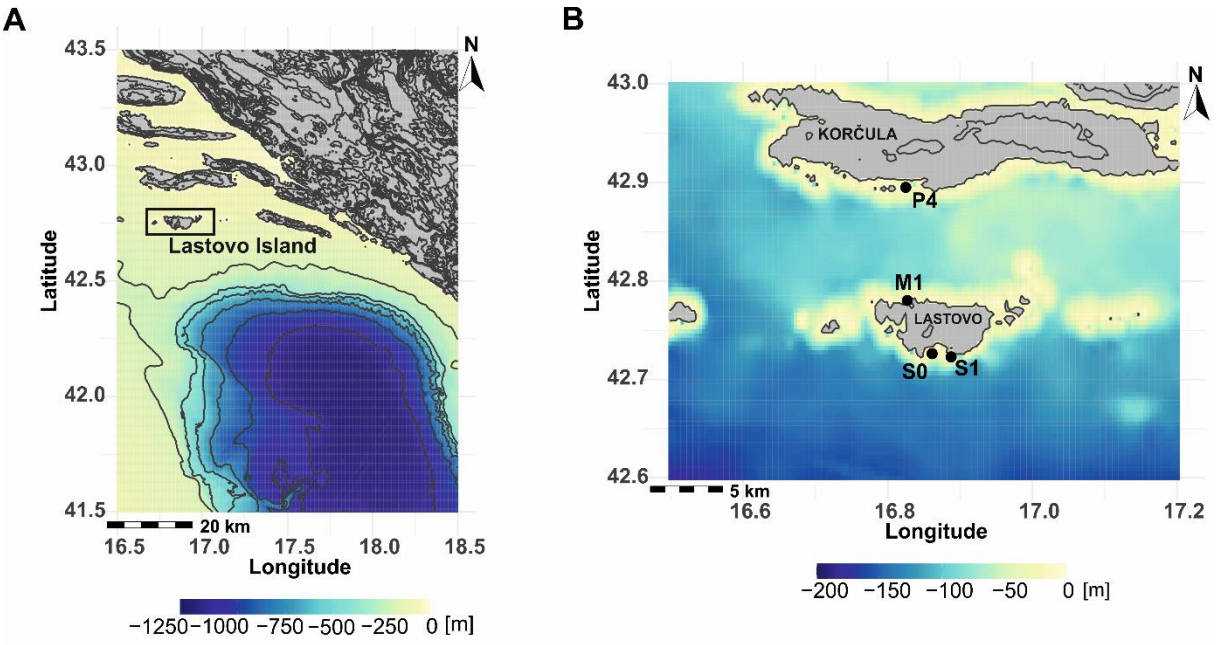

Figure 3. Study area with the research stations. **(A)** Lastovo Island in the southern Adriatic Sea. **(B)** Lastovo Island with station M1 at the northern cliff Maslovnjak, and stations S0 and S1 near the southern cliff Struga; and the Korčula Island with control station P4 (Prižba). The bathymetry map is overlaid.

Intensive sampling of plankton and nutrients, and measurements of physico-chemical parameters were done in July (**Figure 4, Table 1**) when the most intense ITW episodes were expected (Mihanović et al., 2009). Sampling depths were defined *in situ* based on physico-chemical parameters measured with a multi-parametric CTD (Conductivity-Temperature-Depth, SBE 19, Sea-Bird Electronics Inc., USA). Ship-based surveys were carried out twice a day in 2021, at 06:00 h (UTC+2) when the thermocline was deepest, and at 18:00 h (UTC+2) when it was shallowest. Preliminary results indicated that the sampling frequency was insufficient to capture ITWs. Thus, in 2022, a high-frequency adaptive sampling design was

introduced, guided by meteorological and oceanographic model forecasts as described in (Ljubešić et al., 2024). During the ITW episode, sampling and measurements were carried out four times a day, at 06:00, 12:00, 18:00, and 24:00 h (UTC+2) (**Figure 4**) (Ljubešić et al., 2024). ITW episode was considered significant when the diurnal amplitudes of the eastward wind component exceeded 6 m s^{-1}, and thermocline oscillations exceeded 12 m (Ljubešić et al., 2024).

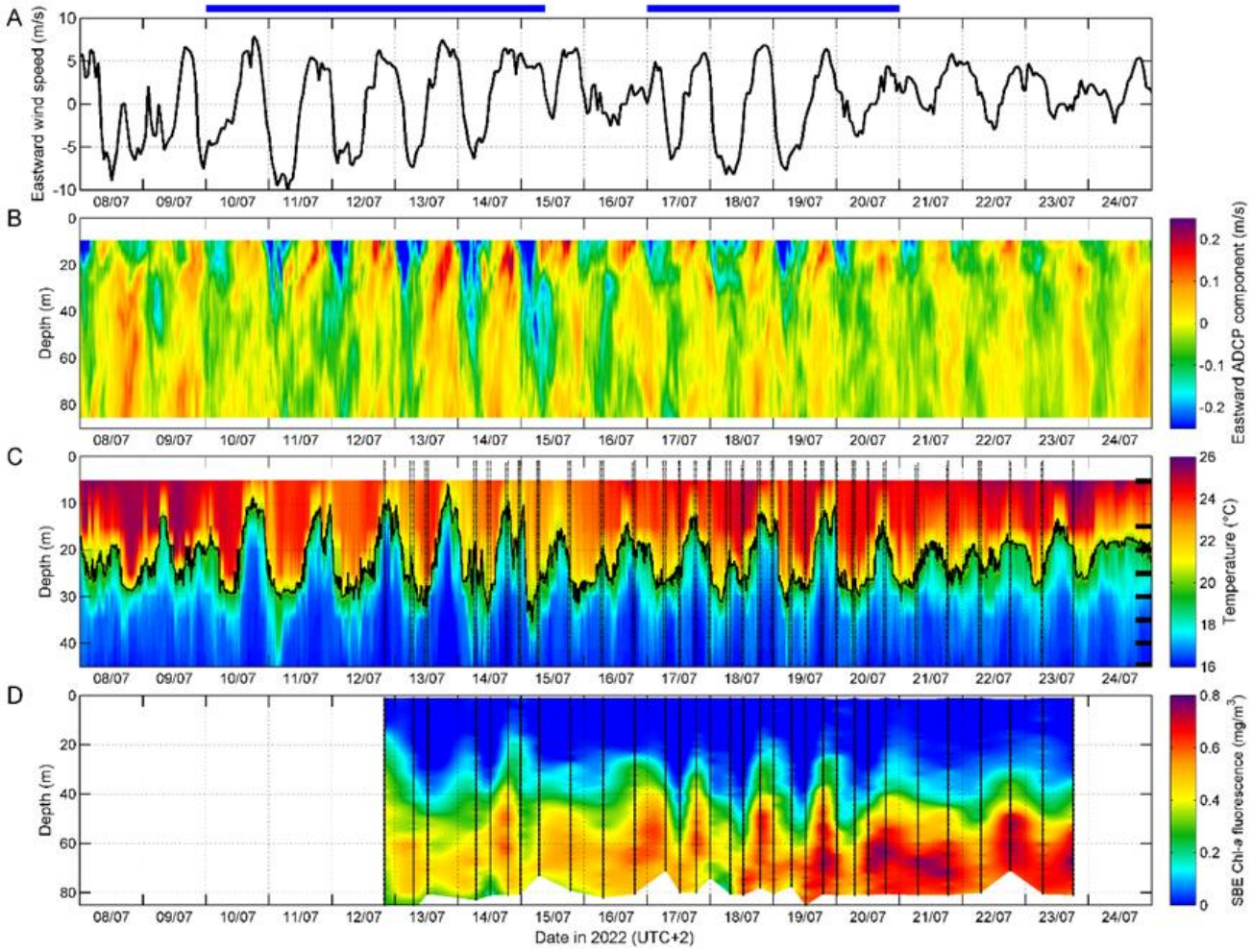

Figure 4. Observations during the field campaign at station S1, the Lastovo Island, in July 2022. **(A)** Eastward wind speed. **(B)** Eastward ADCP component. **(C)** Temperature data measured using thermistors from the cliff at station S1. **(D)** Vertical profiles of Chl *a* fluorescence (Chl F) recovered from CTD casts. ITW events are indicated by blue horizontal lines above panel **(A)**. Vertical dotted lines in **(C)** and **(D)** indicate CTD casts. Black horizontal ticks in the right part of panel **(C)** indicate deployment depths of thermistors, while the thick black contour indicates the 20 °C isotherm (image source: dr. sc. Hrvoje Mihanović, Ljubešić et al. 2024).

Table 1. Sampling design at the Lastovo Island during the 2021–2023 field campaigns at Prižba (P4), Maslovnjak (M1), and Struga (S0, S1). The table summarizes depths of moored measurements (where applicable shown as initial depth : depth interval : final depth), indicates ship-based measurements and discrete sampling (marked with "x"), and lists the sampling periods for each measurement type.

		Moored measurements				**Ship-based measurements**			
		Temperature (dt = 5 min)	**ADCP** (dt = 10 min)	**PAR** (dt = 5 min)	***In situ* PP experiments**	**CTD**	**Nutrients**	**Chl *a***	**Plankton**
	P4	5 m : 5 m : 45 m, except 25 m							
	M1	5, 10, 15, 30, 40 and 45 m							
2021	S1	5, 10, 20, 30, 35 and 45 m				x	x	x	x
	S0		11 m : 4 m : 83 m						
	Period	*June–September*	*June–October*			*July*	*July*	*July*	*July*
	P4	10 m : 5 m : 45 m			x		x		
	M1	15, 25, 30, 35, 40 and 45 m			x	x	x		
2022	S1	5 m : 5 m : 45 m, except 10 m		10 m and 40 m		x	x	x	x
	S0		9.5 m : 4 m : 85.5 m		x	x	x	x	
	Period	*June–September*	*June–September*	*July–October*	*June*	*June and July*	*June and July*	*June and July*	*July*
	P4	15, 20, 25, 35, 40 and 45 m							
	M1	10, 20, 30, 35 and 45 m				x			
2023	S1	10, 15, 20, 25, 30, 35 and 45 m		10 m and 30 m		x			
	S0				x	x	x	x	
	Period	*June–December*		*July*	*July*	*July*	*July*	*July*	

3.2 Continuous measurements of physico-chemical properties

Vertical profiles for temperature, salinity, chlorophyll *a* fluorescence (Chl F) and oxygen were measured using a CTD with 0.5 m depth averaging (Ljubešić et al., 2024) (**Table 1**). An acoustic Doppler current profiler (ADCP) (RDI WorkHorse 300 kHz) was deployed during the entire stratification period from June to October in 2021 and 2022 at the station S0 (Ljubešić et al., 2024) (**Table 1**). Thermistors (HOBO Pendant Temperature/Light Data Logger: models UA-002-64 and MX2202) were mounted on cliffs at S1, M1 and P4 from winter to summer in the period from 2021 to 2023. They were placed at nine equidistant depths between the 5 and 45 m depths, and set to measure temperature [°C] every 5 min (Ljubešić et al., 2024) (**Table 1**). Optical properties were recorded using DEFI2-L sensors that measured PAR at 5 min intervals. Sensors were deployed on the eastern side of the station S1 at 10 m and 40 m from 23 July to 5 October 2022, and on the western side of S1 at 10 and 30 m from 6 to 23 July 2023 (**Table 1**). Optical sensors were mounted horizontally to ensure an upward orientation toward sunlight.

3.3 Discrete sampling of plankton community, nutrients, and Chl *a*

I collected discrete samples of nutrients, picophytoplankton, phytoplankton, and Chl *a* using a 5 L Niskin bottle at predefined depths (**Figure 5, Table 1**). For phytoplankton community analysis, I collected samples in 250 mL bottles and fixed them with hexamine-neutralized formaldehyde (final concentration: 2%). I collected duplicate samples for picophytoplankton and nutrient analysis. I subsampled picophytoplankton (1 mL) into the cryotubes, preserved them using 100 µL of glutaraldehyde (36%), and stored them in the liquid nitrogen until flow cytometry analysis described by Matek et al. (2023). For nutrient analysis, I filtered subsamples through a sterile 0.2 µm Syringe filter into a 15 mL Falcon tube, fixed them with 30 µL of HCl (50%), and stored them in the cold, dark conditions until analysis, as described in Matek et al. (2023). Sampling and analysis for eDNA and zooplankton are described by Ljubešić et al. (2024). Light microscopy was used to determine microphytoplankton (>20 µm) and nanophytoplankton (2–20 µm), as demonstrated by Matek et al. (2023), while picophytoplankton (< 2 µm) was determined using flow cytometry as described by Matek et al. (2023).

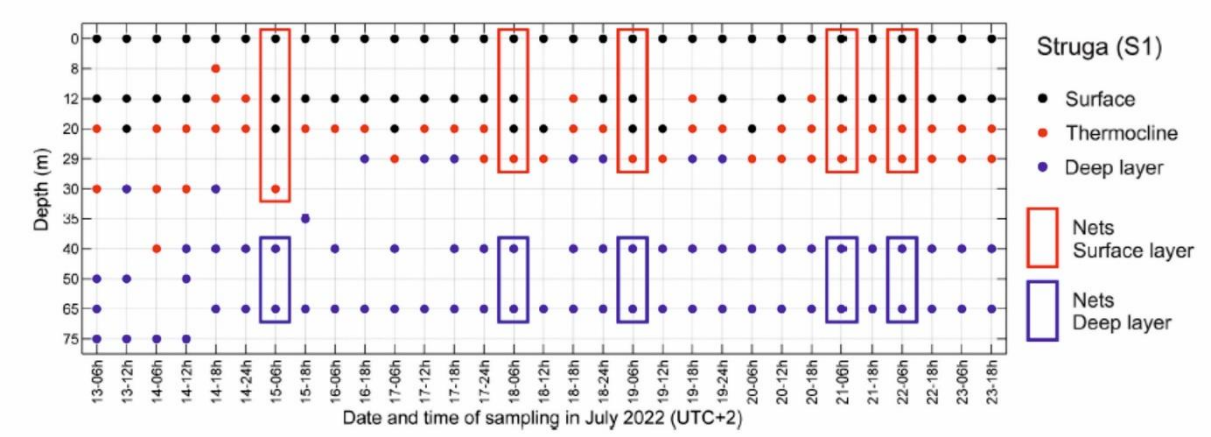

Figure 5. Sampling design during the 2022 field experiment at station S1, Lastovo Island, showing the timing and depths of discrete samples. Depth categories (surface, thermocline, and deep layer) are indicated by color, and the corresponding layers sampled with zooplankton nets are shown by colored squares (image source: dr. sc. Hrvoje Mihanović, Ljubešić et al. 2024).

I sampled from the Niskin bottles for Chl *a* analysis and filtered 1 L of volume through Whatman glass microfiber filters (GF/F) with a pore size of 0.7 μm. I placed the filters in cryovials, fixed them with 1.5 mL of 90% acetone (V1) and stored them at -4 °C in a freezer until laboratory analysis. I conducted fluorometry, the standard method (Holm-Hansen et al., 1965) for accurately determining Chl *a* concentration. The fluorometer was previously calibrated with 90% acetone. I transferred 1.5 mL of extracted Chl *a* (V_1) from the cryovial into a cuvette and diluted it with acetone to 10 mL (V_2). After the first fluorometric reading of the excited Chl *a* ("R_b"), I added 2 to 3 drops of 37% HCl, homogenized the sample, and took the second reading ("R_a"). The value was corrected for significant fluorescence due to phaeopigments by acidification (Holm-Hansen et al., 1965). I estimated Chl *a* concentration [mg m^{-3}] in each sample using the following equation:

$$\text{Chl } a = (R_b - R_a) \times Fs \times (r / r - 1) \times V_1 \times d_f \quad [1]$$

where "R_b" is the sample fluorescence before acidification, "R_a" is the sample fluorescence after acidification, "Fs" is the calibration coefficient, "r" is the maximum acid ratio (R_b/R_a) of pure Chl *a* standard, "V_1" is the volume of extracted Chl *a* (1.5 mL) and "d_f" is the dilution coefficient (V_2/V_1).

3.4 Primary production experiments

3.4.1 Stations and concurrent measurements

I conducted *in situ* primary production measurements at the Lastovo and Korčula islands at stations M1, S0 and P4 in the summer months of 2022 and 2023, and measured NPP under

stratified conditions. A total of six experiments were conducted using the ^{14}C radioactive carbon incubation method (Nielsen, 1952), which is widely used for precise daily NPP measurements at a smaller time scale (minutes, hours, days) (Vandermeulen & Chaves, 2022). Experiment design is presented in **Table 2**.

Table 2. Experimental design of *in situ* ^{14}C primary production incubations at the Lastovo and Korčula islands, including experiment year, station, sampling period, incubation depths, incubation duration and measurements conducted concurrently with the primary production experiments.

					Concurrent measurements		
	Station	**Period**	**Depths**	**Incubation (h:min)**	**CTD**	**Nutrients**	**Chl *a***
2022	P4	8 June	0, 5, 10, 20, 30 and 50 m	6:05	x		x
	M1	7 June	0, 5, 10, 20, 30, 50 and 65 m	6:15	x		x
	S0	10 June	0, 5, 10, 20, 30, 50 and 65 m	7:30	x		x
2023	S0	4 July (S0-04)	0, 5, 10, 20, 30 and 65 m	5:53	x	x	x
		8 July (S0-08)	0, 5, 10, 20, 30 and 65 m	6:30	x	x	x
		16 July (S0-16)	0, 5, 10, 20, 30 and 65 m	6:41	x	x	x

I sampled incubation depths using a 5 L Niskin bottle. Concurrently, I collected Chl *a* samples from the same Niskin bottle prior to each incubation experiment, with additional nutrient sampling conducted in July 2023 (**Table 2**). CTD casts were performed before, during and after all incubation experiments, providing profiles of temperature, salinity, oxygen, density and Chl F (**Table 2**). I conducted *in situ* primary production experiments in four phases: (i) preparation of Winkler glass bottles (100 mL) for incubation, (ii) construction of a deployment system for the incubation bottles, (iii) *in situ* incubation and (iv) filtering incubated samples.

3.4.2 Preparing mooring system and samples

Incubations were done in light and dark Winkler glass bottles (100 mL). I prepared dark bottles using dark tape and waterproof black spray paint. I tied the net around all incubation bottles to secure them to the mooring system. To prevent contamination with trace metals, I cleaned the incubation bottles 12–24 h before each experiment. They were washed in non-ionic detergent, rinsed with distilled water, and then soaked in 10% HCl (1 M hydrochloric acid) solution for 24 hours; afterwards rinsed in tap water, then in distilled water, and dried at 60 °C.

The system for tracking bottles in the field was set up, including a tray with departments for each depth. The mooring system consisted of a buoy, a rope and an anchor. I marked the

incubation depths on the rope and sampled using a 5 L Niskin bottle. I obtained subsamples, filtered them through a 100 μm mesh (to remove zooplankton) and transferred them to 250 mL bottles, then to 100 mL Winkler incubation bottles. I incubated samples with a 2.4 mM aqueous solution of ^{14}C-labelled sodium bicarbonate ($NaH^{14}CO_3$) provided by DHI A/S, Lab Products, Denmark. I collected samples for Chl *a* and nutrient analysis from the same Niskin bottle. I firmly attached the incubation bottles to the rope using zip ties and the mooring system was deployed. The light bottle was always placed above the dark bottle in order to prevent shading.

3.4.3 Analysis of incubated samples

I filtered samples through 47 mm wide Advantec 0.2 μm pore-sized mixed cellulose ester filters using a hand vacuum pump. Filtration was done while on RV oid loss of ^{14}C due to respiration. I rinsed the filters with 100 μL of HCl (10%) to remove excess of inorganic carbon and stored them in vials. After a 24-hour drying period, I stored the samples in the dark at 4 °C. Filters were analyzed in a liquid scintillation counter at DHI A/S, Lab Products (Denmark) to determine ^{14}C activity based on disintegrations per minute (DPM).

3.5 Data analysis and visualization

I analyzed a total of 59 samples from the July 2021 field campaign (Matek et al., 2023) and 180 samples from the July 2022 campaign (Ljubešić et al., 2024); both datasets included plankton community composition and concurrent environmental variables (**Table 1**). Primary production, together with concurrent environmental variables, was analyzed using 37 samples collected during the June 2022 and July 2023 campaigns (**Table 1**). I performed data analysis and visualization across three water column categories: surface, thermocline and deep chlorophyll maximum (DCM) in 2021, or deep layer in 2022 and 2023. I categorized the 2021 data based on CTD-measured temperature and fluorometric Chl *a* values, as described by Matek et al. (2023), whereas data from 2022 and 2023 were categorized solely by CTD-measured temperature (Ljubešić et al., 2024). Additionally, I considered the occurrence of ITWs in analyses and visualizations of the 2022 and 2023 data (Ljubešić et al., 2024). I performed data visualization using Grapher 12 and R Studio, while statistical analyses was conducted in Primer 7.0. (Primer-E Ltd. 2021, Auckland, New Zealand) and R Studio. Modelling was performed in Wolfram Mathematica. Programming packages are specified by Matek et al. (2023) and Ljubešić et al. (2024).

3.5.1 Statistical analyses on in situ data

I conducted multivariate statistical analysis on a log-transformed dataset of biotic variables and a log-transformed, normalized and standardized dataset of abiotic variables. I calculated

resemblance matrices using Euclidean distance for transformed abiotic datasets and Manhattan distance (Bray-Curtis similarity) for transformed biotic datasets. The statistical methods applied included principal component analysis (PCA) and canonical correspondence analysis (CCA). To confirm the significance of the observed differences, I performed similarity tests on the same datasets using analysis of variance (ANOVA), post hoc Tukey HSD (Honest Significance Difference) analysis and analysis of similarities (ANOSIM). I used CCA to estimate the percentage of the plankton community variability explained by environmental factors. To improve CCA accuracy, I calculated variance inflation factors (VIFs) and removed highly correlated variables (VIF > 10). I tested the statistical significance of CCA axes using ANOVA. I described phytoplankton community diversity obtained by light microscopy using biodiversity indices and identified dominant taxa based on maximum abundances and frequency of appearance in samples. I set the significance level for all analyses at p-value < 0.05.

3.5.2 Calculating in situ primary production

Analysis of filters in the liquid scintillation counter resulted in DPM values for each incubated sample. I calculated *in situ* primary production rates based on DPM, specifically daily net primary production at depth $P_T(z)$ [mg C m^{-3}], normalized daily net primary production at depth $P^B_T(z)$ [mg C (mg Chl)$^{-1}$], daily depth-integrated primary production $P_{Z,T}$ [mg C m^{-2}] and daily normalized depth-integrated primary production $P^B_{Z,T}$ [mg C m^{-2}]. Primary production rates at 0 m on 4 July were not calculated due to a missing sample.

I calculated $P_T(z)$ [mg C m^{-3}] by applying the following equation:

$$P_T(z) = [(DPM_L - DPM_D) \times DIC \times K_1 \times K_2 \times K_3) / (DPM_{ST})] \times T \quad [2],$$

where DPM_L and DPM_D represent the ^{14}C radioactive activity in samples incubated in light and dark, respectively. DPM_{ST} is a standard DPM value in the $NaH^{14}CO_3$ solution (9320750 DPM). DIC (dissolved inorganic carbon) is an average concentration in coastal waters (27500 mg C m^{-3}). K_1 = 1.05 and K_2 = 1.06 are correction coefficients. K_1 accounts for the discrimination between ^{14}C and ^{12}C, as ^{14}C is taken up at a rate approximately 5% lower than ^{12}C. K_2 corrects for respiration of organic matter during incubation, with a correction factor of 1.06 to account for approximately 6% respiration loss. K_3 is the reciprocal of the incubation time (K_3 = 1/h: min), and T is the photosynthetic period (T = time of sunset - time of sunrise - 30 min (margin of error)).

I determined $P_{Z,T}$ using trapezoidal integration on vertical profiles of $P_T(z)$ and calculated $P^B_T(z)$ by dividing $P_T(z)$ by Chl *a*. I determined $P^B_{Z,T}$ by applying trapezoidal integration to $P^B_T(z)$ vertical profiles.

The variability of the physico-chemical properties in the incubated water column and the calculated $P_T(z)$ was analyzed using ANOVA and post-hoc Tukey HSD analysis across three factors: *Station*, *Layer* and *ITWs-no ITWs* for all experiments in July 2023. Only significant results (p-value < 0.05) are discussed in the results section. Percentage changes in primary production rates during and after the ITWs in July 2023 were calculated, excluding data at 0 m due to a missing value on 4 July.

3.5.3 Light model

PAR 5-hour interval time-series was measured at station S1 during 23 July–31 August 2022 at depths of 10 m and 40 m, and during 6–21 July 2023 at 10 m and 30 m depths. PAR time series was subsequently smoothed to a 1-hour interval using a moving average and fitted to the following equation to estimate *in situ* attenuation coefficient of PAR (K_{PAR} [m^{-1}]):

$$K_{PAR} = -(1/\Delta z) \times \ln(PAR_2/PAR_1) \quad [3]$$

where PAR_1 represents PAR measured at the shallower depth, PAR_2 represents PAR measured at the deeper depth, and Δz is the vertical distance between these measurements. I processed the K_{PAR} time series by removing outliers, estimating daily averages and interpolating data to 5-minute intervals.

To model surface irradiance (I_0), I used the equation:

$$I_0 = I_0^m \times \sin(\pi \times t/D) \quad [4]$$

where I_0^m [W m^{-2}] and D [h] are the monthly averages of surface irradiance at noon and daylength, respectively, obtained from The Croatian Meteorological and Hydrological Service (DHMZ) and t [h] represents a 24-hour cycle.

I developed a light model for the weeks when ITW episodes occurred during the summer: 31 July to 5 August 2022, 22 to 28 August 2022 and 7 to 19 July 2023. The model was fitted to the K_{PAR} and I_0.

$$I(z, t) = I_0 \times e\text{^}(-(K_{PAR}) \times \sim z) \quad [5]$$

where ~z [m] is a model depth vector. The thermocline was analyzed using temperature data [°C] from loggers, confirming that the 20 °C isotherm is a representative indicator. Depths of

this isotherm (z_i [m]) were calculated. Additionally, I calculated the average depth of the isotherm (z_{avg}). I fitted these depths to the model [5] to obtain I(z_i, t) and I(z_{avg}, t), and I compared the light behaviour between ITW and no-ITW periods by quantifying the difference between the two models.

No concurrent optical measurements were taken during *in situ* primary production experiments in June 2022 and July 2023. Therefore, I removed night-time values from *in situ* measured PAR, smoothed time-series to 1-hour interval by applying moving average and estimated K_{PAR} [3] that was fitted, together with $P_T(z)$ and Chl *a* profiles, to inverse model developed by Kovač et al. (2017)

3.5.4 Inverse model of primary production

Photosynthesis parameters, α_B and P^B_m, are used in photosynthesis irradiance functions that describe the response of primary production to light availability. Common practice is to estimate those parameters from *in vitro* primary production experiments. An inverse model was developed to estimate photosynthesis parameters from *in situ* primary production data (Kovač et al., 2016a, 2016b). In inverse modelling, a forward model of the production profile is tuned until the model data mismatch is minimal and optimal photosynthesis parameters are retrieved. To estimate distribution of optimal α_B and P^B_m values, the model requires data on *in situ* primary production profile that declines with depth, a biomass profile, surface irradiance at noon and attenuation coefficient. Thus, profiles of $P_T(z)$ and Chl *a*, I_0^m and K_{PAR} were applied to the model. However, due to the absence of simultaneous measurements of I_0^m and K_{PAR} during primary production experiments, this method was modified by implementing bootstrapping. For each set of measured profiles of $P_T(z)$ and Chl *a*, the estimation of the photosynthesis parameters was repeated 10 000 times, each with a different combination of I_0^m and K_{PAR}. This allowed us to overcome data limitations and estimate optimal α_B and P^B_m values for which the error between measured and modeled profiles is minimal.

3.5.5 Spatio-temporal analysis of satellite-derived primary production

To identify spatio-temporal patterns of NPP around the Lastovo Island during ITWs, I conducted a spatial autocorrelation analysis of experimental data from July 2023 and operational primary production products from Copernicus Marine Environment Monitoring Services (CMEMS). Specifically, I utilized a daily gap-free multi-sensor L4 Chl *a* product with 1-km spatial resolution (~Chl *a* [mg m^{-3}]) (Berthon & Zibordi, 2004, Volpe et al., 2018, 2019) and a daily 4-km resolution primary production reanalysis model (Salon et al., 2019, Feudale et al., 2023). I estimated depth-integrated primary production (~$P_{Z,T}$ [mg C m^{-2}]) using

trapezoidal integration and performed a Local Indicator of Spatial Association (LISA) analysis. I visualized only statistically significant results, using a significance threshold of z-scores between -1.96 and 1.96 and p-value < 0.05. Additionally, I overlaid log-scaled Chl *a* product on the Local Moran's I and quadrant classification maps. I also implemented ANOVA and post-hoc Tukey HSD test to assess the variance of both operational products in relation to ITW occurrences. Trapezoidal integration was applied to the Copernicus 4-km monthly primary production L4 product (Berthon & Zibordi, 2004, Volpe et al., 2018, 2019) to estimate annual primary production for 2021–2023. The Copernicus 4-km daily product was additionally used to integrate primary production over documented ITW periods at the Lastovo Island and to quantify their contribution to annual estimates.

4 RESULTS

4.1 Water column structure

Thermohaline stratification was primarily determined by temperature, with the 20 °C isotherm representing the thermocline (**Figure 4**). Oligotrophy of the Lastovo Island ecosystem was confirmed by low average nutrient concentrations, particularly nitrite and phosphate (**Table 3**). Among the measured nutrients, silicic acids exhibited the highest concentration in the water column, followed by nitrates (**Table 3**). Nutrient distribution displayed a heterogeneous vertical structure (**Figure 6**). Nitrite, nitrate and silicic acid reached the highest concentration in the deep layer, while the thermocline and surface layers showed the greatest variability and contained the most outliers (**Figure 6**). A DCM was observed, extending between the 40 and 80 m depths (**Figure 4**).

Table 3. Average (Avg), standard deviation (SD), maximum (Max), minimum (Min) and number of samples (N) for physico-chemical parameters measured during the 2021 and 2022 field experiment at station S1 at the Lastovo Island. Shown are values for temperature, salinity, phosphate (PO_4), nitrate (NO_3), nitrite (NO_2), silicic acid (SiO_4) and chlorophyll *a* (Chl *a*).

Parameters	Avg	SD	Min	Max	N
Temperature [°C]	19.66	3.57	15.19	26.79	236
Salinity [PSU]	38.94	1.66	38.46	39.76	236
NO_2 [µmol L^{-1}]	0.035	0.03	0.003	0.137	199
NO_3 [µmol L^{-1}]	0.576	0.94	0.052	10.248	239
PO_4 [µmol L^{-1}]	0.055	0.19	0.007	2.187	238
SiO_4 [µmol L^{-1}]	0.775	0.51	0.323	3.530	239
Chl *a* [mg m^{-3}]	0.317	0.36	0.010	1.960	233

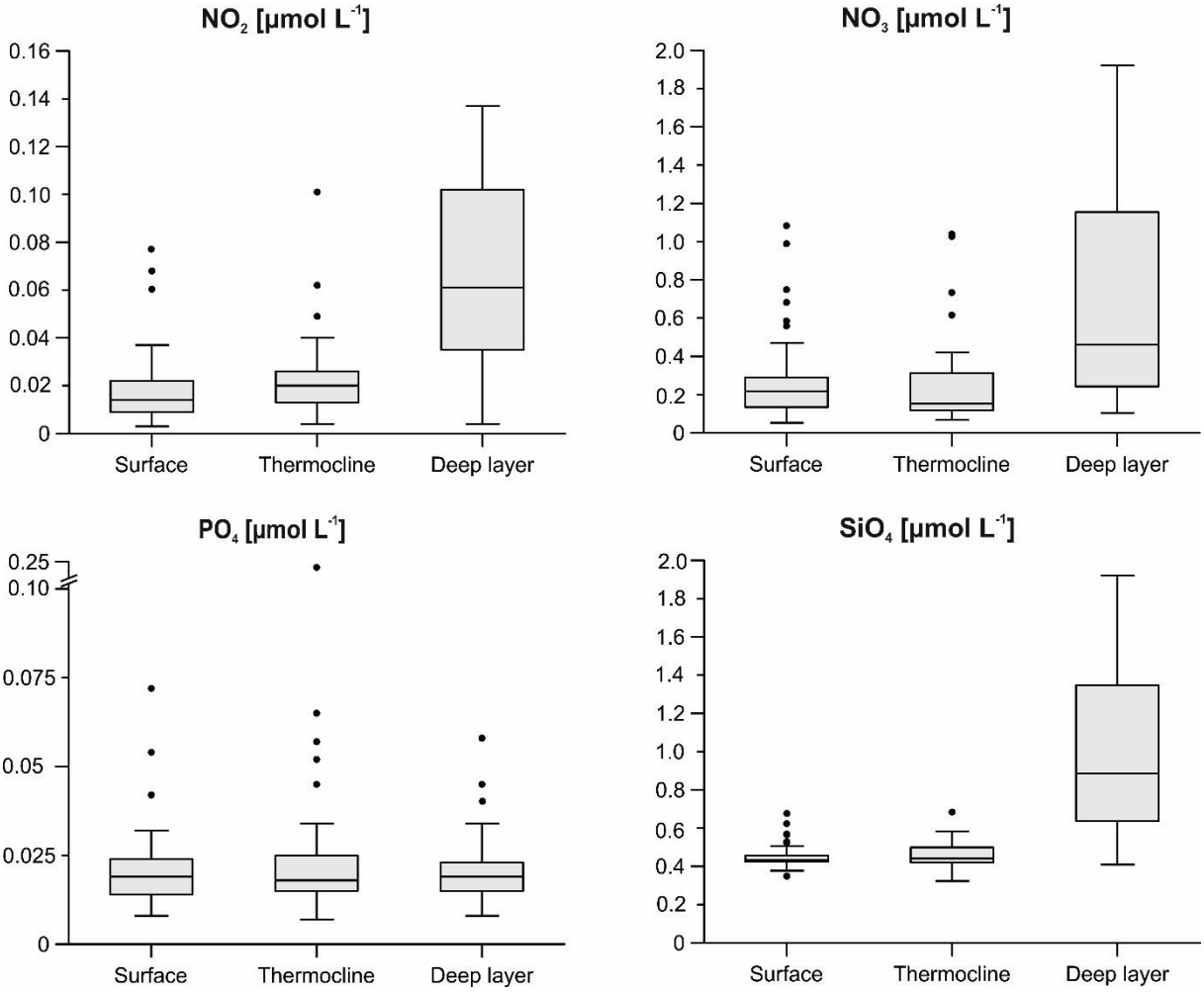

Figure 6. Distribution of nutrient data measured at station S1, Lastovo Island, during the field campaign in July 2022. Shown are the range, mean and outliers of nitrite (NO_2), nitrate (NO_3), phosphate (PO_4) and silicic acid (SiO_4) concentrations.

4.2 Plankton community composition in the stratified oligotrophic ecosystem

A total of 112 taxa were identified, comprising 64 diatoms, 33 dinoflagellates, 11 coccolithophores, and 4 other autotrophs, including cryptophyta, chlorophyceae, chrysophyceae, and *Dictyocha fibula* (**Supplement 1**). Diatoms dominated the microphytoplankton community (84.49%), but were rarely present in the nanophytoplankton (0.06%) (**Figure 7**). In contrast, dinoflagellates dominated the nanophytoplankton (50.59%) and were less abundant in microphytoplankton (9.61%) (**Figure 7**). Coccolitophores were more abundant in the nanophytopankton (24.73%) than in microphytoplankton (5.60%). Other groups contributing to nanophytoplankton were cryptophyta (15.00%), chlorophyceae (9.14%) and chyrosphyceae (0.48%) (**Figure 7**).

Picophytoplankton consisted mainly of *Prochlorococcus* sp. (50.33%) and *Synechococcus* sp. (45.81%), while photosynthetic picoeukaryotes (PPEs) were the least abundant (3.86%) (**Figure 7**). Picoplankton also included heterotrophic bacteria, with an average abundance of 451472 cells mL^{-1} (**Supplement 2**). Overall, picophytoplankton was the most abundant group in the water column, followed by nano- and microphytoplankton (**Supplement 2**).

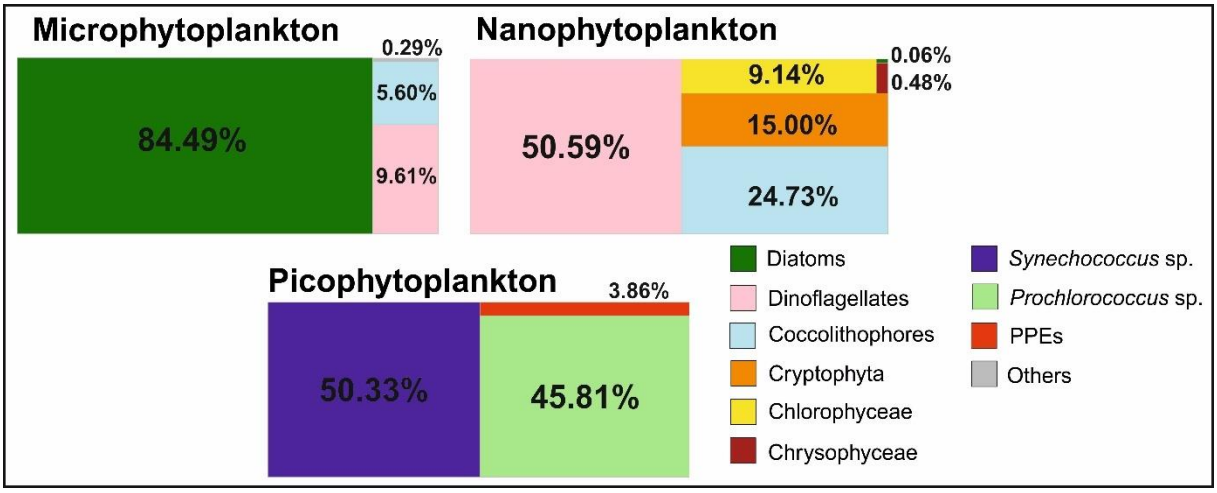

Figure 7. Phytoplankton taxonomic composition at station S1, the Lastovo Island, determined during the July field campaigns in 2021 and 2022. Abbreviations: PPEs (photosynthetic picoeukaryotes).

Dominant taxa/groups at the station S1 were defined as species or groups with maximum abundance greater than 500 cells L^{-1} and a frequency of appearance in samples exceeding 40% in the total samples (N = 156) (**Table 4**). The most abundant group was the nano-fraction dinoflagellates, with a maximum abundance of 23430 cells L^{-1}, appearing in 82.69% of the total samples (**Table 4**). The following were micro-fraction pennate diatoms (78.21%) and micro-fraction coccolithophores (55.13%) (**Table 4**). The most dominant species was *Proboscia alata*, with a maximum abundance of 1325 cells L^{-1} and occurring in 69.23% of the total samples, followed by *Rhizosolenia imbricata*, *Pseudo-nitzschia delicatissima*, *Gyrodinium fusiforme* and *Scripsiella* sp. (**Table 4**).

4.3 Plankton community variability in relation to the environment

4.3.1 Nutrient and Chl a temporal and spatial variability

Temporal variability in nutrient concentrations measured during July 2022 throughout the water column (**Figure 8**) corresponds to fluctuations in the thermocline and surface layers, as indicated by outliers in the distribution of nutrient values (**Figure 6**). Notably, the se outliers were recorded during ITW periods (**Figure 8**). However, no statistically significant variability

in nutrient concentrations was detected in relation to ITWs, as confirmed by the two-way crossed ANOSIM test (**Table 5**). Furthermore, Chl *a* values did not show significant changes in response to ITWs (**Table 5**). In contrast, vertical nutrient distribution was significant, with pronounced dissimilarity in nutrient concentrations between the deep layer and the surface and thermocline layers (**Table 5**).

Table 4. Phytoplankton dominant taxa/groups at station S1, Lastovo Island. Dominance was determined based on frequency of occurrence exceeding 40% in samples (N = 156) and a maximum abundance greater than 500 cells L^{-1}.

Dominant taxa/groups	**Max [cells L^{-1}]**	**Fr[%]**
N.D. dinoflagellates (<20 μm)	23430	82.69
N.D. penatae (micro)	2650	78.21
***Proboscia alata* (Brightwell) Sundström**	1325	69.23
N.D. coccolithophorids (micro)	12770	55.13
***Rhizosolenia imbricata* Brightwell**	755	47.44
***Pseudo-nitzschia delicatissima* (Cleve) Heiden**	14060	46.15
***Gyrodinium fusiforme* Kofoid & Swezy**	570	45.51
***Scripsiella* sp.**	760	42.95

Table 5. Two-way crossed ANOSIM (for factors *Layer* and *ITWs-no ITWs*) of micro- (> 20 μm) and nanophytoplankton (2–20 μm) microscopy counts [cells L^{-1}], picoplankton (< 2 μm) flow cytometry counts [cells mL^{-1}], and nutrient concentrations [μmol L^{-1}] measured at station S1, Lastovo Island. Shown are R values (R = 0; similarity, R = 1; disimilarity, threshold R > 0.5). Level of significance: p-value < 0.05. **Significant R values are bolded**. Abbreviations: PICO (picoplankton), NANO (nanophytoplankton), MICRO (microphytoplankton), Chl *a* (chlorophyll *a*).

	PICO	NANO	MICRO	Nutrients	Chl *a*
ITWs-no ITWs	**0.08** (p = 0.020)	**0.11** (p = 0.003)	**0.05** (p = 0.040)	0 (p = 0.400)	0.06 (p = 0.981)
Surface-Thermocline	**0.77** (p =0.001)	0.03 (p = 0.080)	0.03 (p = 0.080)	0.04 (p = 0.060)	**0.08** (p = 0.003)
Thermocline-Deep layer	**0.52** (p = 0.001)	0 (p = 0.400)	0 (p = 0.300)	**0.25** (p = 0.001)	0 (p = 0.527)
Surface-Deep layer	**0.97** (p = 0.001)	0 (p = 0.300)	**0.03** (p = 0.040)	**0.36** (p = 0.001)	**0.11** (p = 0.001)

.

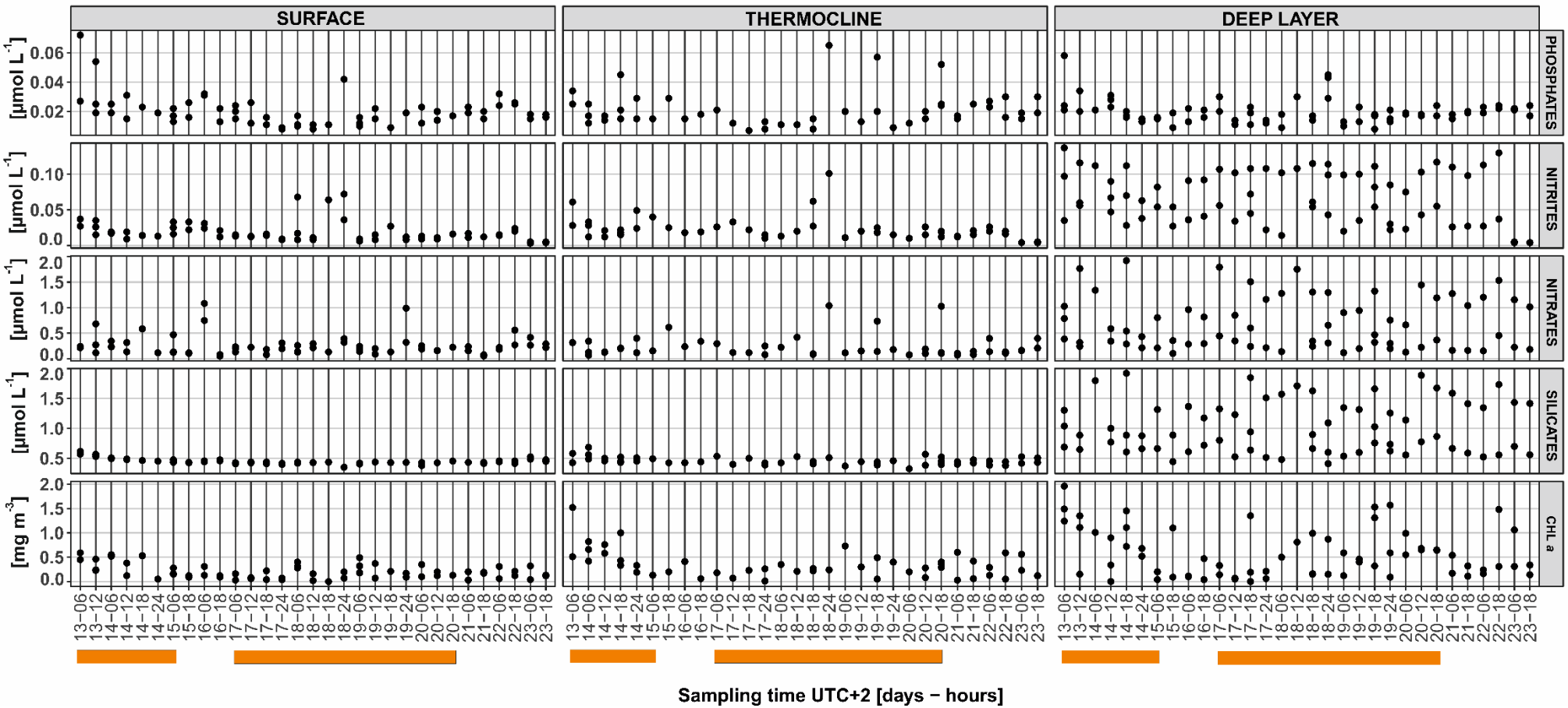

Figure 8. Temporal variations in concentrations of phosphate (PO_4), nitrate (NO_3), nitrite (NO_2), silicic acid (SiO_4) [µmol L^{-1}] and Chl *a* [mg m^{-3}] measured at station S1, Lastovo Island, during the field campaign in July 2022. ITW events are highlighted by orange squares.

4.3.2 Phytoplankton and bacterioplankton succession

Nanophytoplankton consistently exhibited higher abundances [cells L^{-1}] than microphytoplankton (**Figure 9**), with greater average values (**Supplement 2**). Temporal variability did not reveal strong shifts during ITWs in July 2022, except for an increase in heterotrophic bacterial abundances in the thermocline layer and changes in picoplankton composition in the deep layer (**Figure 9**). Specifically, *Prochlorococcus* was more dominant in the deep layer, whereas *Synechococcus* was more abundant in the surface and thermocline layers (**Figure 9**). Overall, *Synechococcus* had higher average abundances than *Prochlorococcus*, while PPEs were the least abundant among picoplankton (**Supplement 2**).

Heterotrophic bacteria exhibited an average abundance of 451472 cells mL^{-1}, with the highest activity observed in the thermocline layer (**Figure 9**). These distribution patterns were further tested using a two-way crossed ANOSIM (**Table 5**), with only significant results ($p < 0.05$) discussed. While plankton community abundances did not vary in relation to ITW occurrence (**Table 5**), vertical structuring of picoplankton was evident, particularly in the dissimilarity between surface and thermocline layers compared to the deep layer (**Table 5**).

The vertical distribution of nutrients and Chl *a* in the stratified water column at station S1 during the field campaign in July 2022 was further confirmed by CCA (**Figure 10A, B**). The surface and thermocline layers were characterized by higher temperature values and increased phosphate concentrations, whereas the DCM/deep layer exhibited high values of Chl *a* along with enhanced nitrite, nitrate and silicic acid concentrations (**Figure 10A, B**).

Environmental variables explained a total of 19.43% ($p = 0.005$) and 11.70% ($p = 0.002$) of the variability in the micro- and nanophytoplankton community during 2021 and 2022, respectively (**Figure 10A, B**). In contrast, the variability in the picoplankton community was more strongly constrained by environmental factors, with 44.82% ($p = 0.001$) and 88.92% ($p = 0.001$) of the variation explained in 2021 and 2022, respectively (**Figure 10A, B**). These results suggest that picoplankton exhibited a stronger response to environmental conditions compared to nano- and microphytoplankton.

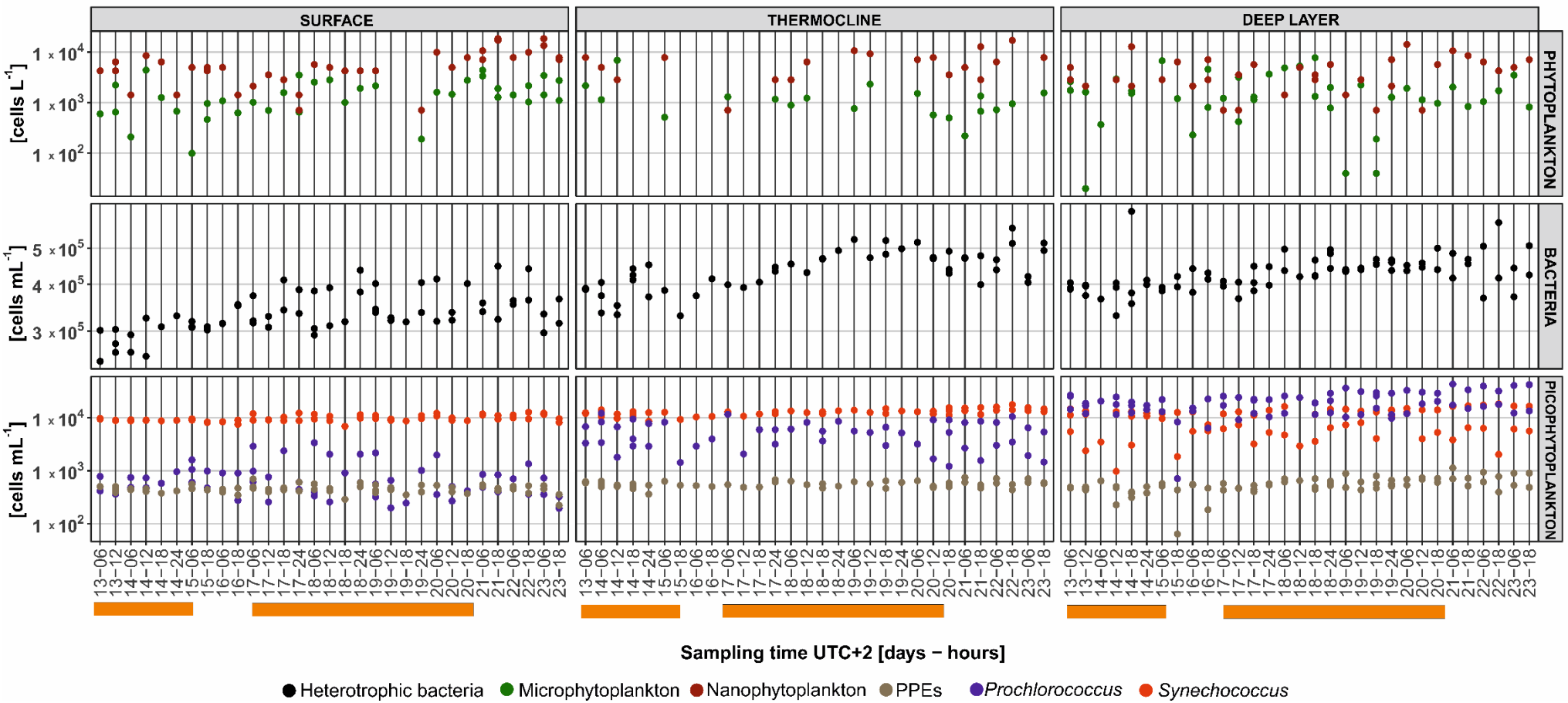

Figure 9. Temporal variations in the abundances of phytoplankton [cells L^{-1}] and picoplankton [cells mL^{-1}] community observed at station S1, Lastovo Island, during the field campaign in July 2022. Plankton groups are indicated by different symbols. ITWs events are highlighted by orange squares.

ANOVA confirmed significant clustering of nano- and microphytoplankton along CCA1 ($p = 0.013$ and $p = 0.011$ in 2021 and 2022, respectively) based on the *Layer* factor (**Figure 10A, B**), further supporting the vertical distribution of these groups (**Figure 9**). Microphytoplankton tended to cluster toward higher concentrations of Chl *a*, nitrite, nitrate and slicic acid in the DCM/deep layer, while nanophytoplankton were associated with higher temperature values and increased phosphate concentrations in the surface and thermocline layers (**Figure 10A, B**).

Similarly, the vertical distribution of picoplankton (**Figure 9**) was confirmed by ANOVA, showing significant clustering across CCA1 ($p = 0.001$ in both 2021 and 2022) (**Figure 10A, B**). *Synechococcus*, heterotrophic bacteria and PPEs clustered toward higher temperatures and phosphate levels in the surface and thermocline layers, while *Prochlorococcus* was associated with increased Chl *a* concentration in the DCM/deep layer (**Figure 10A, B**). CCA scores and egienvalues are provided in the supplementary material (**Supplement 3**).

4.4 Primary production in the stratified ecosystem off the Lastovo and Korčula islands

4.4.1 Physico-chemical dynamics of the incubated water column

During the primary production experiments conducted in June 2022 and July 2023, DCM ranged from 50 to 70 m, while thermocline depths oscillated between the 5 and 30 m depths (**Figure 11**, **Supplement 4**). The lowest oxygen values were recorded in the surface layer (**Figure 11**, **Supplement 4**). Oxygen concentrations varied from 6 to 10 mg L^{-1}, while Chl F ranged between -0.2 and 8 mg m^{-3}, with DCM values from 0.6 to 0.8 mg m^{-3} (**Figure 11**, **Supplement 4**).

On 8 July 2023, during ITWs (S0-08), thermocline oscillations were more pronounced (**Figure 11B**) compared to no-ITW periods (**Figure 11A, C, Supplement 4**). In the morning (before incubation), the thermocline was deeper, whereas in the afternoon (after incubation), it became shallower (**Figure 11B**). Additionally, during S0-08, maximum oxygen concentrations decreased from 8 mg L^{-1} in the morning to 6 mg L^{-1} in the afternoon (**Figure 11B**).

Nutrient concentrations, analyzed prior to incubations in July 2023, confirmed phosphate as the limiting factor for NPP (**Figure 11**). Silicic acid concentrations remained stable throughout the investigation period, whereas nitrate concentrations showed the greatest variability (**Figure 11**). During S0-08, nitrate concentrations increased in the thermocline layer at 20 and 30 m (**Figure 11B**). After ITWs, during S0-16, nitrate concentrations declined at those depths, while a peak at 10 m was observed (**Figure 11C**).

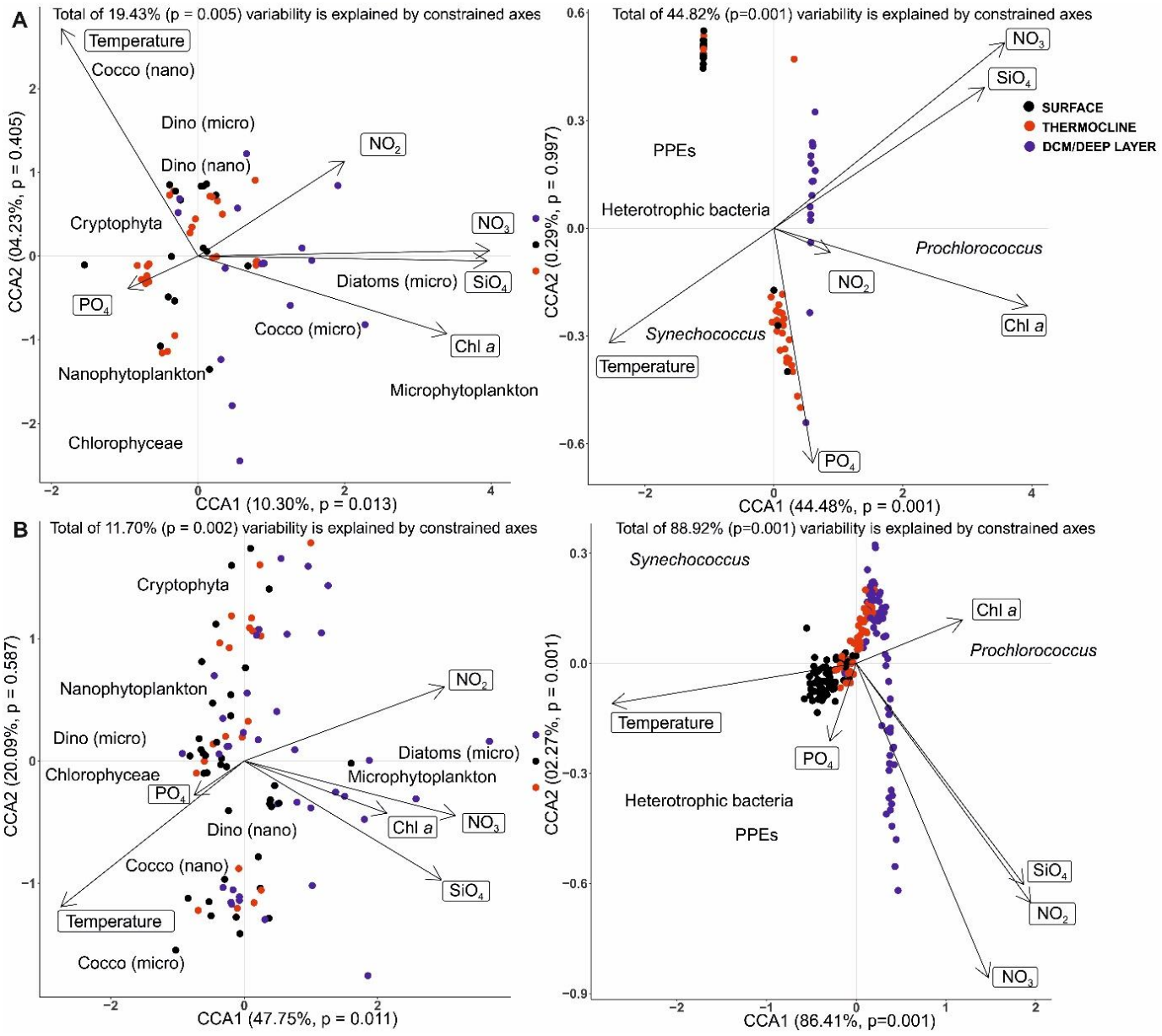

Figure 10. Canonical correspondence analysis (CCA) of constrained environmental variables and the plankton community at station S1, Lastovo Island, in **(A) July 2021** and **(B) July 2022**. Environmental variables included in the analysis are temperature, phosphate (PO_4), nitrate (NO_3), nitrite (NO_2), silicic acid (SiO_4) and chlorophyll *a* (Chl *a*). The plankton community is represented by micro- and nanophytoplankton groups, cyanobacteria, heterotrophic bacteria and PPEs. Symbols represent sample-weighted scores (weighted averages of species) (N = 180 in 2022, N = 59 in 2021) and are colored by the factor *Layer* (surface, thermocline and DCM or deep layer, in 2021 and 2022, respectively). Superimposed vectors (arrows) represent biplot scores of environmental variables. Abbreviations: Dino (dinoflagellates), Cocco (coccolithophores), PPEs (photosynthetic picoeukaryotes)

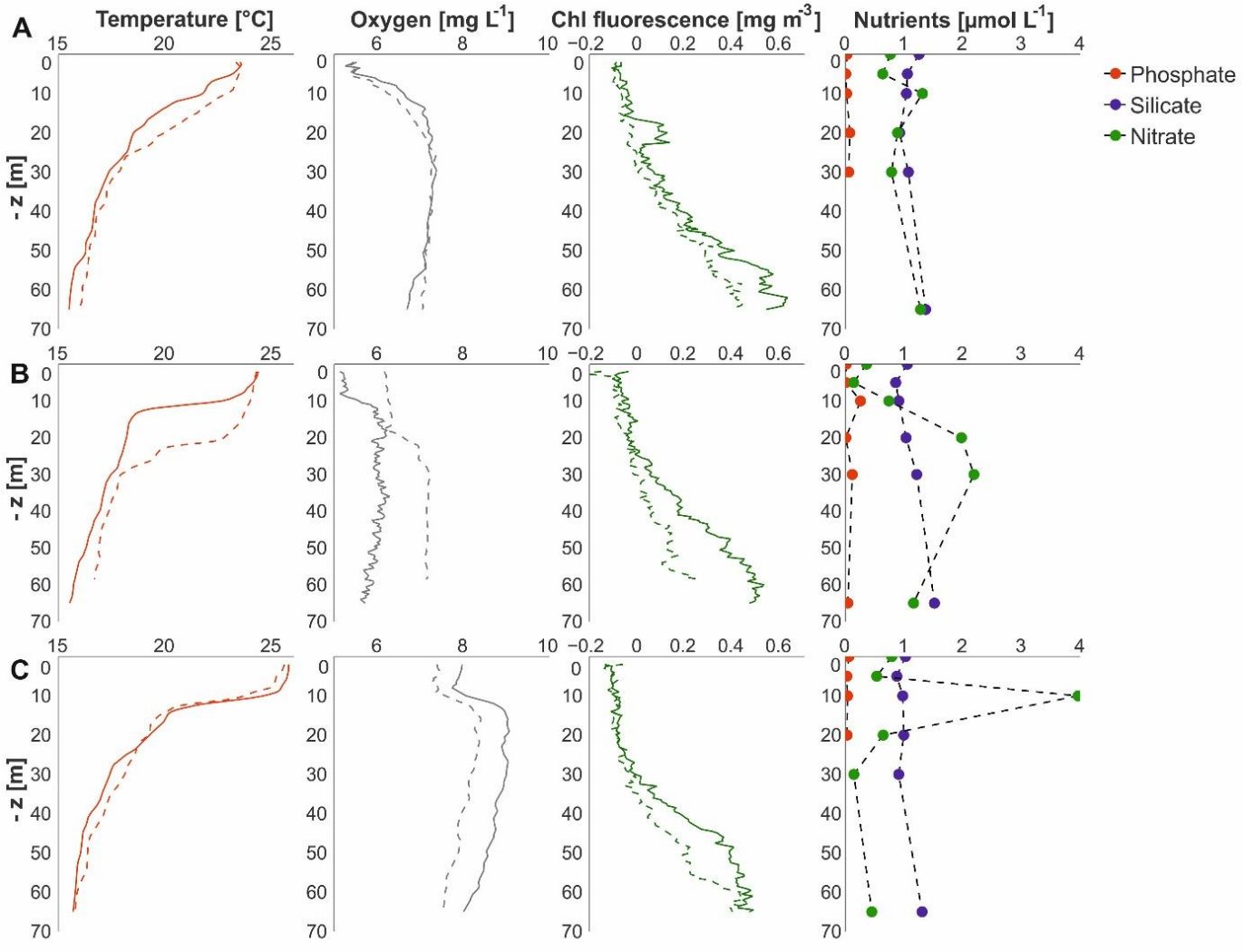

Figure 11. Physico-chemical parameters of the incubated water column in July 2023 before (dashed line) and after (solid line) *in situ* ^{14}C primary production experiments at the station S0, Lastovo Island: **(A)** 4 July (S0-04), **(B)** 8 July (S0-08) and **(C)** 16 July (S0-16). Shown are vertical profiles of temperature [°C], oxygen [mg L^{-1}] and Chl F [mg m^{-3}] measured using CTD and discrete measurements of nutrient concentrations [µmol L^{-1}].

4.4.2 Net primary production at depth and water column production

All experiments indicated the highest photosynthetic activity within the upper 10 m, as shown by $P^B_T(z)$ (**Figure 12A, B**). Chl *a* concentrations ranged from 0 to 1.2 mg m^{-3} in July 2022 (**Figure 12A**) and from 0 to 2 mg m^{-3} in July 2023 (**Figure 12B**). DCM was observed at 50 m at M1 and P4, and at 65 m at S0 during all experiments, except for S0-04, where the highest Chl *a* values occurred at 20 m and no distinct DCM was observed (**Figure 12A, B**).

Compared to June 2022 (**Figure 12A**), NPP at the Lastovo Island in July 2023 exhibited greater variability, particularly during the S0-08 experiment, when ITWs occurred (**Figure 12B**).

During this period, $P_T(z)$ peaked in the thermocline at 20 m and subsequently declined after ITWs (S0-16), as reflected in the twofold decrease in $P_{Z,T}$ values (**Figure 12B**).

The ecosystem off the Korčula Island (station P4) was less productive than that off the Lastovo Island, as indicated by $P_{Z,T}$ values nearly twice as high (**Figure 12A, B**). Only the $P_{Z,T}$ value recorded during S0-16 was comparable to that measured at Korčula Island (**Figure 12A, B**), further confirming the considerable decrease in primary production at the Lastovo Island following ITW occurrence.

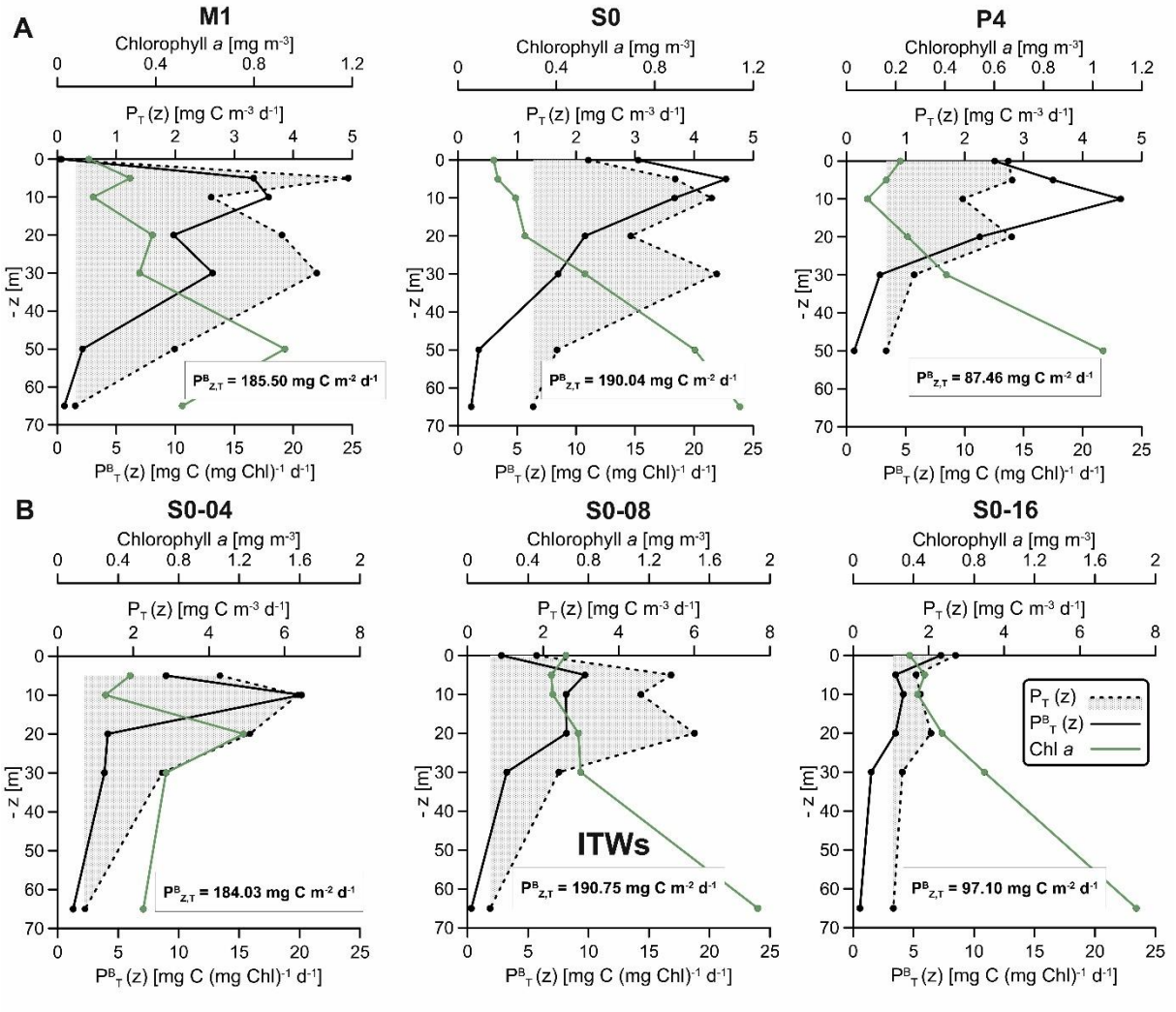

Figure 12. *In situ* ^{14}C primary production experiments at the Lastovo Island with concurrent Chl *a* measurements in **(A)** June 2022 at stations M1, S0 and P4, and **(B)** July 2023 at station S0 on 4, 8 and 16 July (S0-04, S0-08 and S0-16, respectively). Shown are vertical profiles of daily net primary production ($P_T(z)$) and daily normalized net primary production ($P^B_T(z)$). The shaded area beneath $P_T(z)$ represents daily depth-integrated primary production ($P_{Z,T}$).

4.5 ITW-mediated mechanisms affecting NPP in a stratified ecosystem

4.5.1 Nutrient influx in relation to ITWs

Statistical analysis confirmed that nutrient concentrations were not significantly different across ITWs (**Table 5**). However, vertical nutrient profiles measured prior to incubations in July 2023 reveal nitrate response to ITWs in the thermocline layer (**Figure 11**). Although NPP measurements were not conducted in that period, a high-resolution time series of nutrient concentrations was obtained during the July 2022 field experiments (**Figure 8**). When correlated with temperature, distinct patterns emerged based on the water column layers and the presence of ITWs (**Figure 13**). Firstly, the surface, thermocline and deep layers were clearly distinguishable (**Figure 13**). Secondly, while silicic acid remained stable, other nutrients showed variability, with peak values in the surface layer and, notably, in the thermocline layer during ITWs (**Figure 13**). These findings suggest that ITWs may enhance NPP by facilitating nutrient transport from deeper to surface layers.

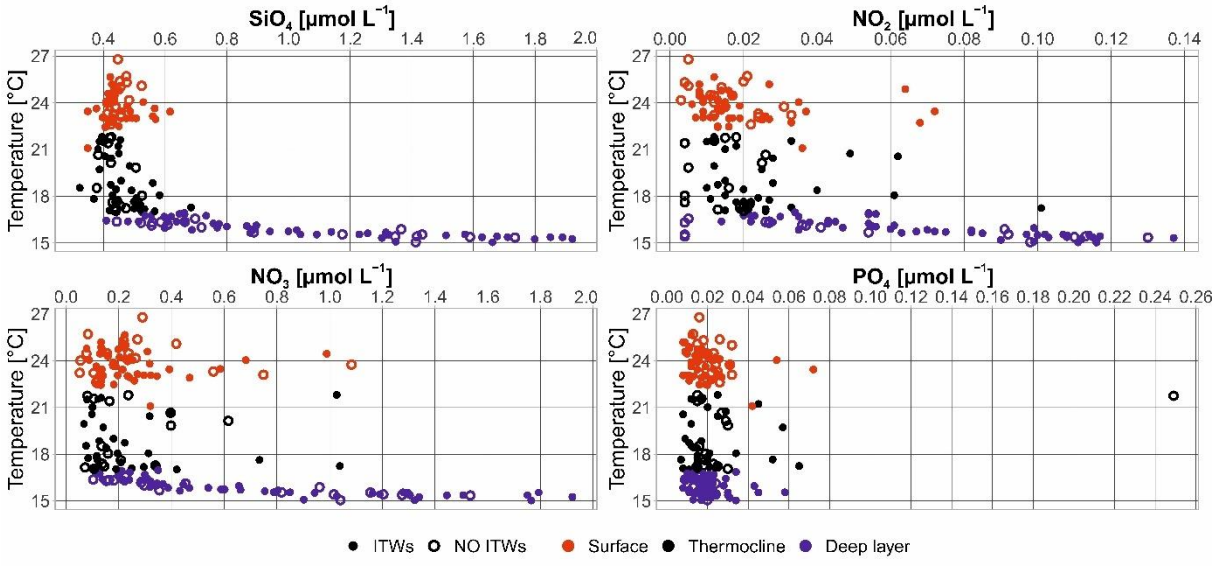

Figure 13. Correlation between nutrient (silicic acid (SiO_4), nitrite (NO_2), nitrate (NO_3) and phosphate (PO_4)) concentrations [µmol L^{-1}] and temperature [°C] measured at station S1, Lastovo Island, during the July 2022 field campaign. Water layers are represented by color and ITW occurrence by symbols.

4.5.2 Dynamics of light properties in response to ITWs

PAR was measured at the station S1 from 23 July to 31 August 2022, and ranged between 1.74 and 505.6 µmol m^{-2} s^{-1} at 10 m (**Supplement 5A**), with the mean value of 169.23 ± 151.29 6 µmol m^{-2} s^{-1}. At 40 m, PAR ranged from 0.43 to 53.9 µmol m^{-2} s^{-1} (**Supplement 5A**), with the mean value of 8.75 ± 10.22 µmol m^{-2} s^{-1}. Estimated K_{PAR} values [3] varied between 0.03 m^{-1} and 0.12 m^{-1} (**Supplement 5A**), with the mean value of 0.1 ± 0.02 m^{-1}. For the period from 6

July to 21 July 2023, PAR values spanned from 3.10 to 642.65 μmol m^{-2} s^{-1} at 10 m (**Supplement 5B**), with the mean value of 319.56 ± 200.92 μmol m^{-2} s^{-1}. At 30 m, PAR ranged from 2.35 to 156.52 μmol m^{-2} s^{-1} (**Supplement 5B**), with the mean value of 73.75 ± 50.68 μmol m^{-2} s^{-1}. K_{PAR} ranged from 0.04 m^{-1} to 0.11 m^{-1} (**Supplement 5B**), with the mean value of 0.08 ± 0.01 m^{-1}.

These *in situ* light measurements were fitted to the light model I(z, t) [W m^{-2}] [5] to examine light dynamics during ITWs. Because the thermocline layer was of primary interest, the 20 °C isotherm depths, used as a proxy for the thermocline, were superimposed on the model output (**Figure 14**). During the most intense ITW episodes, thermocline oscillations ranged approximately from the 5 to 25 m depths (**Figure 14**), whereas a weaker ITW event in late July 2023 produced oscillations between the 10 and 20 m depths (**Figure 14D**). The light model confirmed that thermocline oscillations generated by ITWs can bring this layer into the shallower parts of the water column, particularly in the afternoon at station S1 (**Figure 14**). This pattern is consistent across both summers examined (**Figure 14**).

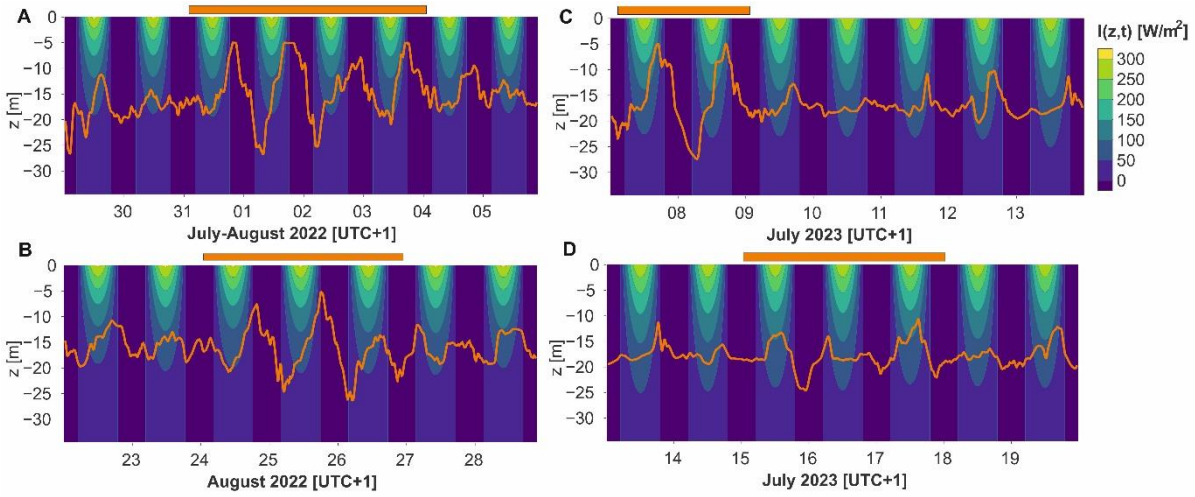

Figure 14. Light model (I(z, t) [W m^{-2}]) with thermocline isotherm depths (red line) for the southern cliff Struga (station S1) at the Lastovo Island during **(A)** 31 July–5 August, **(B)** 22–28 August 2022, **(C)** 7–13 July 2023 and **(D)** 13–19 July 2023. ITW events are indicated by the orange line at the top.

To quantify the extent of excess light available to phytoplankton during ITW events, I modeled light at the 20 °C isotherm depth (representing the thermocline) and at the average isotherm depth, reflecting a no-ITW scenario (**Figure 15**). Light levels at the average isotherm depth did not exceed approximately 90 W m^{-2} (**Figure 15**), indicating nearly twice as low the light availability compared to the surface (**Figure 14**). In contrast, light peaks in the thermocline layer during ITWs suggest enhanced light availability, with irradiance reaching up to 150 W m^{-}

^{2} at solar noon (**Figure 15**). This is far lower than the light intensity at the surface, which is more than double at solar noon (**Figure 14**).

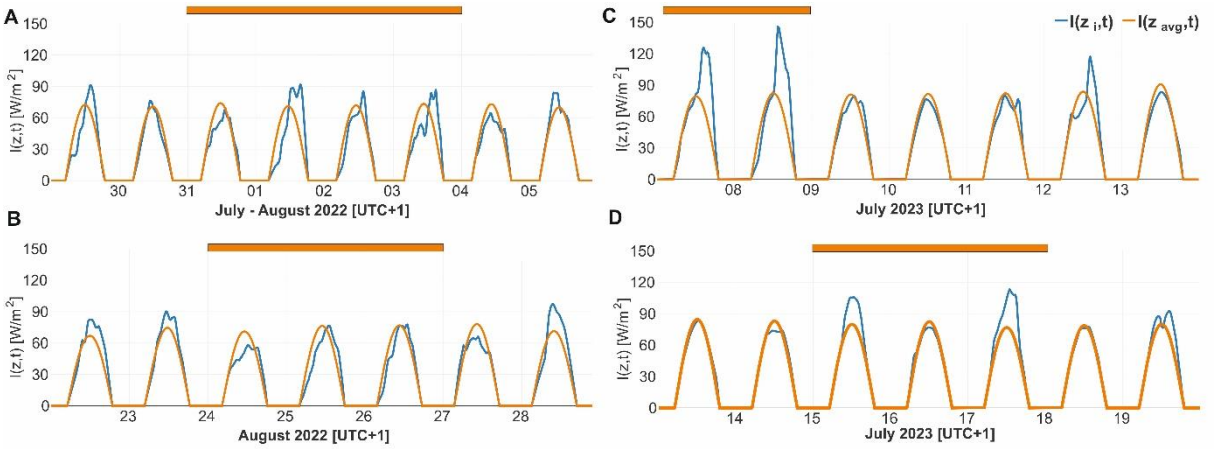

Figure 15. Light model [W m^{-2}] applied to thermocline isotherm depths, (I(z_i, t) [W m^{-2}]), and average thermocline isotherm depth, (I(z_{avg}, t) [W m^{-2}]), for the southern cliff Struga (station S1) at the Lastovo Island during **(A)** 31 July–5 August, **(B)** 22–28 August 2022, **(C)** 7–13 July 2023 and **(D)** 13–19 July 2023. ITW events are indicated by the orange line at the top.

Assuming that the average isotherm depth represents no-ITW conditions with no diurnal thermocline oscillations, it is evident that ITWs exposed the thermocline layer to substantially higher light levels. The strongest increases occurred in early August 2022, when light intensities rose by up to 60 W m^{-2} (**Figure 16A**), and in early July 2023, when increases reached 70 W m^{-2} (**Figure 16C**). Peaks approaching approximately 50 W m^{-2} were also observed during ITWs in early August 2022 (**Figure 16A**) and late July 2023 (**Figure 16D**). In contrast, ITWs observed in late August 2022 produced a more modest increase of up to approximately 20 W m^{-2} (**Figure 16B**), although this may still be ecologically relevant. These results suggest that ITWs can influence the plankton community by vertically displacing water masses toward the surface, thereby increasing their light exposure and enhancing photosynthetic activity.

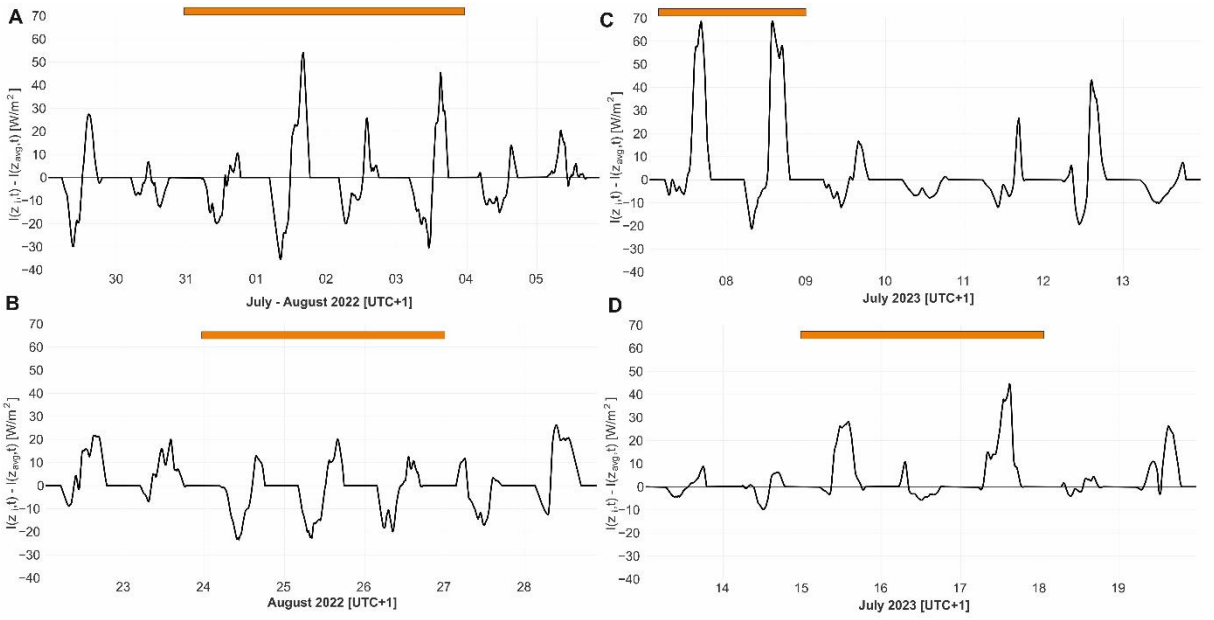

Figure 16. Difference between modeled light at the thermocline isotherm depths ($I(z_i, t)$ [W m^{-2}]) and at the average thermocline depth ($I(z_{avg}, t)$ [W m^{-2}]) for the southern cliff Struga (station S1) during **(A)** 31 July–5 August, **(B)** 22–28 August 2022, **(C)** 7–13 July 2023 and **(D)** 13–19 July 2023. ITW events are indicated by the orange line at the top.

4.6 NPP variability related to ITWs

4.6.1 Ship-based measurements

Oxygen concentrations varied with ITW occurrence, particularly during S0-16 experiment (**Table 6**). Nutrients did not exhibit significant variability, except silicic acid, with significantly different concentrations in the deep layer compared to the surface and thermocline layers (**Table 6**). $P_T(z)$, Chl *a* and temperature contributed to the heterogeneous vertical structure of the water column. Specifically, temperature varied across all layers, while Chl *a* concentrations were significantly different in the deep layer compared to the surface and thermocline layers. $P_T(z)$ varied between the thermocline and deep layers, however did not exhibit significant variability in relation to ITWs (**Table 6**).

Table 6. ANOVA and post-hoc Tukey HSD applied to the 2023 *in situ* daily net primary production at depth ($P_T(z)$) and environmental data across three factors: *Station*, *Layer* and *ITWs-no ITWs*. ANOVA results are shown as „analyzed variable, p-value“, while results of the Post-hoc Tukey HSD test are shown as „tested factor, p-value“ for each variable. Only significant results are shown (significance level p-value < 0.05).

	Station	***Layer***	***ITWs-no ITWs***
ANOVA	**Oxygen**, 0.0002	**$P_T(z)$**, 0.05 **Chl *a***, 0.005 **Temperature**, 6.5×10^{-6} **Silicic acid**, 7.3×10^{-5}	**Oxygen**, 0.008
Post-hoc Tukey HSD	**Oxygen** S0-16; S0-04, 0.005 S0-16; S0-08, 0.0002	**$P_T(z)$** Deep layer-Thermocline, 0.04 **Chl *a*** Deep layer-Surface, 0.004 Deep layer-Thermocline, 0.02 **Temperature** Thermocline-Surface, 0.0002 Deep layer-Surface, 0 Deep layer-Thermocline, 0.009 **Silicic acid** Deep layer-Surface, 0.00009 Deep layer-Thermocline, 0.0002	**Oxygen** ITWs-no ITWs, 0.008

PCA was performed on all six *in situ* experiments, incorporating concurrent measurements of temperature, Chl *a* and oxygen. Along PC2, a distinct cluster of station S0 during ITWs was observed, accounting for 27.95% of the dataset's variability (**Figure 17A**). Specifically, S0-08 grouped towards higher Chl *a* and $P_T(z)$ values (**Figure 17B**). PC1 exhibited three distrinct clusters across water column layers that explained 45.10% of the variability in the dataset, further highlighting the heterogeneous vertical structure of the stratified water column (**Figure 17A, B**). PCA scores for PC1 and PC2, along with the eigenvalues, are provided in the supplementary materials (**Supplement 6**).

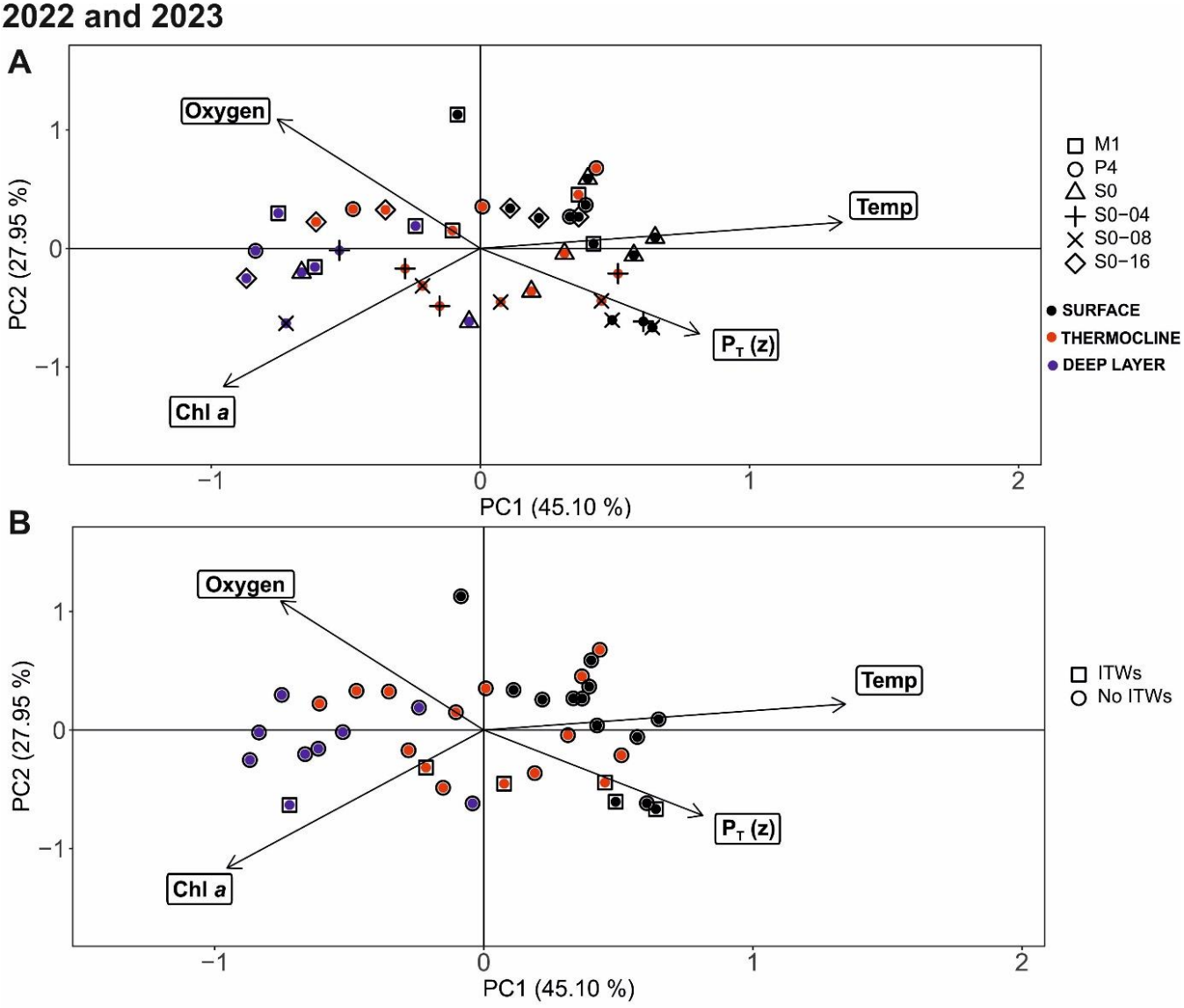

Figure 17. Principal component analysis (PCA) of *in situ* daily net primary production at depth ($P_T(z)$ [mg C m^{-3}]) and concurrent environmental variables measured in June 2022 and July 2023. Ordinations are shown for **(A)** *Station* (symbols) and *Layer* (color), and **(B)** *ITWs-no ITWs* (squares) and *Layer* (color). Each point represents the weighted average scores of a sample (N = 37). Variables were fitted to the ordination as vectors (arrows): temperature (Temp [°C]), oxygen [mg L^{-1}], chlorophyll *a* (Chl *a* [mg m^{-3}]) and $P_T(z)$. The percentage of variability explained by each axis is indicated in the axis title

.

Table 7. Percentage change in primary production rates during and after the ITWs in July 2023 calculated for: daily net primary production at depth ($P_T(z)$ [mg C m^{-3}]), daily normalized net primary production at depth ($P^B_T(z)$ [mg C (mg Chl)$^{-1}$]), daily depth-integrated primary production ($P_{Z,T}$ [mg C m^{-2}]) and daily normalized depth-integrated primary production ($P^B_{Z,T}$ [mg C m^{-2}]). Data at 0 m were excluded due to a missing value on 4 July. Increases in primary production rates at the corresponding depths are indicated in red.

Variable	z [m]	During ITWs [%]	After ITWs [%]
$\mathbf{P^B_{Z,T}}$	integrated	-14.62	-47.27
$\mathbf{P_{Z,T}}$	integrated	3.65	-49.09
$\mathbf{P^B_T(z)}$	0	/	/
	5	8.21	-63.68
	10	-59.61	-48.83
	20	97.90	-57.17
	30	-16.12	-53.54
	65	-75.63	83.61
$\mathbf{P_T(z)}$	0	/	/
	5	25.44	-69.02
	10	-27.92	-61.19
	20	18.12	-65.66
	30	-12.43	-46.09
	65	-17.38	79.21

Percentage change = $(Exp_i - Exp_{i-1})/Exp_{i-1} \times 100$

4.6.2 Inverse model: photosynthesis parameters

The vertical profiles of $P_T(z)$ decreased with depth (**Figure 12**), supporting a key condition for applying the inverse model. Optimal pairs of photosynthesis parameters (α^B, P^B_m) were retrieved through optimization between modeled daily net primary production profile (~$P_T(z)$ [mg C m^{-3}]) and $P_T(z)$ (**Supplement 7**, **Supplement 8**). The distributions of minimal error between ~$P_T(z)$ and $P_T(z)$ elucidate the inverse model accuracy in estimating *in situ* observations (**Supplement 9**).

This was further confirmed by comparing mean ~$P_T(z)$ profiles, computed using mean K_{PAR} (**Supplement 5**), with $P_T(z)$ profiles calculated for each *in situ* primary production experiment (**Figure 18**). Retrieved mean α^B and P^B_m values, along with calculated $P_{Z,T}$, are presented in **Table 8**. While photosynthesis parameters retrieved from June 2022 experiments remained consistent, those estimated for July 2023 showed greater variability among experiments (**Table 8**).

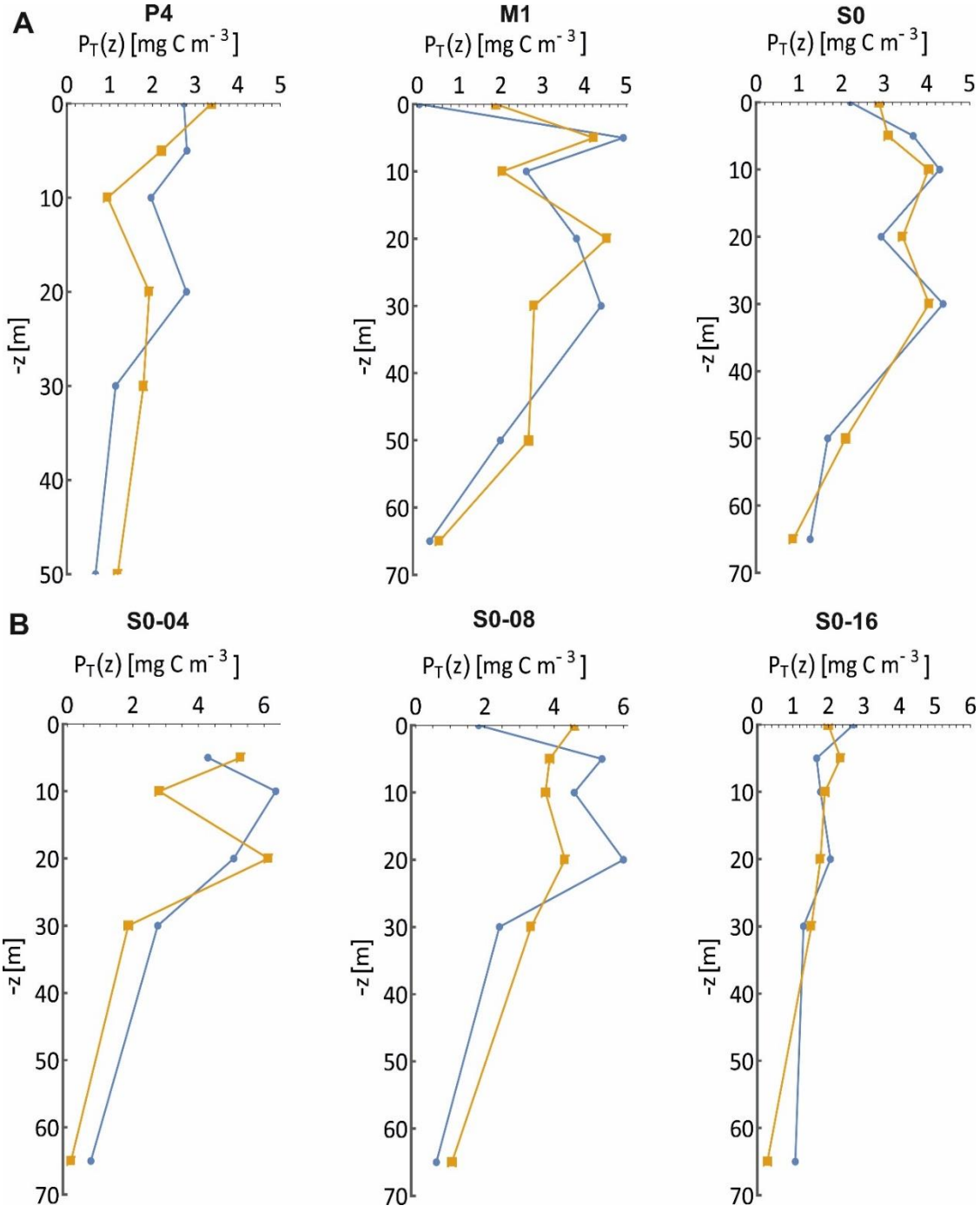

Figure 18. Comparison of *in situ* daily net primary production profiles $P_T(z)$ (orange) versus modeled ~$P_T(z)$ based on mean K_{PAR} (**Supplement 5**). Panels show **(A)** June 2022 at stations P4, M1 and S0 and **(B)** July 2023 at station S0.

Table 8. Daily depth-integrated primary production [$P_{Z,T}$ mg C m^{-2}] with mean and standard deviation values of photosynthesis parameters: initial slope [α^B mg C (mg Chl)$^{-1}$ (W m^{-2})$^{-1}$] and assimilation number [P^B_m mg C (mg Chl)$^{-1}$ h^{-1}], estimated for *in situ* ^{14}C primary production experiments conducted in June 2022 at stations P4, M1 and S0, and in 2023 at station S0 on 4 July (S0-04), 8 July (S0-08) and 16 July (S0-16).

	Experiments	**α^B (mean ± sd)**	**P^B_m (mean ± sd)**	**$P_{Z,T}$**
June 2022	P4	0.02 ± 0.01	1.32 ± 0.28	87.46
	M1	0.05 ± 0.03	1.02 ± 0.11	185.50
	S0	0.04 ± 0.01	1.57 ± 0.25	190.04
July 2023	S0-04	0.009 ± 0.002	1.37 ± 0.39	184.03
	S0-08	0.03 ± 0.009	0.49 ± 0.01	190.75
	S0-16	0.007 ± 0.002	0.44 ± 0.06	97.10

4.6.3 Ocean colour remote sensing

The joined dataset, including *in situ* daily depth-integrated primary production ($P_{Z,T}$ [mg C m^{-2}]) at station S0 and Copernicus model estimates (~$P_{Z,T}$ [mg C m^{-2}]), was used in a spatial autocorrelation analysis, yielding two key findings. First, Moran's I index revealed discrepancies between $P_{Z,T}$ at S0 and ~$P_{Z,T}$, with values aligning most closely on 16 July (**Figure 19C**). The red-to-blue gradient indicates the clustering of similar and dissimilar values, respectively, highlighting the grouping of similar values in the northern and southern regions of the Lastovo Island (**Figure 19**).

Second, quadrant classification revealed a heterogeneous spatial pattern of ~$P_{Z,T}$, with lower values tending to group in "low-low" clusters in the north-eastern region, and higher values forming "high-high" clusters in the south-western and south-eastern regions (**Figure 19**). Notably, after ITWs, higher ~$P_{Z,T}$ values grouped with lower values in a "high-low" cluster in the southern region (**Figure 19C**). However, the drastic decrease in $P_{Z,T}$ after ITWs, which the model ~$P_{Z,T}$ does not accurately reflect, should be considered when interpreting these results. Additionally, Copernicus satellite chlorophyll *a* data (~Chl *a* [mg m^{-3}]) indicated an increase in biomass near the island during ITWs (**Figure 19B**). Spatial analysis was further supported by ANOVA and Post-hoc Tukey HSD test, confirming significant variability in ~$P_{Z,T}$ and ~Chl *a* in relation to ITWs and across the days when *in situ* experiments were conducted: S0-04, S0-08 and S0-16 (**Table 9**).

Annual $P_{Z,T}$ in the Lastovo archipelago was highest in 2021 (122.9 ± 8.38 g C m^{-2}), followed by 2023 (118.0 ± 8.03 g C m^{-2}) and 2022 (114.8 ± 8.24 g C m^{-2}). The contribution of estimated

$P_{Z,T}$ during ITWs to annual $P_{Z,T}$ was highest in 2022 (3.80%), followed by 2021 (1.63%) and 2023 (1.52%) (**Supplement 10**).

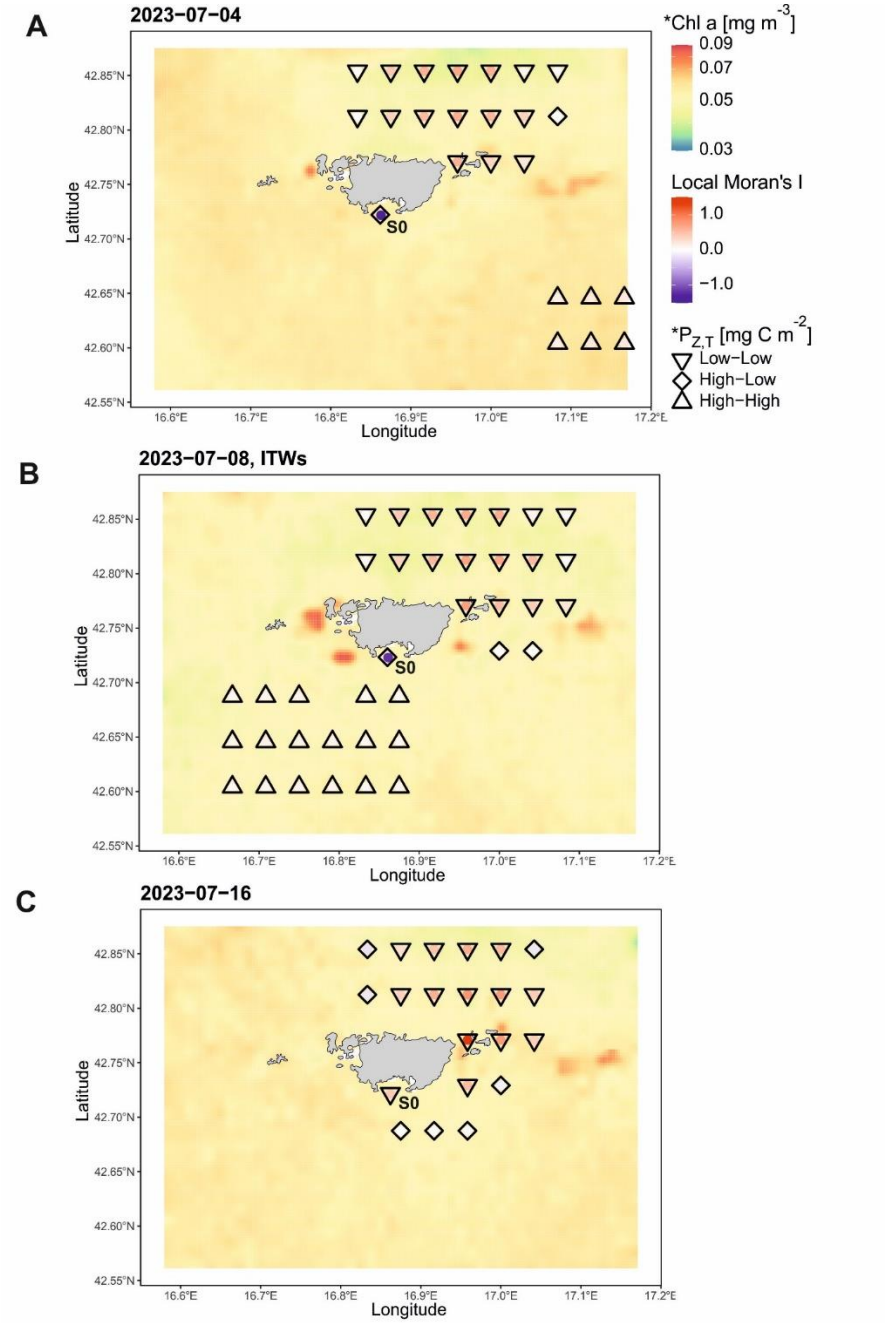

Figure 19. Spatial pattern of NPP at the Lastovo Island in relation to ITWs shown for **(A)** 4 July, **(B)** 8 July and **(C)** 16 July in 2023. Results of the spatial autocorrelation analysis are based on a joined dataset, including *in situ* daily depth-integrated primary production ($P_{Z,T}$ [mg C m^{-2}]) at station S0 and Copernicus operational primary production model (~$P_{Z,T}$ [mg C m^{-2}]). The local Moran's I index is depicted using a blue-white-red color scale, with quadrant classifications represented by symbols. Only significant results are shown (-1.96 ≤ z-score ≤ 1.96, p-value < 0.05). Overlaid are Copernicus daily gap-free L4 chlorophyll *a* data at 1 km resolution (~Chl *a* [mg m^{-3}]), shown on a green-to-red color scale.

Table 9. ANOVA and Post-hoc Tukey HSD applied on Copernicus model estimates of daily depth-integrated primary production (~$P_{Z,T}$ [mg C m^{-2}]), and Copernicus satellite chlorophyll *a* (~Chl *a* [mg m^{-3}]) at the Lastovo Island across two factors: *Station* and *ITWs-no ITWs*. ANOVA results are shown as „analyzed variable, p-value", while results of the Post-hoc Tukey HSD test are shown as „tested factor, p-value" for each variable. Only significant results are shown (significance level n

p-value < 0.05).

	ANOVA	**Post-hoc Tukey HSD**
Station	**~$P_{Z,T}$**, 0.006 **~Chl *a*,** 2 x 10^{-16}	**~$P_{Z,T}$** S0-08;S0-04, 0.004 **~Chl *a*** S0-04; S0-08, 0 S0-04; S0-16, 0.03 S0-08; S0-16, 0
ITWs-no ITWs	**~$P_{Z,T}$**, 0.007 **~Chl *a***, 2 x 10^{-16}	**~$P_{Z,T}$** ITWs-no ITWs, 0.007 **~Chl *a*** ITWs-no ITWs, 0

5 DISCUSSION

5.1 Physico-chemical parameters of the stratified water column

5.1.1 Nutrient and Chl a dynamics in a phosphate-limited ecosystem

The Adriatic Sea, unlike the larger ocean basins, is characterized by relatively low phosphate concentrations, typically below 0.2 μmol L^{-1} (Viličić et al., 1989). Such phosphate-limited ecosystems exhibit distinctive nutrient dynamics shaped by regional bathymetry. In the open southern Adriatic Sea, nitrate concentrations can reach up to 2.5 μmol L^{-1} (Viličić et al., 1989), whereas in eutrophic estuaries, not far from the open ocean, concentrations range between 14 and 20 μmol L^{-1} (Viličić et al., 2008). Reported concentrations of phosphate, nitrate and silicic acid in the open southern Adriatic range between 0.051–0.137 μmol L^{-1}, 0.35–3.81 μmol L^{-1}, and 2.25–12.86 μmol L^{-1}, respectively, while slightly higher values have been recorded at more coastal stations (Viličić & Stojanoski, 1987). Consequently, the nutrient concentrations observed at the Lastovo Island (**Table 3**) are consistent with those typically found in the oligotrophic stratified ecosystems.

The maximum Chl *a* concentration recorded at the Lastovo Island was 1.96 mg m^{-3} in the DCM layer that ranged from the 40 and 80 m depths, coinciding with higher nitrate and silicic acid concentrations (**Table 3**, **Table 5**, **Figure 8**). The mean Chl *a* value of 0.317 mg m^{-3} is consistent with concentrations reported for the southern Adriatic Sea. For instance, at the Otranto Strait, maximum Chl *a* values were recorded from 0.17 to 1.1 mg m^{-3} in the layer from 10 to 50 m (Socal et al., 1999, Turchetto et al., 2000).

5.1.2 Thermocline oscillations during stratified conditions

The Adriatic Sea is a semi-enclosed basin in the northeastern Mediterranean that undergoes pronounced seasonal changes in water-column structure. The average salinity measured at the Lastovo Island was 38.94 (**Table 3**), which aligns with climatological maps for the summer months in the southern Adriatic Sea (Lipizer et al., 2014). Stratification develops seasonally, remaining stable during summer months due to temperature and salinity gradients, and breaking down in winter as strong wind-driven mixing deepens the water column. These variations in the mixed layer depth have been well documented across the Mediterranean using temperature and salinity data (D'Ortenzio et al., 2005) as well as at the Lastovo Island (Hartkamp, 2025).

In the southern Adriatic Sea, the thermal gradient typically forms in April and reaches its maximum stability in August (Viličić et al., 1989), consistent with the study by Ljubešić et al. (2024). ITWs were identified during the stratified summer period at Lastovo using *in situ*

temperature, wind and current data (Matek et al., 2023, Ljubešić et al., 2024). The average water column temperature during all field experiments (2021–2023) ranged from 16 °C to 25 °C (Hartkamp, 2025). Thermocline oscillations reveal interannual variability, with 2023 exhibiting the strongest stratification season and the most pronounced vertical displacements of the thermocline, ranging between the 10 and 35 m depths during July and August (Hartkamp, 2025). A gradual deepening of the thermocline was also observed, with average depths of approximately 10 m in July 2021, 20 m in July 2022 (Ljubešić et al., 2024) and 18 m in July 2023, resembling conditions from 2022. In general, a deeper thermocline is associated with larger oscillations (Mihanović et al., 2014), which is congruent with more pronounced fluctuations observed in 2022 (Ljubešić et al., 2024) and 2023 (Hartkamp, 2025).

These findings suggest that climate-induced changes in the thermohaline properties of the Adriatic could alter the conditions under which ITWs are generated, potentially shifting the timing and intensity of ITW episodes. In the Adriatic Sea, local meteorological conditions, such as heavy rainfall and extended dry periods, may influence the strength of stratification (Verri et al., 2024). Climate projections under the RCP8.5 scenario indicate a 35% reduction in riverine input, which could affect the thermohaline properties of the northern Adriatic by reducing stratification stability (Verri et al., 2024). In contrast, the southern Adriatic is expected to be more influenced by changes in the large-scale thermohaline circulation across the Mediterranean than by river discharge (Verri et al., 2024). In addition to local and regional forcing, marine heatwaves also affect stratification, with projections suggesting longer and more intense stratified periods. Such changes are likely to cascade through the ecosystem, from phytoplankton at the base of the food web to higher trophic levels, thereby altering biogeochemical cycles and energy fluxes (da Costa et al., 2024).

5.1.3 Optical properties of the Adriatic Sea

Estimating K_{PAR} from *in situ* PAR time series obtained from sensors mounted on coastal cliffs (**Supplement 5**) is a novel approach because it enables continuous, shore-based characterization of the underwater light field in the Adriatic Sea, a characterization that has not been reported previously. In previous studies, the optical properties of the northern Adriatic Sea were measured using various techniques, including the Secchi disk (Justić, 1988), spectroradiometers (Lipizer et al., 2006, Lipizer et al., 2007) and profiling PAR sensors (Umer & Malačič, 2022). In contrast, optical measurements in the middle and southern Adriatic Sea employed profiling multispectral radiometers (Morović et al., 2008) and hyperspectral ocean color radiometers (HyperOCR, HOCR) (Puškarić et al., 2024).

In the northern Adriatic Sea, PAR values were calculated by trapezoidal integration of downwelling irradiance (E_d) (Lipizer et al., 2007). Normalized PAR, defined as a percentage of the surface value, decreased to 10% at 15 m depth during summer (Lipizer et al., 2007), indicating waters that are more optically complex than those in the southern basin. Further optical characterization using profiling PAR sensors yielded 81 vertical profiles over different seasons (Umer & Malačič, 2022). PAR exhibited the greatest variability in winter and the lowest in summer, with values ranging from 10^1 to 10^3 μmol m^{-2} s^{-1} near the surface and 10^0 to 10^2 μmol m^{-2} s^{-1} near the bottom (Umer & Malačič, 2022), similar to results presented in this thesis (**Supplement 5**). The average K_{PAR} values were 0.19 m^{-1} for linear fitting, 0.27 m^{-1} for exponential fitting, and 0.14 m^{-1} and 3.20 m^{-1} for biexponential fitting (Umer & Malačič, 2022). These values indicate more turbid coastal waters (Jerlov, 1964) and are higher than those obtained at the Lastovo Island (**Supplement 5**).

Conversely, optical measurements in the middle and southern Adriatic Sea showed that open-sea stations, similar to S1 at the Lastovo Island, match oceanic optical types I–II (Morović et al., 2008). K_d for individual wavelengths ranged from 0.01 m^{-1} to 1.4 m^{-1}. Normalized PAR profiles indicated 10% of incident PAR at 80 m (Morović et al., 2008). These values are deeper than those in the northern Adriatic Sea and are comparable to my findings (**Figure 14**). Additionally, Secchi disk measurements have been conducted in the middle Adriatic Sea as part of a long-term primary production monitoring since 1962 (Kovač et al., 2018). The attenuation coefficient was calculated from the Secchi disk depth (Z_{SD}) as $K = 1.44/Z_{SD}$ (Kirk, 2010). The reported mean K value of 0.077 m^{-1} (median = 0.075 m^{-1}, SD = 0.014 m^{-1}) (Kovač et al., 2018) closely matches my observations of 0.1 ± 0.02 m^{-1} and 0.08 ± 0.01 m^{-1} for 2022 and 2023, respectively (**Supplement 5**).

5.2 Diversity of the summer phytoplankton community at the Lastovo Island

The oligotrophic southern Adriatic Sea has lower phytoplankton abundances than the eutrophic northern region. Phytoplankton blooms typically occur in spring, with pico- and nanophytoplantkon dominating over microphytoplankton (Viličić et al., 1989, 2002). The nano- and microphytoplankton abundances observed in this thesis (**Figure 9**, **Supplement 2**) are characteristic of the southern Adriatic Sea (Viličić, 1991, 1998, Turchetto et al., 2000, Čalić et al., 2013) and other oligotrophic regions of the Mediterranean Sea (Becacos-Kontos, 1977, Berman et al., 1984, Turley, 1999, Yahia-Kefi et al., 2005, Decembrini et al., 2009).

The size structure of phytoplankton communities largely reflects the trophic status of an ecosystem. Pico- and nanophytoplankton are more adapted to nutrient-poor environments, while microphytoplankton dominate eutrophic areas (Thingstad & Sakshaug, 1990). Thus, in oligotrophic offshore areas of the Adriatic Sea, nanophytoplankton typically exhibits higher abundances than microphytoplankton (Viličić et al., 1989, 1998), which aligns with the abundances presented in this thesis (**Figure 9**, **Supplement 2**). At the Lastovo Island, diatoms represent the dominant microphytoplankton group, whereas nanophytoplankton were mostly comprised of dinoflagellates (**Figure 5**, **Supplement 2**), as already reported for other regions in the southern Adriatic Sea (Viličić, 1984, Viličić et al., 1998, 2002, 2008, Ljubimir et al., 2017, Pestorić et al., 2018).

Although nano-scaled dinoflagellates were most dominant, the largest number of identified species using light microscopy were microphytoplankton, particularly diatoms (**Supplement 1**). Differences in taxonomic expertise, sampling location, seasonality, and methodology can explain variations in species composition across studies. Morphological identification by imaging relies heavily on taxonomic expertise, a discipline in decline (McQuatters-Gollop et al., 2017). Yet image-based taxonomy remains among the most widely used methods for assessing phytoplankton composition (Olson & Sosik, 2007, Picheral et al., 2010). Combining this approach with molecular and chemotaxonomic techniques gives a more complete view of phytoplankton structure and dynamics (Matek et al., 2023).

5.2.1 Microphytoplankton

Phytoplankton research in the southern Adriatic Sea (Viličić, 1998, Viličić et al., 1998, 2002, Turchetto et al., 2000, Bosak et al., 2015) reveals a microphytoplankton assemblage similar to what was observed at the Lastovo Island (**Supplement 1**). The microphytoplankton community was composed mainly of diatoms (**Figure 5**, **Supplement 1**, **Supplement 2**). Among the dominant taxa, pennate diatoms accounted for the highest frequency (Fr = 78.21%), followed by *Proboscia alata* (Fr = 69.23%). Other prevalent groups included micro-scaled coccolithophorids (Fr = 55.13%), *Rhizosolenia imbricata* (Fr = 47.44%) and *Pseudo-nitzschia delicatissima* (Fr = 46.15%) (**Supplement 2**).

These findings were further supported by molecular analyses, which confirmed *Pseudo-nitzschia* spp. as the major contributor to the diatom community (Matek et al., 2023). Other identified taxa were primarily *Chaetoceros*, followed by *Minidiscus*, *Thalassiosira*, *Leptocylindrus* and *Hemiaulus* (Matek et al., 2023). As previously discussed, microphytoplankton thrive in nutrient-rich environments and therefore dominate eutrophic

regions (Kimor et al., 1987, Thingstad & Sakshaug, 1990, Mochemadkar et al., 2013). *Pseudo-nitzschia* spp. exhibit low seasonal variability (Ujević et al., 2010), yet they often dominate eutrophic regions of the northern Adriatic Sea (Revelante & Gilmartin, 1977). As recognized indicators of eutrophication (Revelante & Gilmartin, 1980), the dominance of *P. delicatissima* at the Lastovo Island (**Supplement 2**) during the stratified period suggests possible additional sources of nutrient influx to the ecosystem.

The dominant taxa observed at the Lastovo Island correspond to assemblages such as *Chaetoceros-Leptocylindrus-Thalassiosira*, which are typical of coastal European seas (Piredda et al., 2018). Moreover, the phytoplankton diversity presented in this thesis (**Supplement 1**) aligns with the *Chaetoceros-Rhizosolenia* (*Proboscia*) community characteristic of the eastern Adriatic and Mediterranean regions, including genera such as *Bacteriastrum*, *Cerataulina*, *Chaetoceros*, *Leptocylindrus*, *Proboscia*, *Pseudo-nitzschia*, *Rhizosolenia* and *Thalassionema* (Kimor, 1983, Kimor et al.1987, Latasa et al., 1992, Viličić et al., 1995, Latasa et al., 1997). Other species identified at the Lastovo Island (**Supplement 1**) were also observed in deeper layers of the Mediterranean Sea, including *Bacteriastrum* sp., *Dactyliosolen fragilissimus*, *Hemiaulus* sp., *Leptocylindrus danicus*, *Pseudo-nitzschia* sp., *Pseudo-nitzschia delicatissima*, *Rhizosolenia* sp., *Thalassionema frauenfeldii*, *Th. nitzschioides* and *Thalassiosira* sp. (Berland et al., 1987, Gotsis-Skretas et al., 1999, Boldrin et al., 2002).

5.2.2 Nanophytoplankton

Nanophytoplankton were the most diverse group, with more identified taxa compared to pico- and microphytoplankton (**Figure 7**, **Supplement 1**). Among them, dinoflagellates were the most dominant, with an occurrence frequency of 82.69% (**Table 4**). This pattern is consistent with other studies in the stratified Adriatic and Mediterranean Seas, which reported the prevalence of nano-scale dinoflagellates and coccolithophorids over micro-scale diatoms (Ignatiades et al., 2002, Ninčević Gladan et al., 2020). Moreover, these findings were supported by molecular analyses, particularly HTS, which confirmed a greater contribution of dinoflagellates compared to diatoms (Matek et al., 2023), in agreement with other studies in the region (Mucko et al., 2018, Piredda et al., 2018).

The dominant taxa at the Lastovo Island were nano-scaled dinoflagellates (78.21%), *Gyrodinium fusiforme* (45.51%) and *Scripsiella* sp. (42.95%) (**Table 4**). Other taxa were less frequent, except *Oxytoxum* sp. (23.08%), *Tripos furca* (10.26%) and *T. fusus* (7.69%) (**Supplement 1**). The relatively high proportion of undetermined taxa (**Supplement 1**) could be attributed to challenges in identification by light microscopy. The observed diversity aligns

with previous findings from the southern Adriatic Sea (Burić et al., 2007, Drakulović et al., 2010, 2013, Krivokapić et al., 2018) and the broader Mediterranean Sea (Gotsis-Skretas et al., 1999, Vidussi et al., 2001, Marty & Chiavérini, 2002).

Frequent dinoflagellate genera in the southern Adriatic are *Dinophysis*, *Gonyaulax*, *Gymnodinium*, *Oxytoxum*, *Prorocentrum*, *Protoperidinium* and *Tripos* (Viličić, 1985, 1998, Viličić et al., 1998, Drakulović et al., 2013). In the Mediterranean Sea, *Oxytoxum*, *Gymnodinium*, *Gyrodinium*, *Protoperidinium* and *Tripos* are also commonly observed (Giaccone & Geraci, 1989, Estrada, 1991, Gómez, 2006). At the Lastovo Island, 18S rRNA ASVs revealed additional taxa: *Azadinium*, *Ceratoperidinium*, *Karlodinium*, *Karenia*, *Lepidodinium*, etc. (Matek et al., 2023), underscoring the importance of combining imaging and molecular approaches for comprehensive phytoplankton assessment. These findings are consistent with observations from other coastal ecosystems (Lohrenz et al., 1988, Magazzu & Decembrini, 1995, Mucko et al., 2018, Piredda et al., 2018, Wang et al., 2021).

Following dinoflagellates, coccolithophorids were the next most frequently observed group (**Figure 7**, **Supplement 1**). Nano-scaled coccolithophorids were present in 21.15% samples (N = 156) (**Supplement 1**), with the most frequent species being *Calyptrosphaera oblonga* (19.87%), *Calciosolenia brasiliensis* (8.97%), *Rhabdosphaera tignifera* (8.33%), *R. Stylifera* (7.69%), and *Syracosphaera pulchra* (7.05%) (**Supplement 1**). These findings are congruent with previous studies in the southern Adriatic Sea (Skejić et al., 2018) and the Mediterranean Sea (Cros & Fortuño, 2002), although *Emiliana huxley* and *Helicosphaera wallichii* were not detected. Despite *E. huxley* being widely distributed in the Mediterranean (Cros & Fortuño, 2002), its absence in both imaging and molecular analyses (Supplement 1) may be related to its typically higher abundance in late summer and autumn (de Vargas et al., 2015, Piredda et al., 2017).

The silicoflagellate *Dictyocha fibula* was also identified (**Supplement 1**), a species frequently recorded in the southern Adriatic Sea (Drakulović et al., 2013) and occasionally found in the surface waters of the Mediterranean Sea (Estrada, 1991, Gran-Stadniczeñko et al., 2019).

5.2.3 Picophytoplankton

Picophytoplankton abundances and diversity recorded at the Lastovo Island (**Figure 7**, **Figure 9**, **Supplement 2**) are consistent with observations from the oligotrophic Mediterranean Sea (Siokou-Frangou et al., 2010). The picophytoplankton community consisted of cyanobacteria (*Synechococcus* and *Prochlorococcus*) and PPEs (**Figure 7**). Cyanobacteria are widely

distributed across the Mediterranean Sea (Dolan et al., 1999), while PPEs occupy a narrower ecological niche and have been most frequently observed in the Ionian Sea, Strait of Sicily and the Levantine Basin (Siokou-Frangou et al., 2010).

Prochlorococcus sp. and *Synechococcus* sp. abundances (8877 cells mL^{-1} and 9755 cells mL^{-1}, respectively) at the Lastovo Island (**Supplement 2**) are typical for the open oligotrophic southern Adriatic (Šantić et al., 2013, 2020) and comparable to values reported for the wider Mediterranean Sea (Zwirglmaier et al., 2008, Mella-Flores et al., 2011, Larkin et al., 2016). Both taxa were also identified as photosynthetic bacterial ASVs at the Lastovo Island (Matek et al., 2023) and in other molecular studies from the region (Najdek et al., 2014, Korlević et al., 2015, Babić et al., 2018, Mucko et al., 2018).

PPEs abundances (748 cells mL^{-1}) indicated a lower contribution to overall picophytoplankton counts (**Supplement 2**), although their small size and lack of distinct morphological features complicate accurate identification (Henley et al., 2004). Flow cytometry confirmed the presence and abundance of PPEs (**Supplement 2**), while molecular analysis revealed associated heterotrophic picoeukaryotes, predominantly alveolates and stramenopiles (Matek et al., 2023), which likely have a role in bottom-up control through predation and parasitism (Jardillier et al., 2005), as well as in the recycling of inorganic nutrients within water column (Sherr & Sherr, 1991, 1994).

5.3 Phytoplankton community structure in the stratified ecosystem

No significant changes in phytoplankton succession were observed during ITWs at the Lastovo Island (**Table 5**), and the temporal succession of the community remained constant over the study period (**Figure 9**). However, phytoplankton's heterogeneous vertical distribution at the Lastovo Island was significant and constrained by the temperature gradient and the spatial distribution of nutrients (**Figure 4**, **Figure 8**, **Figure 10A, B).** Specifically, microphytoplankton clustered significantly toward the deeper layer characterized by high concentrations of Chl *a*, nitrite, nitrate and silicic acid, whereas pico- and nanophytoplankton were more associated with warmer surface and thermocline layers that were richer in phosphates (**Figure 10A, B**, **Supplement 3**). This structure is typical of a stratified water column and was recently validated using a two-layered nutrient, phytoplankton and zooplankton (NPZ) ecosystem model against a 30-year time series from the Bermuda Atlantic Time-series Study (BATS) (Zheng et al., 2025). The model revealed two distinct communities inhabiting (i) a nutrient-limited surface layer and (ii) a light-limited subsurface layer, both exhibiting different seasonal and interannual dynamics (Zheng et al., 2025).

Several studies in the Adriatic Sea have reported that the dominant microphytoplankton and nanophytoplankton groups, diatoms and dinoflagellates, respectively, prefer contrasting environmental conditions. Generally, diatoms thrive in cold and nutrient-rich waters, whereas dinoflagellates are better adapted to warm, nutrient-poor environments. For instance, observed temperature optima for diatoms range between 16 °C and 24 °C, while dinoflagellates favor temperatures above 24 °C (Viličić et al., 1998). Such temperature-driven vertical structuring during stratification has also been documented across the oligotrophic Mediterranean (Margalef, 1969, Berland et al., 1987, Siokou-Frangou et al., 2010, Mena et al., 2019). Furthermore, diatoms rapidly respond to elevated nitrate concentrations, gaining a competitive advantage over other phytoplankton (Estrada & Blasco, 1979, Estrada et al., 1993, Čalić et al., 2013, Closset et al., 2021). In contrast, dinoflagellates often thrive in nutrient-depleted surface waters of the stratified Adriatic, which can be attributed to their mixotrophic capabilities and diverse feeding strategies (Čalić et al., 2013, Krivokapić et al., 2018).

Vertical structuring of picophytoplankton at the Lastovo Island was reflected in the dominance of *Synechococcus* sp. in the surface and thermocline layers, while *Prochlorococcus* sp. prevailed in the deeper layer (**Table 5**, **Figure 9**, **Figure 10A, B**). Similar vertical partitioning has been reported in other regions of the southern Adriatic Sea (Šilović et al., 2011, Cerino et al., 2012, Šantić et al., 2013, Najdek et al., 2014), as well as across the Mediterranean Sea (Mella-Flores et al., 2011, Pittera et al., 2014), reflecting their distinct ecological niches (Zwirglmaier et al., 2008). *Synechococcus* exhibits broader tolerance to variations in temperature and nutrients (Mackey et al., 2013, Pittera et al., 2014), whereas both cyanobacteria comprise ecotypes adapted to different light regimes and nutrient sources (Mella-Flores et al., 2011, Larkin et al., 2016). Such partitioning is characteristic of the stratified oligotrophic ecosystems (Schmoker & Hernández-León, 2013, Coello-Camba & Agustí, 2021), where picophytoplankton distribution is largely determined by temperature (Mella-Flores et al., 2011, Larkin et al., 2016, Šantić et al., 2020) and nutrient availability (Duarte et al., 2000, Moore et al., 2002, Jardillier et al., 2005). Unlike cyanobacteria, PPEs were relatively homogeneously distributed (**Figure 9**), with a tendency toward warmer surface and thermocline layers (**Figure 10A, B**). Similar patterns have been reported in the southern Adriatic Sea (Šilović et al., 2011, Šantić et al., 2019), driven by nutrient sources (Duarte et al., 2000, Mena et al., 2019) and a temperature gradient (Šantić et al., 2021).

5.4 Succession and correlation between plankton communities in relation to ITWs

5.4.1 Phytoplankton

Environmental variables explained the highest proportion of variability in the picoplankton community (**Figure 10A, B**), indicating that the smaller cells respond more rapidly to environmental changes and suggesting they may be the first to react to oscillations generated by ITWs. These findings align with observations from the South China Sea, where phytoplankton response to internal wave-driven nutrient inputs was influenced by cell size and physiological adaptation (Ma et al., 2020). Pico- and nano-scaled phytoplankton (e.g., haptophytes, prasionophytes and cryptophytes), respond rapidly to vertical advection into high-light environment and nutrient inputs, whereas larger cells, such as micro-scaled diatoms, exhibit a delayed response of 12 to 16 hours (Ma et al., 2020). Similar results for the same region were reported by Guan et al. (2023), demonstrating that nutrient enrichment particularly benefits small phytoplankton. Size-dependent responses are also evident at the molecular level: picoplankton can rapidly increase photosynthetic performance through transcriptional regulation of Rubisco, an enzyme crucial in the process of carbon fixation, whereas larger eukaryotes require more time to refulate and synthesize this enzyme under stress (John et al., 2012).

The effect of ITWs on NPP at the Lastovo Island may also depend on pre-existing ecological equilibria established through interactions among phytoplankton, bacteria and zooplankton. In the stratified South China Sea, Ma et al. (2023) proposed a three-layer phytoplankton community structure in which each layer responds differently to internal waves depending on specific adaptations to light intensity, nutrient availability and top-down control by zooplankton grazing. For instance, although nutrient availability increases in the bottom layer, *Prochlorococcus* abundance decreases due to its inefficiency in nitrate uptake. In contrast, its growth in the surface layer is enhanced since it outcompetes *Synechococcus* for ammonium released by migrating zooplankton (Ma et al., 2023). The community in the middle layer remains stable due to an equilibrium between growth and mortality (Ma et al., 2023). Similar dynamics were observed under internal waves and anticyclonic eddies, where cyanobacteria occupied distinct niches and microphytoplankton were controlled by copepods, allowing pico- and nanophytoplankton to thrive (Zhong et al., 2024).

It is important to note that some phytoplankton groups do not respond to internal waves, either because they are diluted throughout the water column or because they are unable to adapt (Ma et al., 2020). For instance, in a study by Ma et al. (2020), *Synechococcus*, dinoflagellates and

chlorophytes showed no response due to dilution, while *Prochlorococcus*, though advected from deeper layers to the surface, did not respond because it was outcompeted for nutrients and not adapted to higher light conditions (Ma et al., 2020). Although this study did not assess changes in phytoplankton functional groups, internal waves have been shown to shift communities from mixotrophic-dominated to autotrophic- and heterotrophic-dominated states, thereby reducing opportunistic behavior and favoring more direct survival strategies (Guan et al., 2023).

5.4.2 Bacterioplankton

Heterotrophic bacteria observed at the Lastovo Island consisted of high- and low-nucleic-acid (HNA and LNA) cells (Ljubešić et al., 2024). The community was dominated by Proteobacteria (Gammaproteobacteria > Alphaproteobacteria), followed by Bacteroidota and cyanobacteria (Matek et al., 2023). Notably, this composition aligns with other oligotrophic stratified areas in the Adriatic Sea and beyond (Kimor et al., 1987, Marty & Chiavérini, 2002, Babić et al., 2018, Šilović et al., 2018, Becker et al., 2020, Šantić et al., 2020). Furthermore, bacterial abundances at the Lastovo Island (**Supplement 2**) matched summer records for the oligotrophic southern Adriatic Sea (Mackey et al., 2013, Hafner et al., 2018, Šilović et al., 2018, Šantić et al., 2020, 2021). Peak activity, as suggested by high abundances, occurred in the thermocline layer (**Figure 9**), consistent with other studies in the Adriatic Sea (Gallina et al., 2011, Turk et al., 2012, Najdek et al., 2014, Šilović et al., 2018).

At the Lastovo Island, heterotrophic bacteria likely modulated nutrient dynamics in the water column (**Figure 8**, **Figure 10A, B**), reflecting their role in nutrient cycling through utilization and regeneration (Najdek et al., 2014, Mucko et al., 2025). A comparable response was observed in the South China Sea (Chen et al., 2016), where internal waves enhanced bacterial activity through elevated nutrient inputs. Similarly, during ITWs at the Lastovo Island, bacterial functional profiles shifted toward enhanced nitrogen respiration, nitrate reduction, fermentation and (aerobic) chemoheterotrophy (Ljubešić et al., 2024), corroborating the nutrient-driven dynamics reported by Chen et al. (2016). Furthermore, recent findings from the Lastovo Island additionally confirm increased bacterial involvement in nitrogen cycling (nitrification and aerobic ammonia oxidation) and greater metabolic potential in the DCM following ITWs (Mucko et al., 2025), suggesting post-ITW enhanced biomass that simulated microbial processes.

5.4.3 Zooplankton

Zooplankton abundance and composition at the Lastovo Island, characterized using both morphological (Ljubešić et al., 2024, Pestorić et al., 2025) and molecular approaches (Ljubešić et al., 2024, Mucko et al., 2025), reflect the typical coastal oligotrophic community of the southern Adriatic Sea (Miloslavić et al., 2014, Pestorić et al., 2018, Stefanni et al., 2018, Pestorić et al., 2021, Ninčević Gladan et al., 2023). ITWs at the Lastovo Island indirectly affect the zooplankton community by altering phytoplankton abundance (Ljubešić et al., 2024, Pestorić et al., 2025). Both micro- and mesozooplankton abundances responded to ITWs, suggesting adjustments in grazing pressure and feeding preferences in response to altered phytoplankton dynamics (Ljubešić et al., 2024, Pestorić et al., 2025).

For instance, the dominant mesozooplankton species *Centropages typicus* was abundant during ITWs, coinciding with the dominance of nano-scale dinoflagellates (Ljubešić et al., 2024). This association suggests a grazing preference consistent with previous observations under turbulent conditions (Calbet et al., 2007). Furthermore, microzooplankton species such as *Evadne spinifera*, *Oithona* spp. and *Paracalanus parvus parvus* were concentrated in the upper layer during ITWs at the Lastovo Island, preferably grazing on increased nanophytoplankton abundances (Pestorić et al., 2025). Similarly, a mesocosm experiment simulating artificial upwelling in an oligotrophic ecosystem at Gran Canaria demonstrated enhanced microzooplankton grazing on nanophytoplankton following nutrient enrichment. These findings confirm that zooplankton communities rapidly adapt through shifts in prey preferences (Spilling et al., 2023).

Taken together, these findings highlight the complex interplay among ITWs, phytoplankton community structure and broader food web dynamics, and support recent evidence of increased taxonomic diversity and trophic network co-occurrence complexity during ITWs at the Lastovo Island (Mucko et al., 2025).

5.5 Primary production in the stratified oligotrophic ecosystem

Water column properties observed during the *in situ* primary production experiments in June 2022 and July 2023 (**Figure 11, Supplement 4**) are characteristic of a stratified ecosystem (Zheng et al., 2025), with a developing thermocline in the surface layer and a DCM confined to deeper layers (**Figure 11, Supplement 4**). Common primary producers in the oligotrophic Mediterranean Sea are picophytoplankton (Lohrenz et al., 1988, 1992). This was further supported by eDNA metabarcoding of discrete and net water samples at the Lastovo Island, which identified dominant taxa within the pico fraction, including cyanobacteria

(*Synechococcus* strain CC9902) (Ljubešić et al., 2024), Pelagophyceae and Mamiellophyceae (Mucko et al., 2024). Additional primary producers were recognized in other size fractions: stramenopiles (*Pelagomonas*, nanophytoplankton), chlorophytes (*Ostreococcus*, nanophytoplankton) (Ljubešić et al., 2024) and Prymnesiophycae (nano- and microphytoplankton) (Mucko et al., 2024).

$P_{Z,T}$ at the Korčula and Lastovo islands (**Figure 12**) is congruent with other experimental values obtained in oligotrophic ecosystems in the southern Adriatic Sea (Turchetto et al., 2000, La Ferla et al., 2005). In August, daily $P_{Z,T}$ in the South Adriatic Pit reached 236 mg C m^{-2}, notably exceeding values observed in this thesis (**Figure 12**, **Table 8**). Conversely, summer estimates from the northwestern Ionian Sea were approximately 184 mg C m^{-2} (Turchetto et al., 2000), closely matching those recorded at both sides of the Lastovo Island (stations M1 and S0) in June 2022, and during the S0-04 and S0-08 experiments in July 2023 (**Figure 12**). However, in the same area, La Ferla et al. (2005) estimated $P_{Z,T}$ at 249 mg C m^{-2} which is slightly higher than at the Lastovo Island (**Figure 12**, **Table 8**).

Variability in summer primary production is often driven by the dynamics of its limiting factors (Chavez et al., 2011). Local physical processes, such as turbulence disrupting stratification and introducing nutrients to the euphotic zone (Cooper, 1947, Sharples et al., 2007, Villamaña et al., 2017, Tuerena et al., 2019) or horizontal advection of nutrient-rich water masses (Civitarese et al., 2010, 2023), can substantially modulate production levels (De Falco et al., 2022). These mechanisms also appear to operate at the Lastovo Island during ITWs. Specifically, annual $P_{Z,T}$ estimated from ocean colour remote sensing indicates that ITWs contribute approximately 1.5–3.8% to the annual $P_{Z,T}$ (**Supplement 10**). However, the use of a 4-km-resolution data across the broader Lastovo Archipelago likely masks small-scale coastal effects associated with ITWs. High-resolution datasets constrained to the nearshore zone would likely reveal even greater contributions.

Annual $P_{Z,T}$ estimates range approximately 115–123 g C m^{-2} (**Supplement 10**), values comparable to or slightly higher than those reported for the northern Adriatic Sea (Matek & Ljubešić, 2025). They fall within the range documented for the Middle Adriatic, particularly Kaštela Bay, a highly eutrophic system (Matek & Ljubešić, 2024). Unfortunately, comparable annual estimates for the southern Adriatic Sea are currently lacking (Matek & Ljubešić, 2024).

5.6 ITWs as a driver of primary production

NPP dynamics at station S0 were distinct from those at other stations (**Figure 12B**), as reflected by higher $P_{Z,T}$ (**Figure 12A, B**) and confirmed by PCA, which showed significant clustering of S0, particularly during ITWs (**Figure 17A, B, Supplement 6**). In July 2023, $P_T(z)$ and $P^B_T(z)$ at S0 increased by 18.12% and 97.90%, respectively, within the thermocline layer at 20 m during ITWs (**Table 7**). These changes in the thermocline layer were reflected in a 3.65% increase in $P_{Z,T}$ during ITWs (S0-08) (**Table 7**); however, this increase was not statistically significant (**Table 6**). In contrast, $P^B_{Z,T}$ decreased by 14.62% during ITWs (**Table 7**), likely due to elevated photosynthetic activity in the surface layer prior to ITWs (**Figure 12B**). These results are further supported by cxygen-based estimates of NPP, which revealed an increase in the thermocline layer during ITWs at station S1 in July 2022 (Ljubešić et al., 2024).

Seasonal thermocline oscillations at the Lastovo Island, as described by Hartkamp (2025), indicate more frequent advection and convection processes during summer, which may modulate NPP independently of well-defined ITW episodes. In this context, the final *in situ* primary production experiment (S0-16) was conducted outside the main ITW period defined by Ljubešić et al. (2024). However, when a broader view of thermocline variability is taken into account, a weaker ITW event may still have been present, making it relevant to discuss the observed NPP dynamics.

Indeed, thermocline oscillations in July 2023 suggested an additional potential ITW episode from 15 to 18 July (**Figure 14D**, **Figure 15D**), which was not captured by the original ITW classification. Modeled underwater light field in the thermocline layer during this period indicated increased irradiance (**Figure 16D**), implying that the S0-16 experiment may have coincided with the early phase of a newly developing ITW event on 16 July. This is further supported by elevated nitrate concentrations in the thermocline layer during S0-16 (**Figure 11C**). However, no increase in $P_{Z,T}$ was detected during S0-16, as both $P_T(z)$ and $P^B_T(z)$ increased only at 65 m by 79.21% and 83.61%, respectively, while a similarly strong decrease was observed in the rest of the water column (**Table 7**).

These NPP dynamics are likely shaped by a combination of factors: phytoplankton photoacclimation processes, taxonomic composition, cell size and whether the response to ITWs is primarily physiological or physical. Ma et al. (2020) reported that nanophytoplankton vertically advected to higher light conditions exhibit a rapid, light-driven response. In contrast, microphytoplankton responses to nutrient influx occur with a temporal lag.

In this chapter, I will build on these findings by discussing mechanisms in detail, with emphasis on nutrient dynamics, photoacclimation inferred from photosynthesis parameters and the influence of ITWs on the NPP spatio-temporal distribution.

5.6.1 Nutrient enrichment during advection processes

Several global studies have shown that sporadic nutrient inputs occur through disruption of stratification caused by internal waves (Garrett & Munk, 1979, Garrett, 2003, Li et al., 2018, Whalen et al., 2020, Dematteis et al., 2024). As previously discussed, these processes affect various aspects of the phytoplankton community, including shifts in community structure (Ma et al., 2020, Wang et al., 2021) and functionality (Ma et al., 2023, Guan et al., 2023), increases in Chl *a* (Sangrà et al., 2001), particulate organic carbon (POC) (Li et al., 2018), primary production (Pan et al., 2012) and bacterial activity (Chen et al., 2016).

At the Lastovo Island, the deeper layer was richer in nutrients than the thermocline and surface layers (**Figure 8**) and significant nutrient outliers (calculated using z-scores) were observed within the thermocline layer (**Figure 6**, **Figure 13**). These outliers were sporadic and not frequent enough to discuss their effect on NPP. However, similarly small and recurrent nutrient inputs have been shown to increase primary production (Spilling et al., 2023). I did not observe a significant response in nutrient concentrations to ITWs (**Table 9**), and thus cannot conclude whether detected outliers in the thermocline layer reflect ITW-driven nutrient transport from the deeper layer.

Nutrient profiles measured concurrently with *in situ* ^{14}C primary production experiments do not fully conform to the typical stratified ecosystem model described by Zheng et al. (2025), in which surface waters are nutrient-replete and deeper layers are nutrient-depleted. However, at the Lastovo Island, silicic acid and phosphate remained constant throughout the water column, while only nitrates were elevated in the thermocline at 20 and 30 m depths (**Figure 11**). Furthermore, if ITWs had caused nutrient influx, an increase in all nutrients within the thermocline would be expected; this was not observed during primary production experiments (**Figure 11**). The observed nutrient time-series (**Figure 13)** also indicates dynamics unrelated to ITWs. Specifically, in July 2022, high variability in nitrate and nitrite was observed, with elevated levels in the thermocline during ITWs, while phosphate and silicic acid remained more constant (**Figure 13**).

Collectively, these findings suggest that nutrient dynamics at the Lastovo Island are complex and likely mediated by plankton activity and trophic interactions, rather than directly driven by

ITWs. Furthermore, these observations do not match the typical stratified ecosystem model described by Zheng et al. (2025), in which the upper layer is nutrient-rich and the bottom layer is nutrient-depleted. In the case of the Lastovo Island, nutrient profiles before and after incubations indicate a constant concentration throughout the water column of nitrites and silicic acids, while nitrates only follow the so-called model of stratified water column, with elevated levels in the surface and thermocline layer (**Figure 13**).

Wang et al. (2007) also reported a nonlinear relationship between nutrients and internal waves, evident in time-lagged response in Chl *a* that increased 7–8 days after wave events. Internal waves advected organic matter from depth, which was remineralized via microbial processes in the surface layer, promoting regenerated primary production (Wang et al., 2007). Similarly, biomass increased by internal waves enhances bacterial remineralization, resulting in elevated nutrient levels, particularly nitrates (Chen et al., 2016). This corroborates the hypothesis that nutrient dynamics in the thermocline at the Lastovo Island during ITWs may be strongly influenced by the plankton community, particularly bacterioplankton, which exhibited increased abundances during ITWs in July 2022 (**Figure 9**), suggesting enhanced activity. However, further research is needed to test this hypothesis.

In contrast, the idealized model of ITWs at the Lastovo Island supports nutrient transport as an important mechanism driving increased primary production (Jacobsen et al., 2023). The discrepancies with *in situ* observations may arise from the model not accounting for biological feedback within the plankton community. Furthermore, the smaller changes in nutrient concentrations observed *in situ* compared to those estimated by the model may reflect the rapid response of dominant pico- and nanophytoplankton (Ljubešić et al., 2024, Mucko et al., 2024), which the model did not account for. As previously discussed, smaller phytoplankton are more efficient at nutrient uptake (John et al., 2012, Ma et al., 2020). At the Lastovo Island, this may be linked to the high abundance of the primary producer *Synechococcus* in the thermocline layer (Ljubešić et al., 2024) (**Supplement 2**), a genus well adapted to high light intensity and elevated nutrient conditions (Moore et al., 2002, Mackey et al., 2013).

5.6.2 Variability in the underwater light field in the southern Adriatic Sea

The influence of internal waves on the underwater light field is well known (Holloway, 1984). To account for increased phytoplankton light exposure in such environments, correction factors have been introduced into primary production models (Platt & Sathyendranath, 1993, Lande & Yentsch, 1988). Furthermore, field and modeling studies have shown that the vertical displacement of phytoplankton by internal waves can increase photosynthesis by up to 200%

in light-limited ecosystems, depending on cloud cover (Evans et al., 2008), though this estimate was derived for a lake. Consistent with these findings, this thesis results show increased afternoon light conditions at S1 by up to 70 W m^{-2} during ITWs (**Figure 15, Figure 16**), suggesting a potential effect on NPP (Matek et al., 2024).

Similarly, Muacho et al. (2013) observed internal waves in the Nazaré Canyon (western Iberian Peninsula) and reported up to an 8.7% daily increase in photosynthesis and a 50% increase in Chl *a* compared with areas without internal waves. They also identified horizontal Chl *a* patches along internal wave trajectories, highlighting spatial effects, particularly where wave crests (shallow thermocline) coincided with peak surface irradiance at noon. These findings suggest that primary production may increase when ITWs crest and high irradiance coincide. Modeling studies further support this mechanism, showing that the most favorable photosynthetic conditions occur when ITW crests coincide with solar noon (Kamykowski, 1974). Therefore, it is reasonable to assume that even higher primary production might have occurred at the Lastovo Island in areas where ITW crests align more closely with solar noon, rather than around 17:00 (UTC+1) at station S1 (Ljubešić et al., 2024).

Kamykowski (1974) also emphasized that photosynthetic efficiency depends on the rate at which phytoplankton acclimate to changing light intensities during the internal wave cycle. This adaptation likely shapes community composition, favoring taxa that tolerate light fluctuations. Accordingly, phytoplankton groups dominating the thermocline at the Lastovo Island, mainly nanophytoplankton (dinoflagellates, followed by coccolithophorids, cryptophytes and chlorophyceae) and picophytoplankton (*Synechococcoccus* sp. and PPEs) (**Figure 10A, B**), appear well adapted to the variable light regime during ITWs. Furthermore, phytoplankton modify their biochemical composition in response to changes in light spectrum (Marmelstein, 1970) or other qualitative chemical changes (Wallen & Geen, 1971), which may alter their nutritional quality, especially when adapting to different light environments. This can corroborate observed zooplankton migrations between stratified layers and shifts in their prey preferences during ITWs at the Lastovo Island (Pestorić et al., 2025).

5.6.3 Photoacclimation revealed through photosynthesis parameters

A decrease in P^B_m was observed during and after ITWs at the Lastovo Island (**Supplement 8**), suggesting reduced photosynthesis efficiency under high-light conditions. A similar pattern was reported by Gaxiola-Castro et al. (2002), who attributed the decline in P^B_m during internal waves to the upward advection of phytoplankton acclimated to light-limited deeper layers. However, photoacclimation during ITWs cannot be confirmed in this thesis due to a lack of concurrent

measurements of the underwater light field and phytoplankton community structure. Nevertheless, these *in situ* data are valuable and should be more adequately assessed in the future, since regionally derived photosynthesis parameters can improve regional estimates of primary production (Bouman et al., 2018). For instance, the distribution of P^B_m retrieved from *in situ* primary production profiles using an inverse model (Kovač et al., 2016a, 2016b) allowed correction of overestimates in monthly measurements of a 55-year *in situ* primary production time series in the Middle Adriatic (Kovač et al., 2018). The same model was applied in this thesis, and its accuracy was confirmed by the low error distribution (**Supplement 9**) and the good agreement between modeled and *in situ* profiles (**Figure 18**).

It is also important to note that both α^B and P^B_m measured at the Lastovo and Korčula islands (**Supplement 7**, **Supplement 8**, **Table 8**) represent the first available estimates for the southern Adriatic Sea (Matek & Ljubešić, 2024). In contrast, photosynthesis parameters have been estimated for some regions in the northern Adriatic Sea, such as the Gulf of Trieste (Malej et al., 1995, Talaber et al., 2014), the Po River delta (Vadrucci et al., 2002, Pugnetti et al., 2003, 2004, Mangoni et al., 2008, 2020) and the Venice Lagoon (Pugnetti et al., 2003, 2004). However, these studies are not directly comparable due to seasonal, regional and methodological differences.

5.6.4 Spatio-temporal distribution of primary production at the Lastovo Island

Ocean colour remote sensing revealed a significant increase in $\sim P_{Z,T}$ and ~Chl *a* during ITWs (**Table 9**). Spatial heterogeneity in primary production was evident, with the highest $\sim P_{Z,T}$ in the southern region near S0 (**Figure 19B**). This aligns with previous studies identifying ITWs as physical drivers of IME (De Falco et al., 2022) typically expressed through spatio-temporal heterogeneity in biogeochemical parameters (Kahru, 1983, Kamykowski, 1974, Bourdin et al., 2024), as observed at the Lastovo Island (**Table 8**, **Figure 18**).

Ocean colour remote sensing often tracks IME as Chl *a* patches advected horizontally from the island coast (Bourdin et al., 2024). Several studies have confirmed that such patches can form in response to internal waves (Sangrà et al., 2001, da Silva et al., 2002, Wang et al., 2007, Muacho et al., 2013). This corroborates the results presented in this thesis, which confirm an increase in Chl *a* concentrations along the southern coast of the Lastovo Island (**Figure 19B**). However, no further horizontal advection was observed (**Figure 19C**), in contrast with reports by Messié et al. (2020) and Bourdin et al. (2024). However, unlike the coastal Adriatic Sea, these studies investigated the open Pacific, where long retention times and decoupling of water

masses can allow phytoplankton blooms to persist for months and spread over 1000 km from the coast (Messié et al., 2020, Bourdin et al., 2024).

It should also be noted that I used a 4-km spatial resolution of the primary production product, which likely limited the detection of short-term and small-scale increases in Chl *a* associated with ITWs, as discussed in Bourdin et al. (2024). Since Chl *a* is applied in models of primary production, this can affect the observed patterns. Discrepancies between *in situ* and remote sensing data were revealed by Moran's I values. *In situ* primary production at S0 was underestimated before and during ITWs, while estimates aligned better afterwards (**Figure 19A, B**). These results highlight the need for a higher resolution remote sensing product, ideally daily 1-km data with improved atmospheric correction that accounts for glint and adjacency effects. This is particularly relevant around small islands in coastal seas (Bourdin et al., 2024), especially since it could improve the ability to detect ITW-related changes in NPP at the Lastovo Island, which are likely underestimated in the current dataset.

Despite these limitations, spatio-temporal heterogeneity was observed during ITWs, with enhanced NPP in the southern region of the island (**Figure 19B**). This finding is supported by my model of the underwater light field in the thermocline layer at S1 (**Figure 14**, **Figure 15**, **Figure 16**) and further coroborated in aforementioned studies confirming the increased photosynthetic efficiency in response to more favorable light conditions during internal waves (Holloway, 1984, Lande & Yentsch, 1988, Evans et al., 2008), especially when diurnal light cycle and internal wave are in phase (Kamykowski, 1974, Muacho et al., 2013, Jacobsen, 2024). The observed spatial pattern is influenced by island shape and size. At the Lastovo Island, the 24-hour ITW cycle aligns with the diurnal light cycle, while a similar effect may occur at Bermuda (with a 26.1-hour period) (Brink, 1999). In contrast, in Hawaii, where ITWs exhibit a 59-hour period (Luther, 1985), such phasing is unlikely to influence spatial production patterns.

An idealized model of ITWs at the Lastovo Island was recently developed by Jacobsen (2024). Numerical experiments conducted with the Regional Ocean Modeling System (ROMS) coupled to a simplified NPZD (nutrient, phytoplankton, zooplankton, detritus) ecosystem model quantified the response of nutrients, phytoplankton biomass and primary production to ITWs under varying light and wind conditions (Jacobsen, 2024). Under constant light, nutrient availability and primary production increased by 6.1% and 5.4% at 23 m (thermocline), and by 20.5% and 15.9% at 40 m (below thermocline), respectively. A more pronounced effect below the thermocline (Jacobsen, 2024) contrasts with *in situ* observations at the Lastovo Island,

which revealed decreases in both $P_T(z)$ and $P^B_T(z)$ below thermocline (**Table 7**). This discrepancy likely arises because the model does not account for complex plankton community interactions or their feedback on nutrient dynamics. Nevertheless, both the model and *in situ* data consistently demonstrate enhanced primary production within the thermocline layer, as reflected by high percentage change in both $P_T(z)$ and $P^B_T(z)$ at 20 m (**Table 7**).

A second experiment incorporating a diel light cycle produced responses similar to those under constant light, indicating that the light cycle does not alter the underlying mechanism by which ITWs affect the ecosystem (Jacobsen, 2024). However, it does influence the spatial distribution of primary production. Congruent with my findings, the diel light cycle introduced strong spatial heterogeneity in primary production at the Lastovo Island (Jacobsen, 2024). However, the spatial pattern simulated by Jacobsen et al. (2023) shows that the western side of the island is the most productive, while my observations identified the highest productivity in the southern region, a discrepancy that requires further research.

6 CONCLUSION

This research presents the first interdisciplinary oceanographic study investigating the effects of ITWs on biology in the Adriatic Sea, specifically plankton community diversity, succession and NPP. The objectives were achieved and the hypotheses confirmed: (i) nano- and pico-fraction dominate the phytoplankton community in the stratified oligotrophic water column off the Lastovo Island in the Southern Adriatic Sea; (ii) changes in physico-chemical conditions of the water column due to vertical thermocline oscillations define plankton succession and correlations between plankton communities; (iii) island trapped waves influence daily net phytoplankton primary production in the oligotrophic ecosystem off the Lastovo Island; (iv) inverse numerical model defines daily net primary production profile, and daily and yearly water column production off the Lastovo Island. However, the fourth hypothesis was only partially tested as the inverse numerical model could not be fully applied. This limitation arose from the lack of concurrent measurements of the underwater light field, which prevented conclusions on phytoplankton photoacclimation during primary production measurements. Consequently, the retrieved photosynthesis parameters were not suitable for further modeling of daily and annual water column production at the Lastovo Island. Nevertheless, Copernicus-derived ocean colour remote sensing data were successfully used to estimate annual water-column production.

The main findings of this dissertation can be summarized for each objective under the following points:

O1: Describe taxonomic composition of phytoplankton in the stratified oligotrophic ecosystem influenced by rare oceanographic phenomena - island trapped waves (ITWs).

- A total of 112 taxa were identified, comprising 64 diatoms, 33 dinoflagellates, 11 coccolithophores and 4 other autotrophs, including Cryptophyta, Chlorophyceae, Chrysophyceae and *Dictyocha fibula*.
- The phytoplankton community composition was characteristic of a stratified oligotrophic ecosystem, with picophytoplankton being the most abundant group in the water column, followed by nano- and microphytoplankton.
- Diatoms and dinoflagellates contributed the most to micro- and nanophytoplankton, respectively. Picophytoplankton consisted mainly of *Prochlorococcus* sp. and *Synechococcus* sp., while PPEs were the least abundant.

- The most abundant group was nano-fraction dinoflagellates, followed by micro-fraction penatae diatoms and micro-fraction coccolithophores. The most dominant species was *Proboscia alata*, followed by *Rhizosolenia imbricata*, *Pseudo-nitzschia delicatissima*, *Gyrodinium fusiforme* and *Scripsiella* sp.

O2: Describe succession and correlation between plankton communities, and their response to changes in the physco-chemical conditions of the oligotrophic stratified water column.

- The temporal succession of phytoplankton abundances did not change in relation to ITWs. However, the vertical distribution of the phytoplankton community was defined by the stratification influenced by ITWs.
- The surface and thermocline layers, characterized by high temperature and increased phosphate concentrations, were dominated by pico- and nanophytoplankton, while microphytoplankton contributed the most to the deep layer, which showed elevated concentrations of Chl *a*, nitrite, nitrate and silicic acid.
- A clear niche partitioning of *Synechococcus* and *Prochlorococcus* was observed, with the highest abundances in the surface and deep layers, respectively. The highest proportion of variability explained by environmental parameters was found in the picophytoplankton community, confirming that these organisms are strongly constrained by temperature, light and nutrient conditions, and suggesting that they are the first to respond to ITW-related changes.
- ITWs effect was indirectly reflected in both bacterioplankton and zooplankton communities, as revealed by concurrent research alongside this dissertation.
- An increase in bacterial abundance was observed within the thermocline layer during ITWs, accompanied by a shift in bacterial functional profiles toward enhanced nutrient cycling, particularly nitrites and nitrates, consistent with distinct nutrient dynamics observed during ITWs.
- The abundances of certain micro- and mesozooplankton groups shift during ITWs, suggesting adaptation to changes in grazing pressure and feeding preferences. This was further corroborated by analyses of co-occurrence trophic networks, which became more complex during ITWs.

O3: Determine in situ daily net primary production in the oligotrophic stratified ecosystem off the Lastovo Island influenced by ITWs.

- *In situ* daily net primary production ($P_T(z)$) and daily depth-integrated water column production ($P_{Z,T}$) measured at the Korčula and Lastovo islands are characteristic of oligotrophic Adriatic Sea.
- No significant change in $P_T(z)$ and $P_{Z,T}$ was detected in response to ITWs. Nevertheless, the thermocline layer showed notable variability: $P_T(z)$ and $P^B_T(z)$ at 20 m increased by 18.12% and 97.90%, respectively. However, this is not reflected in daily $P_{Z,T}$ which changes by only 3.65%, while normalized $P_{Z,T}$ decreases during ITWs by 14.62%, driven in part by elevated photosynthetic activity in the surface layer before ITWs.
- Nutrient concentrations did not show a clear, consistent signal of ITW-driven flux. A few outlying observations within the thermocline are compatible with episodic upward nutrient transport, but the data suggest nutrient levels are influenced more by biological activity, notably bacterial dynamics.
- Underwater light-field modelling indicated that when ITWs and diel light cycle are in phase, light availability increases in the thermocline layer. At the southern station S1, afternoon irradiance increased by up to 60 W m^{-2} when the thermocline was displaced toward the surface, a change that could enhance photosynthesis locally and thereby affect primary production.

O4: Implement inverse numerical model to determine daily net primary production profile, and daily and yearly water column production in the stratified island ecosystem of the Southern Adriatic Sea.

- The inverse numerical model was successfully applied, accurately reproducing *in situ* profiles with minimal error. This study confirmed its efficiency in modeling regional daily NPP at depth. However, due to the lack of concurrent underwater light-field data, the resulting photosynthetic parameters were not suitable for modeling daily and annual water column production at the Lastovo Island.
- The Copernicus biogeochemical model for the Mediterranean Sea was used to estimate daily water column production, which was found to overestimate the experimental results.
- Annual primary production at the Lastovo Island (approximately 115–123 g C m^{-2}) together with an ITWs contribution of approximately 1.5–3.8% demonstrate that ITWs, though episodic and local, provide a measurable boost to the regional productivity budget.

- Remote sensing data indicated a heterogeneous spatial distribution of NPP, with higher values observed in the southern region, particularly during ITWs. This pattern aligns with the observed increase in light availability when ITW and light cycles coincide and is consistent with previous studies showing that the interaction between these cycles governs the spatial distribution of primary production.

Research on the impact of ITWs on marine ecosystems is still emerging but holds significant implications for understanding the adaptive strategies of plankton communities, particularly primary producers, in stratified systems that are expected to become more widespread under climate change-driven ocean warming. The research of this dissertation demonstrated that the Lastovo Island is an ideal natural laboratory for coupled physico-chemical and biological studies. When integrated with operational meteo-oceanographic forecasts, it enables adaptive and efficient sampling at scale where physical and biological processes interact, thereby capturing rapid shifts in the marine environment with high spatio-temporal resolution. ITWs forming at the Lastovo Island represent a phenomenon in which a nutrient-poor, stratified system temporarily transforms into a more favorable environment for primary producers. On a broader scale, such atypical ecosystems may serve as critical refuges under future climate scenarios where ocean productivity is projected to decline. Understanding these dynamics is crucial, since primary production remains essential for supporting and regulating our global ocean ecosystems, serving as a pillar of the marine food web and of global biogeochemical cycles.

Following this research, future studies should focus on more detailed *in situ* primary production measurements during ITWs on the opposite sides of the Lastovo Island, particularly at Struga and Maslovnjak. These measurements should be complemented by concurrent measurements of underwater light field and phytoplankton community composition, providing a more comprehensive understanding of ecosystem dynamics during ITWs. It would be particularly valuable to investigate how phytoplankton acclimate to light conditions and to quantify the time lag in their response to increased light availability and nutrient input, thereby distinguishing whether the response is primarily light- or nutrient-driven, or both. Further research is also needed to clarify the extent to which nutrient dynamics are modulated by bacterial activity during ITWs at the Lastovo Island. Moreover, assessing the influence of ITWs on NPP spatio-temporal distribution using high-resolution (300 m–1 km) coastal products would better capture localized nearshore effects. Such datasets would also improve the accuracy of annual NPP estimates and, when compared with open-sea values, allow a clearer quantification of the ITW

contribution to both summer and annual ecosystem productivity. This requires future tailoring of regional ocean colour remote sensing products specifically for the southern Adriatic Sea.

Further integration of operational meteo-oceanographic forecasts in marine ecology research should be strongly encouraged, as it is essential for accurately assessing the physico-biological interactions. More *in situ* observations of primary production are needed, especially in oligotrophic regions. Conducting experiments in accordance with standardized protocols is essential to enhance comparability between ocean regions. Promoting optical oceanography is also crucial, as investigation of the underwater light field can enhance understanding of phytoplankton photoacclimation and enable more accurate estimates of regional daily and annual water column production, as well as its variability under the influence of regional physical processes and climate change. In the future, particularly for semi-enclosed coastal systems such as the Adriatic Sea, it is imperative to accurately integrate *in situ* observations with ocean colour remote sensing and models to build a holistic view of primary production across broader spatial and temporal scales. Ultimately, effective monitoring of primary production is fundamental to achieving a comprehensive understanding of ocean productivity in a rapidly changing world.

7 REFERENCES

Babić, I., Mucko, M., Petrić, I., Bosak, S., Mihanović, H., Vilibić, I., Dupčić Radić, I., Cetinić, I., Balestra, C., Casotti, R., & Ljubešić, Z. (2018). Multilayer approach for characterization of bacterial diversity in a marginal sea: From surface to seabed. *Journal of Marine Systems*, *184*, 15–27. https://doi.org/10.1016/j.jmarsys.2018.04.002

Balch, W. M., Carranza, M., Cetinić, I., Chaves, J. E., Duhamel, S., Erickson, Z., Fassbender, A., Fernandez-Carrera, A., Ferrón, S., García-Martín, E., Goes, J., Gomes, H., Gorbunov, M., Gundersen, K., Halsey, K., Hirawake, T., Isada, T., Juranek, L., Kulk, G., … Vandermeulen, R. A. (2022). Aquatic primary productivity field protocols for satellite validation and model synthesis. In R. A. Vandermeulen & J. E. Chaves (Eds.), *IOCCG Ocean Optics and Biogeochemistry Protocols for Satellite Ocean Colour Sensor Validation, Volume 7.0* (IOCCG Protocol Series). International Ocean Colour Coordinating Group (IOCCG).

Becacos-Kontos, T. (1977). Primary production and environmental factors in an oligotrophic biome in the Aegean Sea. *Marine Biology*, *42*(2), 93–98. https://doi.org/10.1007/BF00391559

Becker, S., Aoyama, M., Woodward, E., Bakker, K., Coverly, S., Mahaffey, C., & Tanhua, T. (2020). GO-SHIP repeat hydrography nutrient manual: The precise and accurate determination of dissolved inorganic nutrients in seawater, using continuous flow analysis methods. *Frontiers in Marine Science*, *7*, 581790. https://doi.org/10.3389/fmars.2020.581790

Begouen Demeaux, C., Boss, E., Graff, J. R., Behrenfeld, M. J., & Westberry, T. K. (2025). Phytoplanktonic photoacclimation under clouds. *Geophysical Research Letters*, *52*(6), e2024GL112274. https://doi.org/10.1029/2024GL112274

Behrenfeld, M. J., Halsey, K. H., & Milligan, A. J. (2008). Evolved physiological responses of phytoplankton to their integrated growth environment. *Philosophical Transactions of the Royal Society B: Biological Sciences*, *363*(1504), 2687–2703. https://doi.org/10.1098/rstb.2008.0019

Berland, B., Burlakova, Z. P., Georgieva, L., Izmestieva, M., Kholodov, V., Krupatkina, D. K., Maestrini, S., & Zaika, V. E. (1987). *Phytoplancton estival de la mer du Levant, biomasse et facteurs limitants*. *2*, 61–83.

Berman, T., Townsend, D., Elsayed, S., Trees, C., & Azov, Y. (1984). Optical transparency, chlorophyll and primary productivity in the eastern mediterranean near the israeli coast. *Oceanologica Acta*, *7*(3), 367–372.

Berthon, J.-F., & Zibordi, G. (2004). Bio-optical relationships for the northern Adriatic Sea. *International Journal of Remote Sensing*, *25*(7–8), 1527–1532. https://doi.org/10.1080/01431160310001592544

Boldrin, A., Miserocchi, S., Rabitti, S., Turchetto, M. M., Balboni, V., & Socal, G. (2002). Particulate matter in the southern Adriatic and Ionian Sea: Characterisation and downward fluxes. *Journal of Marine Systems*, *33–34*, 389–410. https://doi.org/10.1016/S0924-7963(02)00068-4

Bosak, S., Mejdandžić, M., Bošnjak, I., Godrijan, J., & Ljubešić, Z. (2015). Taxonomy and spatial distribution of phytoplankton in the South Adriatic: Winter aspect. In *Book of Abstracts of the 12th Croatian Biological Congress* (p. 83).

Bouman, H. A., Platt, T., Doblin, M., Figueiras, F. G., Gudmundsson, K., Gudfinnsson, H. G., Huang, B., Hickman, A., Hiscock, M., Jackson, T., Lutz, V. A., Melin, F., Rey, F., Pepin, P., Segura, V., Tilstone, G. H., van Dongen-Vogels, V., & Sathyendranath, S. (2018). Photosynthesis-irradiance parameters of marine phytoplankton: Synthesis of a global data set. *Earth System Science Data*, *10*(1), 251–266. https://doi.org/10.5194/essd-10-251-2018

Bourdin, G., Karp-Boss, L., Lombard, F., Gorsky, G., & Boss, E. (2024). Dynamic island mass effect from space. Part I: Detecting the extent. *EGUsphere*, 1–38. https://doi.org/10.5194/egusphere-2024-2670

Brink, K. H. (1991). Coastal-trapped waves and wind-driven currents over the continental shelf. *Annual Review of Fluid Mechanics*, *23*, 389–412. https://doi.org/10.1146/annurev.fl.23.010191.002133

Brink, K. H. (1999). Island-trapped waves, with application to observations off Bermuda. *Dynamics of Atmospheres and Oceans*, *29*(2), 93–118. https://doi.org/10.1016/S0377-0265(99)00003-2

Brush, M. J., Mozetič, P., Francé, J., Aubry, F. B., Djakovac, T., Faganeli, J., Harris, L. A., & Niesen, M. (2020). Phytoplankton dynamics in a changing environment. In *Coastal Ecosystems in Transition* (Vol. 256, pp. 49–74). American Geophysical Union (AGU). https://doi.org/10.1002/9781119543626.ch4

Buljan, M. (1964). An estimate of productivity of the Adriatic Sea made on the basis of its hydrographic properties. *Acta Adriatica*, *11*, 35–45.

Burić, Z., Cetinić, I., Viličić, D., Mihalić, K. C., Carić, M., & Olujić, G. (2007). Spatial and temporal distribution of phytoplankton in a highly stratified estuary (Zrmanja, Adriatic Sea). *Marine Ecology*, *28*(S1), 169–177. https://doi.org/10.1111/j.1439-0485.2007.00180.x

Calbet, A., Carlotti, F., & Gaudy, R. (2007). The feeding ecology of the copepod *Centropages typicus* (Kröyer). *Progress in Oceanography*, *72*(2–3), 137–150. https://doi.org/10.1016/j.pocean.2007.01.003

Čalić, M., Carić, M., Kršinić, F., Jasprica, N., & Pećarević, M. (2013). Controlling factors of phytoplankton seasonal succession in oligotrophic Mali Ston Bay (south-eastern Adriatic). *Environmental Monitoring and Assessment*, *185*(9), 7543–7563. https://doi.org/10.1007/s10661-013-3118-2

Cantoni, C., Cozzi, S., Pecchiar, I., Cabrini, M., Mozetič, P., Catalano, G., & Umani, S. F. (2003). Short-term variability of primary production and inorganic nitrogen uptake related to the environmental conditions in a shallow coastal area (Gulf of Trieste, N Adriatic Sea). *Oceanologica Acta*, *26*(5), 565–575. https://doi.org/10.1016/S0399-1784(03)00050-1

Cerino, F., Bernardi Aubry, F., Coppola, J., La Ferla, R., Maimone, G., Socal, G., & Totti, C. (2012). Spatial and temporal variability of pico-, nano- and microphytoplankton in the offshore waters of the southern Adriatic Sea (Mediterranean Sea). *Continental Shelf Research*, *44*(1), 94–105. https://doi.org/10.1016/j.csr.2011.06.006

Cervantes-Duarte, R., González-Rodríguez, E., Funes-Rodríguez, R., Ramos-Rodríguez, A., Torres-Hernández, M. Y., & Aguirre-Bahena, F. (2021). Variability of net primary productivity and associated biophysical drivers in Bahía de La Paz (Mexico). *Remote Sensing*, *13*(9), 1644. https://doi.org/10.3390/rs13091644

Cetinić, I., Rousseaux, C. S., Carroll, I. T., Chase, A. P., Kramer, S. J., Werdell, P. J., Siegel, D. A., Dierssen, H. M., Catlett, D., Neeley, A., Soto Ramos, I. M., Wolny, J. L., Sadoff, N., Urquhart, E., Westberry, T. K., Stramski, D., Pahlevan, N., Seegers, B. N., Sirk, E., … Sayers, M. (2024). Phytoplankton composition from sPACE: Requirements, opportunities, and challenges. *Remote Sensing of Environment*, 302, 113964. https://doi.org/10.1016/j.rse.2023.113964

Chavez, F. P., Messié, M., & Pennington, J. T. (2011). Marine primary production in relation to climate variability and change. *Annual Review of Marine Science*, *3*(1), 227–260. https://doi.org/10.1146/annurev.marine.010908.163917

Chen, T.-Y., Tai, J.-H., Ko, C.-Y., Hsieh, C., Chen, C.-C., Jiao, N., Liu, H.-B., & Shiah, F.-K. (2016). Nutrient pulses driven by internal solitary waves enhance heterotrophic bacterial growth in the South China Sea. *Environmental Microbiology*, *18*(12), 4312–4323. https://doi.org/10.1111/1462-2920.13273

Chen, Z., Sun, J., Gu, T., Zhang, G., & Wei, Y. (2021). Nutrient ratios driven by vertical stratification regulate phytoplankton community structure in the oligotrophic western Pacific Ocean. *Ocean Science, 17*(6), 1775–1789. https://doi.org/10.5194/os-17-1775-2021

Civitarese, G., Gačić, M., Batistić, M., Bensi, M., Cardin, V., Dulčić, J., Garić, R., & Menna, M. (2023). The BiOS mechanism: History, theory, implications. *Progress in Oceanography, 216*, 103056. https://doi.org/10.1016/j.pocean.2023.103056

Civitarese, G., Gačić, M., Lipizer, M., & Eusebi Borzelli, G. L. (2010). On the impact of the Bimodal Oscillating System (BiOS) on the biogeochemistry and biology of the Adriatic and Ionian Seas (Eastern Mediterranean). *Biogeosciences*, *7*(12), 3987–3997. https://doi.org/10.5194/bg-7-3987-2010

Closset, I., McNair, H. M., Brzezinski, M. A., Krause, J. W., Thamatrakoln, K., & Jones, J. L. (2021). Diatom response to alterations in upwelling and nutrient dynamics associated with climate forcing in the California Current System. *Limnology and Oceanography*, *66*(4), 1578–1593. https://doi.org/10.1002/lno.11705

Coello-Camba, A., & Agustí, S. (2021). Picophytoplankton niche partitioning in the warmest oligotrophic sea. *Frontiers in Marine Science*, 8, 651877. https://doi.org/10.3389/fmars.2021.651877

Coma, R., Ribes, M., Serrano, E., Jiménez, E., Salat, J., & Pascual, J. (2009). Global warming-enhanced stratification and mass mortality events in the Mediterranean. *Proceedings of*

the National Academy of Sciences, *106*(15), 6176–6181. https://doi.org/10.1073/pnas.0805801106

Cooper, L. H. N. (1947). Internal waves and upwelling of oceanic water from mid-depths on to a continental shelf. *Nature*, *159*(4043), 579–580. https://doi.org/10.1038/159579c0

Cozzi, S., & Giani, M. (2011). River water and nutrient discharges in the Northern Adriatic Sea: Current importance and long term changes. *Continental Shelf Research*, *31*(18), 1881–1893. https://doi.org/10.1016/j.csr.2011.08.010

Cozzi, S., Ibáñez, C., Lazar, L., Raimbault, P., & Giani, M. (2019). Flow regime and nutrient-loading trends from the largest South European watersheds: Implications for the productivity of Mediterranean and Black Sea's coastal areas. *Water*, *11*(1), 1. https://doi.org/10.3390/w11010001

Cros, L., & Fortuño, J. M. (2002). Atlas of Northwestern Mediterranean coccolithophores. *Scientia Marina*, *66*(S1), 1–182. https://doi.org/10.3989/scimar.2002.66s11

da Costa, V. S., Alessandri, J., Verri, G., Mentaschi, L., Guerra, R., & Pinardi, N. (2024). Marine climate indicators in the Adriatic Sea. *Frontiers in Climate*, *6*, 1449633. https://doi.org/10.3389/fclim.2024.1449633

da Silva, J. C. B., New, A. L., Srokosz, M. A., & Smyth, T. J. (2002). On the observability of internal tidal waves in remotely-sensed ocean colour data. *Geophysical Research Letters*, *29*(12), 10–14. https://doi.org/10.1029/2001GL013888

De Falco, C., Desbiolles, F., Bracco, A., & Pasquero, C. (2022). Island mass effect: A review of oceanic physical processes. *Frontiers in Marine Science*, *9*, 894860. https://doi.org/10.3389/fmars.2022.894860

De Falco, C., Bracco, A., Desbiolles, F., & Pasquero, C. (2024). Kilometer-scale ocean processes behind the variability of the Island Mass Effect in the Maldives. *Scientific Reports*, *14*(1), 17568. https://doi.org/10.1038/s41598-024-63836-9

De La Rocha, C. L., & Passow, U. (2007). Factors influencing the sinking of POC and the efficiency of the biological carbon pump. *Deep Sea Research Part II: Topical Studies in Oceanography*, *54*(5), 639–658. https://doi.org/10.1016/j.dsr2.2007.01.004

de Vargas, C., Audic, S., Henry, N., Decelle, J., Mahé, F., Logares, R., Lara, E., Berney, C., Le Bescot, N., Probert, I., Carmichael, M., Poulain, J., Romac, S., Colin, S., Aury, J.-M., Bittner, L., Chaffron, S., Dunthorn, M., Engelen, S., … Karsenti, E. (2015). Eukaryotic plankton diversity in the sunlit ocean. *Science*, *348*(6237), 1261605. https://doi.org/10.1126/science.1261605

Decembrini, F., Caroppo, C., & Azzaro, M. (2009). Size structure and production of phytoplankton community and carbon pathways channelling in the Southern Tyrrhenian Sea (Western Mediterranean). *Deep Sea Research Part II: Topical Studies in Oceanography*, *56*(11–12), 687–699. https://doi.org/10.1016/j.dsr2.2008.07.022

Degobbis, D., Gilmartin, M., & Revelante, N. (1986). An annotated nitrogen budget calculation for the northern Adriatic Sea. *Marine Chemistry*, *20*(2), 159–177. https://doi.org/10.1016/0304-4203(86)90037-X

Dematteis, G., Le Boyer, A., Pollmann, F., Polzin, K. L., Alford, M. H., Whalen, C. B., & Lvov, Y. V. (2024). Interacting internal waves explain global patterns of interior ocean mixing. *Nature Communications*, *15*(1), 7468. https://doi.org/10.1038/s41467-024-51503-6

Denamiel, C. (2025). Far-future climate projection of the Adriatic marine heatwaves: A kilometre-scale experiment under extreme warming. *Ocean Science*, *21*(5), 1909–1931. https://doi.org/10.5194/os-21-1909-2025

Denman, K. L. (1994). Scale-determining biological-physical interactions in oceanic food webs. In *Aquatic Ecology: Scale, Pattern and Process.* (pp. 377–402). Blackwell Science.

Dolan, J. R., Vidussi, F., & Claustre, H. (1999). Planktonic ciliates in the Mediterranean Sea: Longitudinal trends. *Deep Sea Research Part I: Oceanographic Research Papers*, *46*(12), 2025–2039. https://doi.org/10.1016/S0967-0637(99)00043-6

D'Ortenzio, F., Iudicone, D., de Boyer Montegut, C., Testor, P., Antoine, D., Marullo, S., Santoleri, R., & Madec, G. (2005). Seasonal variability of the mixed layer depth in the Mediterranean Sea as derived from *in situ* profiles. *Geophysical Research Letters*, *32*(12), L12605. https://doi.org/10.1029/2005GL022463

Doty, M. S., & Oguri, M. (1956). The Island Mass Effect. *ICES Journal of Marine Science*, *22*(1), 33–37. https://doi.org/10.1093/icesjms/22.1.33

Drakulović, D., Krivokapić, S., Mandić, M., & Redžic, A. (2013). Phytoplankton community in Boka Kotorska bay (South-Eastern Adriatic). *Rapports et Procès-Verbaux Des Réunions de La Commission Internationale Pour l'Exploration Scienti-Fique de La Mer Méditerranée*, *40*, 428.

Drakulović, D., Vuksanović, N., & Joksimović, D. (2010). Dynamics of phytoplankton in Boka Kotorska bay. *Studia Marina*, *25*(1), 1–20.

Duarte, C. M., Agustí, S., Gasol, J. M., Vaqué, D., & Vazquez-Dominguez, E. (2000). Effect of nutrient supply on the biomass structure of planktonic communities: An experimental test on a Mediterranean coastal community. *Marine Ecology Progress Series*, *206*, 87–95. https://doi.org/10.3354/meps206087

Durkin, C. A., Buesseler, K. O., Cetinić, I., Estapa, M. L., Kelly, R. P., & Omand, M. (2021). A visual tour of carbon export by sinking particles. *Global Biogeochemical Cycles*, *35*(10), e2021GB006985. https://doi.org/10.1029/2021GB006985

Durkin, C. A., Cetinić, I., Estapa, M., Ljubešić, Z., Mucko, M., Neeley, A., & Omand, M. (2022). Tracing the path of carbon export in the ocean though DNA sequencing of individual sinking particles. *The ISME Journal*, *16*(8), 1941–1951. https://doi.org/10.1038/s41396-022-01239-2

Ercegović, A. (1938). Productivity of the East Adriatic waters [in Croatian]. *Godišnjak Oceanografskog Instituta Kraljevine Jugoslavije*, *1*, 1–50.

Estrada, M. (1991). Phytoplankton assemblages across a NW Mediterranean front: changes from winter mixing to spring stratification. In J. Ros & N. Pratt (Eds.), *Homage to Ramon Margalef; or, Why There Is Such Pleasure in Studying Nature* (*Oecologia Aquatica*, Vol. 10, pp. 157-185).

Estrada, M., & Blasco, D. (1979). Two phases of the phytoplankton community in the Baja California upwelling. *Limnology and Oceanography*, *24*(6), 1065–1080. https://doi.org/10.4319/lo.1979.24.6.1065

Estrada, M., Marrase, C., Latasa, M., Berdalet, E., Delgado, M., & Riera, T. (1993). Variability of deep chlorophyll maximum characteristics in the northwestern Mediterranean. *Marine Ecology Progress Series*, *92*(3), 289–300.

Evans, M. A., MacIntyre, S., & Kling, G. W. (2008). Internal wave effects on photosynthesis: Experiments, theory, and modeling. *Limnology and Oceanography*, *53*(1), 339–353. https://doi.org/10.4319/lo.2008.53.1.0339

Falkowski, P. G., Katz, M. E., Knoll, A. H., Quigg, A., Raven, J. A., Schofield, O., & Taylor, F. J. R. (2004). The evolution of modern eukaryotic phytoplankton. *Science*, *305*(5682), 354–360. https://doi.org/10.1126/science.1095964

Feudale, L., Bolzon, G., Lazzari, P., Salon, S., Teruzzi, A., Di Biagio, V., Coidessa, G., Alvarez, E., Amadio, C., & Cossarini, G. (2023). *Mediterranean Sea biogeochemical analysis and forecast (Copernicus Marine Service MED-Biogeochemistry, MedBFM4 system) (Version 2)* [Data set]. Copernicus Marine Service. https://doi.org/10.25423/cmcc/medsea_analysisforecast_bgc_006_014_medbfm4

Field, C. B., Behrenfeld, M. J., Randerson, J. T., & Falkowski, P. (1998). Primary production of the biosphere: Integrating terrestrial and oceanic components. *Science (New York, N.Y.)*, *281*(5374), 237–240. https://doi.org/10.1126/science.281.5374.237

Freilich, M. A., & Mahadevan, A. (2019). Decomposition of vertical velocity for nutrient transport in the upper ocean. *Journal of Physical Oceanography*, *49*(6), 1561-1575. https://doi.org/10.1175/JPO-D-19-0002.1

Freilich, M., Flierl, G., & Mahadevan, A. (2022). Diversity of growth rates maximizes phytoplankton productivity in an eddying ocean. *Geophysical Research Letters*, *49*(3), e2021GL096180. https://doi.org/10.1029/2021GL096180

Frouin, R. J., Franz, B. A., Ibrahim, A., Knobelspiesse, K., Ahmad, Z., Cairns, B., Chowdhary, J., Dierssen, H. M., Tan, J., Dubovik, O., Huang, X., Davis, A. B., Kalashnikova, O., Thompson, D. R., Remer, L. A., Boss, E., Coddington, O., Deschamps, P.-Y., Gao, B.-C., … Zhai, P.-W. (2019). Atmospheric correction of satellite ocean-color imagery suring the PACE era. *Frontiers in Earth Science*, *7*, 145. https://doi.org/10.3389/feart.2019.00145

Gallina, A. A., Celussi, M., & Del Negro, P. (2011). Large-scale distribution and production of bacterioplankton in the Adriatic Sea. *Journal of Sea Research*, *66*(1), 1–8. https://doi.org/10.1016/j.seares.2011.03.009

Garrett, C. (2003). Internal tides and ocean mixing. *Science*, *301*(5641), 1858–1859. https://doi.org/10.1126/science.1090002

Garrett, C., & Munk, W. (1979). Internal waves in the ocean. *Annual Review of Fluid Mechanics*, *11*, 339–369. https://doi.org/10.1146/annurev.fl.11.010179.002011

Gaxiola-Castro, G., Alvarez-Borrego, S., Nájera-Martínez, S., & Zirino, A. (2002). Internal waves effect on the Gulf of California phytoplankton. *Ciencias Marinas*, *28*, 297–309. https://doi.org/10.7773/cm.v28i3.222

Getzner, M., Jungmeier, M., & Špika, M. (2017). Willingness-to-pay for improving marine biodiversity: A case study of Lastovo Archipelago Marine Park (Croatia). *Water*, *9*(1), 2. https://doi.org/10.3390/w9010002

Giaccone, G., & Geraci, R. (1989). Biogeografia delle alghe del Mediterráneo. *Anales Del Jardin Botanico De Madrid*, *1*, 27–34.

Gilmartin, M., & Revelante, N. (1983). The phytoplankton of the Adriatic Sea: Standing crop and primary production. *Thalassia Jugoslavica*, *19*, 173–188.

Giordani, P., Miserocchi, S., Balboni, V., Malaguti, A., Lorenzelli, R., Honsell, G., & Poniz, P. (1997). Factors controlling trophic conditions in the north-west Adriatic basin: Seasonal variability. *Marine Chemistry*, *58*(3–4), 351–360. https://doi.org/10.1016/S0304-4203(97)00061-3

Gómez, F. (2006). Endemic and Indo-Pacific plankton in the Mediterranean Sea: A study based on dinoflagellate records. *Journal of Biogeography*, *33*(2), 261–270. https://doi.org/10.1111/j.1365-2699.2005.01373.x

Goryl, P., Fox, N., Donlon, C., & Castracane, P. (2023). Fiducial Reference Measurements (FRMs): What are they? *Remote Sensing*, *15*(20), 5017. https://doi.org/10.3390/rs15205017

Goto, N., Kawamura, T., Mitamura, O., & Terai, H. (1999). Importance of extracellular organic carbon production in the total primary production by tidal-flat diatoms in comparison to phytoplankton. *Marine Ecology Progress Series*, *190*, 289–295. https://doi.org/10.3354/meps190289

Gotsis-Skretas, O., Pagou, K., Moraitou-Apostolopoulou, M., & Ignatiades, L. (1999). Seasonal horizontal and vertical variability in primary production and standing stocks of phytoplankton and zooplankton in the Cretan Sea and the Straits of the Cretan Arc (March 1994–January 1995). *Progress in Oceanography*, *44*(4), 625–649. https://doi.org/10.1016/S0079-6611(99)00048-8

Gran, H. H., & Braarud, T. (1935). A quantitative study on the phytoplankton of the bay of fundy and the gulf of Maine (including observations on hydrography, chemistry and morbidity). *Journal of the Biological Board of Canada*, 1, 219–467.

Granéli, E., Carlsson, P., Turner, J. T., Tester, P. A., Béchemin, C., Dawson, R., & Funari, E. (1999). Effects of N:P:Si ratios and zooplankton grazing on phytoplankton communities in the northern Adriatic Sea.: I.: Nutrients, phytoplankton biomass, and polysaccharide production. *Aquatic Microbial Ecology*, *18*(1), 37–54. https://doi.org/10.3354/ame018037

Gran-Stadniczeñko, S., Egge, E., Hostyeva, V., Logares, R., Eikrem, W., & Edvardsen, B. (2019). Protist diversity and seasonal dynamics in Skagerrak plankton communities as revealed by metabarcoding and microscopy. *Journal of Eukaryotic Microbiology*, *66*(3), 494–513. https://doi.org/10.1111/jeu.12700

Grbec, B., Morović, M., Paklar, G. B., Kušpilić, G., Matijević, S., Matić, F., & Gladan, Ž. N. (2009). The relationship between the atmospheric variability and productivity in the Adriatic Sea area. *Journal of the Marine Biological Association of the United Kingdom*, *89*(8), 1549–1558. https://doi.org/10.1017/S0025315409000708

Grilli, F., Accoroni, S., Acri, F., Bernardi Aubry, F., Bergami, C., Cabrini, M., Campanelli, A., Giani, M., Guicciardi, S., Marini, M., Neri, F., Penna, A., Penna, P., Pugnetti, A., Ravaioli, M., Riminucci, F., Ricci, F., Totti, C., Viaroli, P., & Cozzi, S. (2020). Seasonal and interannual trends of oceanographic parameters over 40 years in the northern Adriatic Sea in relation to nutrient loadings using the EMODnet chemistry data portal. *Water*, *12*(8), 2280. https://doi.org/10.3390/w12082280

Gržetić, Z., Precali, R., Degobbis, D., & Škrivanić, A. (1991). Nutrient enrichment and phytoplankton response in an Adriatic karstic estuary. *Marine Chemistry*, *32*(2–4), 313–331. https://doi.org/10.1016/0304-4203(91)90046-Y

Guan, Z., Ge, R., Li, Y., Zou, L., & Yang, S. (2023). Diel variation of phytoplankton communities in the northern South China Sea under the effect of internal solitary waves and its response to environmental factors. *Water*, *15*(13), 2422. https://doi.org/10.3390/w15132422

Hafner, D., Car, A., Jasprica, N., Kapetanović, T., & Radić, I. D. (2018). Relationship between marine epilithic diatoms and environmental variables in oligotrophic bay, NE Mediterranean. *Mediterranean Marine Science*, *19*(2), 245–256. https://doi.org/10.12681/mms.14151

Harris, G. P. (1987). *Phytoplankton Ecology: Structure, Function and Fluctuation*. Springer Netherlands. https://doi.org/10.1007/978-94-009-4081-9

Harris, G. P., & Trimbee, A. M. (1986). Phytoplankton population dynamics of a small reservoir: Physical/biological coupling and the time scales of community change. *Journal of Plankton Research*, *8*(6), 1011–1025. https://doi.org/10.1093/plankt/8.6.1011

Harrison, W. G. (1980). Nutrient regeneration and primary production in the sea. In P. G. Falkowski (Ed.), *Primary Productivity in the Sea* (pp. 433–460). Springer US. https://doi.org/10.1007/978-1-4684-3890-1_24

Hartkamp, J. (2025). *Response of planktonic and benthic communities to small-scale physical processes - case study of island-trapped waves* [Bachelor's thesis, University of Zagreb, Faculty of Science].

Henley, W. J., Hironaka, J. L., Guillou, L., Buchheim, M. A., Buchheim, J. A., Fawley, M. W., & Fawley, K. P. (2004). Phylogenetic analysis of the 'Nannochloris-like' algae and diagnoses of *Picochlorum oklahomensis* gene. et sp. nov. (Trebouxiophyceae, Chlorophyta). *Phycologia*, *43*(6), 641–652. https://doi.org/10.2216/i0031-8884-43-6-641.1

Henson, S. A., Sanders, R., & Madsen, E. (2012). Global patterns in efficiency of particulate organic carbon export and transfer to the deep ocean. *Global Biogeochemical Cycles*, *26*(1), GB1028. https://doi.org/10.1029/2011GB004099

Hieronymi, M., Bi, S., Müller, D., Schütt, E. M., Behr, D., Brockmann, C., Lebreton, C., Steinmetz, F., Stelzer, K., & Vanhellemont, Q. (2023). Ocean color atmospheric correction methods in view of usability for different optical water types. *Frontiers in Marine Science*, *10*, 1129876. https://doi.org/10.3389/fmars.2023.1129876

Hogg, N. G. (1980). Observations of internal kelvin waves trapped round Bermuda. *Journal of Physical Oceanography*, *10*(9), 1353–1376. https://doi.org/10.1575/1912/10248

Holloway, G. (1984). Effects of velocity fluctuations on vertical distributions of phytoplankton. *Journal of Marine Research*, *42*, 559–571.

Holloway, G., & Denman, K. (1989). Influence of internal waves on primary production. *Journal of Plankton Research*, *11*(2), 409–413. https://doi.org/10.1093/plankt/11.2.409

Holm-Hansen, O., Lorenzen, C. J., Holmes, R. W., & Strickland, J. D. H. (1965). Fluorometric determination of Chlorophyll. *ICES Journal of Marine Science*, *30*(1), 3–15. https://doi.org/10.1093/icesjms/30.1.3

Huthnance, J. M. (1978). On coastal trapped waves: Analysis and numerical calculation by inverse iteration. *Journal of Physical Oceanography*, *8*(1), 74–92.

Ignatiades, L., Psarra, S., Zervakis, V., Pagou, K., Souvermezoglou, E., Assimakopoulou, G., & Gotsis-Skretas, O. (2002). Phytoplankton size-based dynamics in the Aegean Sea (Eastern Mediterranean). *Journal of Marine Systems*, *36*(1–2), 11–28. https://doi.org/10.1016/S0924-7963(02)00132-X

Ingrosso, G., Giani, M., Cibic, T., Karuza, A., Kralj, M., & Del Negro, P. (2016). Carbonate chemistry dynamics and biological processes along a river-sea gradient (Gulf of Trieste, northern Adriatic Sea). *Journal of Marine Systems*, *155*, 35–49. https://doi.org/10.1016/j.jmarsys.2015.10.013

Jacobsen, J. R. (2024). *The effect of baroclinic processes on marine primary production* [Doctoral dissertation, University of California, Santa Cruz]. https://escholarship.org/uc/item/8pz4z8qv

Jacobsen, J. R., Edwards, C. A., Powell, B. S., Colosi, J. A., & Fiechter, J. (2023). Nutricline adjustment by internal tidal beam generation enhances primary production in idealized numerical models. *Frontiers in Marine Science*, *10*, 1309011. https://doi.org/10.3389/fmars.2023.1309011

Jardillier, L., Boucher, D., Personnic, S., Jacquet, S., Thénot, A., Sargos, D., Amblard, C., & Debroas, D. (2005). Relative importance of nutrients and mortality factors on prokaryotic community composition in two lakes of different trophic status: Microcosm experiments. *FEMS Microbiology Ecology*, *53*(3), 429–443. https://doi.org/10.1016/j.femsec.2005.01.011

Jassby, A. D., & Platt, T. (1976). Mathematical formulation of the relationship between photosynthesis and light for phytoplankton. *Limnology and Oceanography*, *21*(4), 540–547. https://doi.org/10.4319/lo.1976.21.4.0540

Jerlov, N. G. (1964). Optical classification of ocean water. In *Physical Aspects of Light in the Sea* (pp. 45–49). University of Hawaii Press.

John, D. E., López-Díaz, J. M., Cabrera, A., Santiago, N. A., Corredor, J. E., Bronk, D. A., & Paul, J. H. (2012). A day in the life in the dynamic marine environment: How nutrients shape diel patterns of phytoplankton photosynthesis and carbon fixation gene expression in the Mississippi and Orinoco River plumes. *Hydrobiologia*, *679*(1), 155–173. https://doi.org/10.1007/s10750-011-0862-6

Jordi, A., Basterretxea, G., & Wang, D.-P. (2009). Evidence of sediment resuspension by island trapped waves. *Geophysical Research Letters*, *36*(18), L18610. https://doi.org/10.1029/2009GL040055

Justić, D. (1988). Trend in the transparency of the northern Adriatic Sea 1911–1982. *Marine Pollution Bulletin*, *19*(1), 32–35. https://doi.org/10.1016/0025-326X(88)90751-5

Kahru, M. (1983). Phytoplankton patchiness generated by long internal waves: A model. *Marine Ecology Progress Series*, *10*(111–117).

Kamykowski, D. (1974). Possible interactions between phytoplankton and semidiurnal internal tides. *Journal of Marine Research*, *32*(1), 65–87.

Karl, D. M., & Lukas, R. (1996). The Hawaii Ocean Time-series (HOT) program: Background, rationale and field implementation. *Deep Sea Research Part II: Topical Studies in Oceanography*, *43*(2), 129–156. https://doi.org/10.1016/0967-0645(96)00005-7

Kimor, B. (1983). Distinctive features of the plankton of the eastern Mediterranean. *Annales de l'Institut Océanographique*, *59*, 97–106.

Kimor, B., Berman, T., & Schneller, A. (1987). Phytoplankton assemblages in the deep chlorophyll maximum layers off the Mediterranean coast of Israel. *Journal of Plankton Research*, *9*, 433–443.

Kirk, J. T. O. (2010). *Light and Photosynthesis in Aquatic Ecosystems* (3rd ed.). Cambridge University Press. https://doi.org/10.1017/CBO9781139168212

Kong, F., Dong, Q., Xiang, K., Yin, Z., Li, Y., & Liu, J. (2019). Spatiotemporal variability of remote sensing ocean net primary production and major forcing factors in the tropical Eastern Indian and Western Pacific Ocean. *Remote Sensing*, *11*(4), 391. https://doi.org/10.3390/rs11040391

Korlević, M., Pop Ristova, P., Garić, R., Amann, R., & Orlić, S. (2015). Bacterial diversity in the Southern Adriatic Sea during a strong deep winter convection year. *Applied and Environmental Microbiology*, *81*(5), 1715–1726. https://doi.org/10.1128/AEM.03410-14

Körner, M., Brandt, P., Illig, S., Dengler, M., Subramaniam, A., Bachèlery, M.-L., & Krahmann, G. (2024). Coastal trapped waves and tidal mixing control primary production in the tropical Angolan upwelling system. *Science Advances*, *10*(4), eadj6686. https://doi.org/10.1126/sciadv.adj6686

Kovač, Ž., Platt, T., Ninčević Gladan, Ž., Morović, M., Sathyendranath, S., Raitsos, D. E., Grbec, B., Matić, F., & Veža, J. (2018). A 55-year time series station for primary production in the Adriatic Sea: Data correction, extraction of photosynthesis parameters and regime shifts. *Remote Sensing*, *10*(9), 1460. https://doi.org/10.3390/rs10091460

Kovač, Ž., Platt, T., Sathyendranath, S., & Antunović, S. (2017). Models for estimating photosynthesis parameters from *in situ* production profiles. *Progress in Oceanography, 159*, 255–266. https://doi.org/10.1016/j.pocean.2017.10.013

Kovač, Ž., Platt, T., Sathyendranath, S., Morović, M., & Jackson, T. (2016a). Recovery of photosynthesis parameters from *in situ* profiles of phytoplankton production. *ICES Journal of Marine Science, 73*(2), 275–285. https://doi.org/10.1093/icesjms/fsv204

Kovač, Ž., Platt, T., Sathyendranath, S., & Morović, M. (2016b). Analytical solution for the vertical profile of daily production in the ocean. *Journal of Geophysical Research: Oceans, 121*(5), 3532–3548. https://doi.org/10.1002/2015JC011293Kovač, Ž., & Sathyendranath, S. (2025). Critical times for the Critical Depth Theory. *Journal of Geophysical Research: Oceans*, *130*(4), e2024JC021415. https://doi.org/10.1029/2024JC021415

Kramer, S. J., Maritorena, S., Cetinić, I., Werdell, P. J., & Siegel, D. A. (2024). Phytoplankton communities quantified from hyperspectral ocean reflectance correspond to pigment-based communities. *Optics Express*, *32*(20), 34482–34491. https://doi.org/10.1364/OE.529906

Krivokapić, S., Bosak, S., Viličić, D., Kušpilić, G., Drakulović, D., & Pestorić, B. (2018). Algal pigments distribution and phytoplankton group assemblages in coastal transitional environment - Boka Kotorska Bay (southeastern Adriatic Sea). *Acta Adriatica, 59*(1), 35–49. https://doi.org/10.32582/aa.59.1.3

Kveder, S., & Kečkeš, S. (1969). Hydrographic and biotical conditions in North Adriatic. V. Primary phytoplankton productivity. *Ekologija, 2*, 185–191.

Kveder, S., Revelante, N., Smodlaka, N., & Škrivanić, A. (1971). Some characteristics of phytoplankton and phytoplankton productivity in the Northern Adriatic. *Thalassia Jugoslavica, 7*, 151–158.

La Ferla, R., Azzaro, F., Azzaro, M., Caruso, G., Decembrini, F., Leonardi, M., Maimone, G., Monticelli, L. S., Raffa, F., Santinelli, C., Zaccone, R., & Ribera d'Alcalà, M. (2005). Microbial contribution to carbon biogeochemistry in the central Mediterranean Sea: Variability of activities and biomass. *Journal of Marine Systems, 57*(1), 146–166. https://doi.org/10.1016/j.jmarsys.2005.05.001

Lande, R., & Yentsch, C. S. (1988). Internal waves, primary production and the compensation depth of marine phytoplankton. *Journal of Plankton Research, 10*(3), 565–571. https://doi.org/10.1093/plankt/10.3.565

Larkin, A. A., Blinebry, S. K., Howes, C., Lin, Y., Loftus, S. E., Schmaus, C. A., Zinser, E. R., & Johnson, Z. I. (2016). Niche partitioning and biogeography of high light adapted *Prochlorococcus* across taxonomic ranks in the North Pacific. *The ISME Journal, 10*(7), 1557–1567. https://doi.org/10.1038/ismej.2015.244

Latasa, M., Estrada, M., & Delgado, M. (1992). Plankton-pigment relationships in the Northwestern Mediterranean during stratification. *Marine Ecology Progress Series, 88*(1), 61–73. https://doi.org/10.3354/meps088061

Latasa, M., Landry, M. R., Schlüter, L., & Bidigare, R. R. (1997). Pigment-specific growth and grazing rates of phytoplankton in the central equatorial Pacific. *Limnology and Oceanography*, *42*, 289–298. https://doi.org/10.4319/lo.1997.42.2.0289

Lazure, P., Le Cann, B., & Bezaud, M. (2018). Large diurnal bottom temperature oscillations around the Saint Pierre and Miquelon archipelago. *Scientific Reports*, *8*(1), 14167. https://doi.org/10.1038/s41598-018-31857-w

Li, D., Chou, W.-C., Shih, Y.-Y., Chen, G.-Y., Chang, Y., Chow, C. H., Lin, T.-Y., & Hung, C.-C. (2018). Elevated particulate organic carbon export flux induced by internal waves in the oligotrophic northern South China Sea. *Scientific Reports*, *8*(1), 2042. https://doi.org/10.1038/s41598-018-20184-9

Li, G., Cheng, L., Zhu, J., Trenberth, K. E., Mann, M. E., & Abraham, J. P. (2020). Increasing ocean stratification over the past half-century. *Nature Climate Change*, *10*(12), 1116–1123. https://doi.org/10.1038/s41558-020-00918-2

Lindeman, R. L. (1942). The trophic-dynamic aspect of ecology. *Ecology*, *23*(4), 399–417. https://doi.org/10.2307/1930126

Lipizer, M., Gerin, R., Spoto, M., & Mosetti, R. (2006). Seawater optical properties in the Gulf of Trieste during algal blooms. *Biologia Marina Mediterranea*, *13*, 1011–1014.

Lipizer, M., Gerin, R., Spoto, M., & Mosetti, R. (2007). Optical properties and light penetration in the waters of the Gulf of Trieste (northern Adriatic Sea). *Bollettino di Geofisica Teorica ed Applicata*, *48*, 65–78.

Lipizer, M., Partescano, E., Rabitti, A., Giorgetti, A., & Crise, A. (2014). Qualified temperature, salinity and dissolved oxygen climatologies in a changing Adriatic Sea. *Ocean Science*, *10*(5), 771–797. https://doi.org/10.5194/os-10-771-2014

Ljubešić, Z., Mihanović, H., Matek, A., Mucko, M., Achterberg, E. P., Omand, M., Pestorić, B., Lučić, D., Čižmek, H., Čolić, B., Balestra, C., Casotti, R., Janeković, I., & Orlić, M. (2024). Marine plankton community and net primary production responding to island-trapped waves in a stratified oligotrophic ecosystem. *Heliyon*, *10*(18), e37788. https://doi.org/10.1016/j.heliyon.2024.e37788

Ljubimir, S., Jasprica, N., Čalić, M., Hrustić, E., Dupčić Radić, I., Car, A., & Batistić, M. (2017). Interannual (2009–2013) variability of winter-spring phytoplankton in the open Southern Adriatic Sea: Effects of deep convection and lateral advection. *Continental Shelf Research*, *143*, 311–321. https://doi.org/10.1016/j.csr.2017.05.007

Lohrenz, S. E., Arnone, R. A., Wiesenburg, D. A., & DePalma, I. P. (1988). Satellite detection of transient enhanced primary production in the western Mediterranean Sea. *Nature*, *335*(6187), 245–247. https://doi.org/10.1038/335245a0

Lohrenz, S. E., Knauer, G. A., Asper, V. L., Tuel, M., Michaels, A. F., & Knap, A. H. (1992). Seasonal variability in primary production and particle flux in the northwestern Sargasso Sea: U.S. JGOFS Bermuda Atlantic time-series study. *Deep Sea Research Part A: Oceanographic Research Papers*, *39*(7), 1373–1391. https://doi.org/10.1016/0198-0149(92)90074-4

Luther, D. S. (1985). Trapped waves around the Hawaiian Islands. In *Hawaiian Ocean Experiment: Proceedings of the 3rd ʻAha Hulikoʻa Hawaiian Winter Workshop* (pp. 261–301).

Ma, L., Bai, X., Laws, E. A., Xiao, W., Guo, C., Liu, X., Chiang, K.-P., Gao, K., & Huang, B. (2023). Responses of phytoplankton communities to internal waves in oligotrophic oceans. *Journal of Geophysical Research: Oceans*, *128*(10), e2023JC020201. https://doi.org/10.1029/2023JC020201

Ma, L., Xiao, W., Laws, E. A., Bai, X., Chiang, K.-P., Liu, X., Chen, J., & Huang, B. (2020). Responses of phytoplankton communities to the effect of internal wave-powered upwelling. *Limnology and Oceanography*, *66*(4), 1083–1098. https://doi.org/10.1002/lno.11666

Mackey, K. R. M., Paytan, A., Caldeira, K., Grossman, A. R., Moran, D., McIlvin, M., & Saito, M. A. (2013). Effect of temperature on photosynthesis and growth in marine *Synechococcus* spp. *Plant Physiology*, *163*(2), 815–829. https://doi.org/10.1104/pp.113.221937

Magazzu, G., & Decembrini, F. (1995). Primary production, biomass and abundance of phototrophic picoplankton in the Mediterranean-Sea: A review. *Aquatic Microbial Ecology*, *9*(1), 97–104. https://doi.org/10.3354/ame009097

Mahadevan, A. (2016). The impact of submesoscale physics on primary productivity of plankton. *Annual Review of Marine Science*, *8*, 161–184. https://doi.org/10.1146/annurev-marine-010814-015912

Malej, A., Mozetič, P., Malačič, V., Terzić, S., & Ahel, M. (1995). Phytoplankton responses to fresh-water inputs in a small semienclosed gulf (Gulf of Trieste, Adriatic Sea). *Marine Ecology Progress Series*, *120*(1–3), 111–121. https://doi.org/10.3354/meps120111

Mangoni, O., Bolinesi, F., Saggiomo, V., & Saggiomo, M. (2020). Photosynthetic rate and size structure of the phytoplankton community in transitional waters of the Northern Adriatic Sea. *Ecological Questions*, *31*(4), 11–20. https://doi.org/10.12775/EQ.2020.025

Mangoni, O., Modigh, M., Mozetič, P., Bergamasco, A., Rivaro, P., & Saggiomo, V. (2008). Structure and photosynthetic properties of phytoplankton assemblages in a highly dynamic system, the Northern Adriatic Sea. *Estuarine, Coastal and Shelf Science*, *77*(4), 633–644. https://doi.org/10.1016/j.ecss.2007.10.023

Mann, K. H., & Lazier, J. R. N. (2005a). Marine ecology comes of age. In *Dynamics of Marine Ecosystems: Biological-Phyical Interactions in the Oceans* (3rd ed., pp. 1–6). Wiley. https://doi.org/10.1002/9781118687901.ch1

Mann, K. H., & Lazier, J. R. N. (2005b). Variability in ocean circulation: Its biological consequences. In *Dynamics of Marine Ecosystems: Biological-Phyical Interactions in the Oceans* (3rd ed., pp. 337–389). Wiley. https://doi.org/10.1002/9781118687901.ch9

Marasović, I., Grbec, B., & Morović, M. (1995). Long-term production changes in the Adriatic. *Netherlands Journal of Sea Research*, *34*(4), 267–273. https://doi.org/10.1016/0077-7579(95)90037-3

Marasović, I., Ninčević, Ž., Kušpilić, G., Marinović, S., & Marinov, S. (2005). Long-term changes of basic biological and chemical parameters at two stations in the middle Adriatic. *Journal of Sea Research*, *54*(1), 3–14. https://doi.org/10.1016/j.seares.2005.02.007

Marasović, I., Viličić, D., & Ninčević, Ž. (1999). South Adriatic ecosystem: Interaction wić with the Mediterranean Sea. In P. Malanotte-Rizzoli & V. N. Eremeev (Eds.), *The Eastern Mediterranean as a Laboratory Basin for the Assessment of Contrasting Ecosystems* (Vol. 51, pp. 383–405). Springer Netherlands. https://doi.org/10.1007/978-94-011-4796-5_25

Margalef, R. (1969). Composición específica del fitoplancton de la costa catalano-levantina (Mediterráneo occidental) en 1962-1967. *Investigación Pesquera*, *33*, 345–380.

Marmelstein, A. D. (1970). *The effect of light intensity on the organic composition of marine phytoplankton diatoms* [Doctoral dissertation, Oregon State University].

Marra, J. F., Barber, R. T., Barber, E., Bidigare, R. R., Chamberlin, W. S., Goericke, R., Hargreaves, B. R., Hiscock, M., Iturriaga, R., Johnson, Z. I., Kiefer, D. A., Kinkade, C., Knudson, C., Lance, V., Langdon, C., Lee, Z.-P., Perry, M. J., Smith, W. O., Vaillancourt, R., & Zoffoli, L. (2021). A database of ocean primary productivity from the ^{14}C method. *Limnology and Oceanography Letters*, *6*(2), 107–111. https://doi.org/10.1002/lol2.10175

Marty, J.-C., & Chiavérini, J. (2002). Seasonal and interannual variations in phytoplankton production at DYFAMED time-series station, northwestern Mediterranean Sea. *Deep Sea Research Part II: Topical Studies in Oceanography*, *49*(11), 2017–2030. https://doi.org/10.1016/S0967-0645(02)00025-5

Marzetz, V., Spijkerman, E., Striebel, M., & Wacker, A. (2020). Phytoplankton community responses to interactions between light intensity, light variations, and phosphorus supply. *Frontiers in Environmental Science*, *8*, 539733. https://doi.org/10.3389/fenvs.2020.539733

Matek, A., Bosak, S., Šupraha, L., Neeley, A., Višić, H., Cetinić, I., & Ljubešić, Z. (2023). Phytoplankton diversity and chemotaxonomy in contrasting North Pacific ecosystems. *PeerJ*, *11*, e14501. https://doi.org/10.7717/peerj.14501

Matek, A., & Ljubešić, Z. (2024). Primary production research in the Adriatic Sea - A review. *Acta Adriatica*, *65*(2), Article 2. https://doi.org/10.32582/aa.65.2.1

Matek, A., Mucko, M., Casotti, R., Trano, A., Achterberg, E., Mihanović, H., Cižmek, H., Čolić, B., Cuculić, V., & Ljubešić, Z. (2023). Phytoplankton diversity and co-dependency in a stratified oligotrophic ecosystem in the South Adriatic Sea. *Water*, *15*(12), 2299. https://doi.org/10.3390/w15122299

Matek, A., Omand, M., Mihanović, H., Čižmek, H., & Ljubešić, Z. (2024). Optical properties of the Adriatic Sea: Light the way to the preservation of coastal island ecosystem. *Rapports et Procès-Verbaux Des Réunions de La Commission Internationale Pour l'Exploration Scienti-Fique de La Mer Méditerranée, 43*, 311–311.

Matić, F., Grbec, B., & Morović, M. (2011). Indications of climate regime shifts in the Middle Adriatic Sea. *Acta Adriatica*, *52*(2), 235–246.

Matić, F., Kovač, Ž., Vilibić, I., Mihanović, H., Morović, M., Grbec, B., Leder, N., & Džoić, T. (2017). Oscillating Adriatic temperature and salinity regimes mapped using the Self-Organizing Maps method. *Continental Shelf Research*, *132*, 11–18. https://doi.org/10.1016/j.csr.2016.11.006

McQuatters-Gollop, A., Johns, D., Bresnan, E., Skinner, J., Rombouts, I., Stern, R., Aubert, A., Johansen, M., Bedford, J., & Knights, A. (2017). From microscope to management: The critical value of plankton taxonomy to marine policy and biodiversity conservation. *Marine Policy*, *83*, 1–10. https://doi.org/10.1016/j.marpol.2017.05.022.

Mella-Flores, D., Mazard, S., Humily, F., Partensky, F., Mahé, F., Bariat, L., Courties, C., Marie, D., Ras, J., Mauriac, R., Jeanthon, C., Mahdi Bendif, E., Ostrowski, M., Scanlan, D. J., & Garczarek, L. (2011). Is the distribution of *Prochlorococcus* and *Synechococcus* ecotypes in the Mediterranean Sea affected by global warming? *Biogeosciences*, *8*(9), 2785–2804. https://doi.org/10.5194/bg-8-2785-2011

Mena, C., Reglero, P., Hidalgo, M., Sintes, E., Santiago, R., Martín, M., Moyà, G., & Balbín, R. (2019). Phytoplankton community structure is driven by stratification in the oligotrophic Mediterranean Sea. *Frontiers in Microbiology*, *10*, 1698. https://doi.org/10.3389/fmicb.2019.01698

Messié, M., Petrenko, A., Doglioli, A. M., Aldebert, C., Martinez, E., Koenig, G., Bonnet, S., & Moutin, T. (2020). The delayed island mass effect: How islands can remotely trigger blooms in the oligotrophic ocean. *Geophysical Research Letters*, *47*(2), e2019GL085282. https://doi.org/10.1029/2019GL085282

Messié, M., Petrenko, A., Doglioli, A. M., Martinez, E., & Alvain, S. (2022). Basin-scale biogeochemical and ecological impacts of islands in the tropical Pacific Ocean. *Nature Geoscience*, *15*(6), 469–474. https://doi.org/10.1038/s41561-022-00957-8

Mifka, B., Prtenjak, M. T., Kuzmić, J., Čanković, M., Mateša, S., & Ciglenečki, I. (2022). Climatology of dust deposition in the Adriatic Sea: A possible impact on marine production. *Journal of Geophysical Research: Atmospheres*, *127*(7), e2021JD035783. https://doi.org/10.1029/2021JD035783

Mihanović, H., Beg Paklar, G., & Orlić, M. (2014). Resonant excitation of island-trapped waves in a shallow, seasonally stratified sea. *Continental Shelf Research*, *77*, 24–37. https://doi.org/10.1016/j.csr.2014.01.014

Mihanović, H., Orlić, M., & Pasarić, Z. (2006). Diurnal internal tides detected in the Adriatic. *Annales Geophysicae*, *24*(11), 2773–2780. https://doi.org/10.5194/angeo-24-2773-2006

Mihanović, H., Orlić, M., & Pasarić, Z. (2009). Diurnal thermocline oscillations driven by tidal flow around an island in the Middle Adriatic. *Journal of Marine Systems*, *78*, S157–S168. https://doi.org/10.1016/j.jmarsys.2009.01.021

Miloslavić, M., Lučić, D., Gangai, B., & Onofri, I. (2014). Mesh size effects on mesozooplankton community structure in a semi-enclosed coastal area and surrounding

sea (South Adriatic Sea). *Marine Ecology*, *35*(4), 445–455. https://doi.org/10.1111/maec.12101

Mobley, C. D. (1994). *Light and Water: Radiative Transfer in Natural Waters*. Academic Press.

Mobley, C. D. (2022). *The Oceanic Optics Book*. International Ocean Colour Coordinating Group (IOCCG). http://dx.doi.org/10.25607/OBP-1710

Mochemadkar, S., Gauns, M., Pratihary, A., Thorat, B., Roy, R., Pai, I. K., & Naqvi, S. (2013). Response of phytoplankton to nutrient enrichment with high growth rates in a tropical monsoonal estuary - Zuari estuary, India. *Indian Journal of Geo-Marine Sciences*, *42*(3), 314–325.

Moore, L. R., Post, A. F., Rocap, G., & Chisholm, S. W. (2002). Utilization of different nitrogen sources by the marine cyanobacteria *Prochlorococcus* and *Synechococcus*. *Limnology and Oceanography*, *47*(4), 989–996. https://doi.org/10.4319/lo.2002.47.4.0989

Morel, A. (1991). Light and marine photosynthesis: A spectral model with geochemical and climatological implications. *Progress in Oceanography*, *26*(3), 263–306. https://doi.org/10.1016/0079-6611(91)90004-6

Morel, A., Antoine, D., Babin, M., & Dandonneau, Y. (1996). Measured and modeled primary production in the northeast Atlantic (EUMELI JGOFS program): The impact of natural variations in photosynthetic parameters on model predictive skill. *Deep Sea Research Part I: Oceanographic Research Papers*, *43*(8), 1273–1304. https://doi.org/10.1016/0967-0637(96)00059-3

Morović, M., Matić, F., Grbec, B., Bone, M., & Matijević, S. (2008). Optical characterization of the eastern Adriatic waters. *Fresenius Environmental Bulletin*, *17*, 1679–1687.

Muacho, S., da Silva, J. C. B., Brotas, V., & Oliveira, P. B. (2013). Effect of internal waves on near-surface chlorophyll concentration and primary production in the Nazaré Canyon (west of the Iberian Peninsula). *Deep Sea Research Part I: Oceanographic Research Papers*, *81*, 89–96. https://doi.org/10.1016/j.dsr.2013.07.012

Mucko, M., Bosak, S., Casotti, R., Balestra, C., & Ljubešić, Z. (2018). Winter picoplankton diversity in an oligotrophic marginal sea. *Marine Genomics*, *42*, 14–24. https://doi.org/10.1016/j.margen.2018.09.002

Mucko, M., Matek, A., Bosak, S., Čolić, B., & Ljubešić, Z. (2024). Plankton community composition in Southern Adriatic Sea during summer stratification period. *Rapports et Procès-Verbaux Des Réunions de La Commission Internationale Pour l'Exploration Scienti-Fique de La Mer Méditerranée, 43*, 202–202.

Mucko, M., Russo, L., Matek, A., Grgurević, F., Pestorić, B., Achterberg, E. P., D'Alelio, D., & Ljubešić, Z. (2025). Influence of internal island-trapped waves on plankton structure and trophic networks in stratified oligotrophic coastal waters. *Marine Environmental Research*, *212*, 107578. https://doi.org/10.1016/j.marenvres.2025.107578

Najdek, M., Paliaga, P., Šilović, T., Batistić, M., Garić, R., Supić, N., Ivančić, I., Ljubimir, S., Korlević, M., Jasprica, N., Hrustić, E., Dupčić-Radić, I., Blažina, M., & Orlić, S. (2014). Picoplankton community structure before, during and after convection event in the

offshore waters of the Southern Adriatic Sea. *Biogeosciences, 11*(10), 2645–2659. https://doi.org/10.5194/bg-11-2645-2014

Nielsen, E. S. (1952). The use of radioactive carbon (C14) for measuring organic production in the sea. *ICES Journal of Marine Science, 18*(2), 117–140. https://doi.org/10.1093/icesjms/18.2.117

Ninčević Gladan, Ž., Marasović, I., Grbec, B., Skejić, S., Bužančić, M., Kušpilić, G., Matijević, S., & Matić, F. (2010). Inter-decadal variability in phytoplankton community in the Middle Adriatic (Kaštela Bay) in relation to the North Atlantic Oscillation. *Estuaries and Coasts, 33*(2), 376–383. https://doi.org/10.1007/s12237-009-9223-3

Ninčević Gladan, Ž., Matić, F., Arapov, J., Skejić, S., Bužančić, M., Bakrač, A., Straka, M., Dekneudt, Q., Grbec, B., Garber, R., & Nazlić, N. (2020). The relationship between toxic phytoplankton species occurrence and environmental and meteorological factors along the eastern Adriatic coast. *Harmful Algae, 92*, 101745. https://doi.org/10.1016/j.hal.2020.101745

Ninčević Gladan, Ž., Mihanović, H., Bužančić, M., Vidjak, O., Šestanović, S., Veža, J., Šantić, D., Šolić, M., Grbec, B., Matić, F., Udovičić, D., & Prelesnik, H. (2023). *Plankton communities in oligotrophic offshore environments in the eastern Adriatic Sea in relation to mesoscale hydrodynamic fluctuations* [Preprint] (SSRN Scholarly Paper No. 4551183). https://doi.org/10.2139/ssrn.4551183

Ninčević, Z., & Marasović, I. (1998). Chlorophyll and primary production of size fractionated phytoplankton in the middle Adriatic Sea. *Rapports et Procès-Verbaux Des Réunions de La Commission Internationale Pour l'Exploration Scienti-Fique de La Mer Méditerranée, 35*.

Novosel, M., Požar-Domac, A., & Pasarić, M. (2004). Diversity and distribution of the bryozoa along underwater cliffs in the Adriatic Sea with special reference to thermal regime. *Marine Ecology, 25*(2), 155–170. https://doi.org/10.1111/j.1439-0485.2004.00022.x

Olson, R. J., & Sosik, H. M. (2007). A submersible imaging-in-flow instrument to analyze nano- and microplankton: Imaging FlowCytobot. *Limnology and Oceanography: Methods, 5*, 195–203. https://doi.org/10.4319/lom.2007.5.195

Orlić, M., Beg Paklar, G., Dadić, V., Leder, N., Mihanović, H., Pasarić, M., & Pasarić, Z. (2011). Diurnal upwelling resonantly driven by sea breezes around an Adriatic island. *Journal of Geophysical Research, 116*(C9), C09025. https://doi.org/10.1029/2011JC006955

Orr, M. H., & Mignerey, P. C. (2003). Nonlinear internal waves in the South China Sea: Observation of the conversion of depression internal waves to elevation internal waves. *Journal of Geophysical Research: Oceans, 108*(C3). https://doi.org/10.1029/2001JC001163

Pan, X., Wong, G. T. F., Shiah, F.-K., & Ho, T.-Y. (2012). Enhancement of biological productivity by internal waves: Observations in the summertime in the northern South China Sea. *Journal of Oceanography, 68*(3), 427–437. https://doi.org/10.1007/s10872-012-0107-y

Parasyris, A., Metheniti, V., Kampanis, N., & Darmaraki, S. (2025). Marine heatwaves in the Mediterranean Sea: A convolutional neural network study for extreme event prediction. *Ocean Science*, *21*(3), 897–912. https://doi.org/10.5194/os-21-897-2025

Pestorić, B., Drakulović, D., Lučić, D., Đorđević, N., & Joksimović, D. (2021). Zooplankton in Montenegrin Adriatic offshore waters. In A. Joksimović, M. Đurović, I. S. Zonn, A. G. Kostianoy, & A. V. Semenov (Eds.), *The Montenegrin Adriatic Coast: Marine Biology* (Vol. 109, pp. 107–128). Springer International Publishing. https://doi.org/10.1007/698_2020_703

Pestorić, B., Drakulović, D., Mandić, M., & López Abbate, C. (2018). Distribution changes of plankton communities in the harbour Porto Montenegro (South Adriatic Sea). *Studia Marina, 31*(2), 5–31. https://doi.org/10.5281/zenodo.2412386

Pestorić, B., Mucko, M., Matek, A., Lučić, D., & Ljubešić, Z. (2025). Structure of the zooplankton community and trophic interactions in a pelagic system influenced by internal island-trapped waves. *Acta Adriatica*, *66*(2), 163–178. https://doi.org/10.32582/aa.66.2.4

Picheral, M., Guidi, L., Stemmann, L., Karl, D. M., Iddaoud, G., & Gorsky, G. (2010). The Underwater Vision Profiler 5: An advanced instrument for high spatial resolution studies of particle size spectra and zooplankton. *Limnology and Oceanography: Methods*, *8*, 462–473. https://doi.org/10.4319/lom.2010.8.462

Piredda, R., Claverie, J.-M., Decelle, J., de Vargas, C., Dunthorn, M., Edvardsen, B., Eikrem, W., Forster, D., Kooistra, W. H. C. F., Logares, R., Massana, R., Montresor, M., Not, F., Ogata, H., Pawlowski, J., Romac, S., Sarno, D., Stoeck, T., & Zingone, A. (2018). Diatom diversity through HTS-metabarcoding in coastal European seas. *Scientific Reports*, *8*(1), 18045. https://doi.org/10.1038/s41598-018-36345-9

Piredda, R., Tomasino, M. P., D'Erchia, A. M., Manzari, C., Pesole, G., Montresor, M., Kooistra, W. H. C. F., Sarno, D., & Zingone, A. (2017). Diversity and temporal patterns of planktonic protist assemblages at a Mediterranean Long Term Ecological Research site. *FEMS Microbiology Ecology*, *93*(1), fiw200. https://doi.org/10.1093/femsec/fiw200

Pittera, J., Humily, F., Thorel, M., Grulois, D., Garczarek, L., & Six, C. (2014). Connecting thermal physiology and latitudinal niche partitioning in marine *Synechococcus*. *The ISME Journal*, *8*(6), 1221–1232. https://doi.org/10.1038/ismej.2013.228

Pizarro, O., & Shaffer, G. (1998). Wind-driven, coastal-trapped waves off the island of Gotland, Baltic Sea. *Journal of Physical Oceanography*, *28*(11), 2117–2129. https://doi.org/10.1175/1520-0485(1998)028<2117:WDCTWO>2.0.CO;2

Platt, T., Denman, K., & Jassby, A. (1977). Modeling the productivity of phytoplankton. In E. D. Goldberg, I. N. McCave, J. J. O'Brien, & J. H. Steele (Eds.), *The sea: Ideas and observations on progress in the study of the seas* (Vol. 6, pp. 807–856). Wiley.

Platt, T., Gallegos, C., & Harrison, W. (1980). Photoinhibition of photosynthesis in natural assemblages of marine phytoplankton. *Journal of Marine Research*, *38*(4), 687–701.

Platt, T., Rao, D. V. S., & Irwin, B. (1983). Photosynthesis of picoplankton in the oligotrophic ocean. *Nature, 301*(5902), 702–704. https://doi.org/10.1038/301702a0

Platt, T., & Sathyendranath, S. (1993). Estimators of primary production for interpretation of remotely sensed data on ocean color. *Journal of Geophysical Research: Oceans, 98*(C8), 14561–14576. https://doi.org/10.1029/93JC01001

Platt, T., Sathyendranath, S., White, G. N., Jackson, T., Saux Picart, S., & Bouman, H. (2017). Primary production: Sensitivity to surface irradiance and implications for archiving data. *Frontiers in Marine Science, 4*, 387. https://doi.org/10.3389/fmars.2017.00387

Pojed, I., & Kveder, S. (1977). Investigation of nutrient limitation of phytoplankton production in the Northern Adriatic by enrichment experiments. *Thalassia Jugoslavica, 13*(1/2), 13–24.

Polovina, J. J., Howell, E. A., & Abecassis, M. (2008). Ocean's least productive waters are expanding. *Geophysical Research Letters, 35*, L03618. https://doi.org/10.1029/2007GL031745

Pucher-Petković, T. (1971). Recherches sur la production primaire et la densité des populations du Phytoplancton en Adriatique moyenne (1962-1967). *Rapports et Procès-Verbaux Des Réunions de La Commission Internationale Pour l'Exploration Scienti-Fique de La Mer Méditerranée, 20*, 339–343.

Pucher-Petković, T. (1974). Essai d'évaluation de la production primaire annuelle dans l'Adriatique. *Rapports et Procès-Verbaux Des Réunions de La Commission Internationale Pour l'Exploration Scienti-Fique de La Mer Méditerranée, 22*(9), 71–72.

Pucher-Petković, T., & Zore-Armanda, M. (1973). Essai d'évaluation et pronostic de la production en fonction des facteurs du milieu dans l'Adriatique. *Acta Adriatica, 15*, 1–39.

Pugnetti, A., Acri, F., Alberighi, L., Barletta, D., Bastianini, M., Bernardi-Aubry, F., Berton, A., Bianchi, F., Socal, G., & Totti, C. (2004). Phytoplankton photosynthetic activity and growth rates in the NW Adriatic Sea. *Chemistry and Ecology, 20*(6), 399–409. https://doi.org/10.1080/02757540412331294902

Pugnetti, A., Acri, F., Bastianini, M., Bernardi Aubry, F., Berton, A., Bianchi, F., Noack, P., & Socal, G. (2003). Primary production processes in the north-western Adriatic Sea. *Atti dell'Associazione Italiana Di Oceanologia e Limnologia (Proceedings of the Italian Association of Oceanology and Limnology), 16*, 15–28.

Puškarić, S., Sokač, M., Ninčević, Ž., Šantić, D., Skejić, S., Džoić, T., Prelesnik, H., & Børsheim, K. Y. (2024). Extracted spectral signatures from the water column as a tool for the prediction of the structure of a marine microbial community. *Journal of Marine Science and Engineering, 12*(2), 286. https://doi.org/10.3390/jmse12020286

Revelante, N., & Gilmartin, M. (1977). The effects of northern italian rivers and eastern Mediterranean ingressions on the phytoplankton of the Adriatic Sea. *Hydrobiologia, 56*(3), 229–240. https://doi.org/10.1007/BF00017509

Revelante, N., & Gilmartin, M. (1980). Microplankton diversity indices as indicators of eutrophication in the northern Adriatic Sea. *Hydrobiologia*, *70*(3), 277–286. https://doi.org/10.1007/BF00016772

Richardson, K., Bendtsen, J., Kragh, T., & Mousing, E. A. (2016). Constraining the distribution of photosynthetic parameters in the global ocean. *Frontiers in Marine Science*, *3*, 269. https://doi.org/10.3389/fmars.2016.00269

Sakshaug, E., Bricaud, A., Dandonneau, Y., Falkowski, P. G., Kiefer, D. A., Legendre, L., Morel, A., Parslow, J., & Takahashi, M. (1997). Parameters of photosynthesis: Definitions, theory and interpretation of results. *Journal of Plankton Research*, *19*(11), 1637–1670. https://doi.org/10.1093/plankt/19.11.1637

Salon, S., Cossarini, G., Bolzon, G., Feudale, L., Lazzari, P., Teruzzi, A., Solidoro, C., & Crise, A. (2019). Novel metrics based on Biogeochemical Argo data to improve the model uncertainty evaluation of the CMEMS Mediterranean marine ecosystem forecasts. *Ocean Science*, *15*(4), 997–1022. https://doi.org/10.5194/os-15-997-2019

Sangrà, P., Basterretxea, G., Pelegrí, J. L., & Arístegui, J. (2001). Chlorophyll increase due to internal waves in the shelf-break of Gran Canaria Island (Canary Islands). *Scientia Marina*, *65*(S1), 189–198. https://doi.org/10.3989/scimar.2001.65s189

Šantić, D., Kovačević, V., Bensi, M., Giani, M., Vrdoljak Tomaš, A., Ordulj, M., Santinelli, C., Šestanović, S., Šolić, M., & Grbec, B. (2019). Picoplankton distribution and activity in the deep waters of the southern Adriatic Sea. *Water*, *11*(8), 1655. https://doi.org/10.3390/w11081655

Šantić, D., Krstulović, N., Šolić, M., Ordulj, M., & Kušpilić, G. (2013). Dynamics of prokaryotic picoplankton community in the central and southern Adriatic Sea (Croatia). *Helgoland Marine Research*, *67*(3), 471–481. https://doi.org/10.1007/s10152-012-0336-x

Šantić, D., Piwosz, K., Matić, F., Vrdoljak Tomaš, A., Arapov, J., Dean, J. L., Šolić, M., Koblížek, M., Kušpilić, G., & Šestanović, S. (2021). Artificial neural network analysis of microbial diversity in the central and southern Adriatic Sea. *Scientific Reports*, *11*(1), 12348. https://doi.org/10.1038/s41598-021-90863-7

Šantić, D., Vrdoljak Tomaš, A., & Lušić, J. (2020). Spatial and temporal patterns of picoplankton community in the central and southern Adriatic Sea. In A. Joksimović, M. Đurović, I. S. Zonn, A. G. Kostianoy, & A. V. Semenov (Eds.), *The Montenegrin Adriatic Coast: Marine Biology* (pp. 29–51). Springer International Publishing. https://doi.org/10.1007/698_2020_645

Sathyendranath, S., & Platt, T. (1989). Computation of aquatic primary production: Extended formalism to include effect of angular and spectral distribution of light. *Limnology and Oceanography*, *34*(1), 188–198. https://doi.org/10.4319/lo.1989.34.1.0188

Sathyendranath, S., Platt, T., Caverhill, C. M., Warnock, R. E., & Lewis, M. R. (1989). Remote sensing of oceanic primary production: Computations using a spectral model. *Deep Sea Research Part A. Oceanographic Research Papers*, *36*(3), 431–453. https://doi.org/10.1016/0198-0149(89)90046-0

Schmoker, C., & Hernández-León, S. (2013). Stratification effects on the plankton of the subtropical Canary Current. *Progress in Oceanography, 119,* 24–31. https://doi.org/10.1016/j.pocean.2013.08.006

Sharples, J., Tweddle, J. F., Mattias Green, J. A., Palmer, M. R., Kim, Y.-N., Hickman, A. E., Holligan, P. M., Moore, C. M., Rippeth, T. P., Simpson, J. H., & Krivtsov, V. (2007). Spring-neap modulation of internal tide mixing and vertical nitrate fluxes at a shelf edge in summer. *Limnology and Oceanography, 52*(5), 1735–1747. https://doi.org/10.4319/lo.2007.52.5.1735

Sherr, E. B., & Sherr, B. F. (1991). Planktonic microbes: Tiny cells at the base of the ocean's food webs. *Trends in Ecology & Evolution*, *6*(2), 50–54. https://doi.org/10.1016/0169-5347(91)90122-E

Sherr, E. B., & Sherr, B. F. (1994). Bacterivory and herbivory: Key roles of phagotrophic protists in pelagic food webs. *Microbial Ecology*, *28*(2), 223–235. https://doi.org/10.1007/BF00166812

Shih, Y.-Y., Shiah, F.-K., Lai, C.-C., Chou, W.-C., Tai, J.-H., Wu, Y.-S., Lai, C.-Y., Ko, C.-Y., & Hung, C.-C. (2021). Comparison of primary production using *in situ* and satellite-derived values at the SEATS station in the South China Sea. *Frontiers in Marine Science*, *8*, 747763. https://doi.org/10.3389/fmars.2021.747763

Sieburth, J., Smetacek, V., & Lenz, J. (1978). Pelagic ecosystem structure: Heterotrophic compartments of the plankton and their relationship to plankton size fractions. *Limnology and Oceanography*, *23*(6), 1256–1263. https://doi.org/10.4319/lo.1978.23.6.1256

Šilović, T., Ljubešić, Z., Mihanović, H., Olujić, G., Terzić, S., Jakšić, Ž., & Viličić, D. (2011). Picoplankton composition related to thermohaline circulation: The Albanian boundary zone (southern Adriatic) in late spring. *Estuarine, Coastal and Shelf Science*, *91*(4), 519–525. https://doi.org/10.1016/j.ecss.2010.12.012

Šilović, T., Mihanović, H., Batistić, M., Radić, I. D., Hrustić, E., & Najdek, M. (2018). Picoplankton distribution influenced by thermohaline circulation in the southern Adriatic. *Continental Shelf Research*, *155*(1), 21–33. https://doi.org/10.1016/j.csr.2018.01.007

Silsbe, G. M., Fox, J., Westberry, T. K., & Halsey, K. H. (2025). Global declines in net primary production in the ocean color era. *Nature Communications*, *16*(1), 5821. https://doi.org/10.1038/s41467-025-60906-y

Simoes-Sousa, I. T., Tandon, A., Pereira, F., Lazaneo, C. Z., & Mahadevan, A. (2022). Mixed layer eddies supply nutrients to enhance the spring phytoplankton bloom. *Frontiers in Marine Science, 9*, 825027. https://doi.org/10.3389/fmars.2022.825027

Siokou-Frangou, I., Christaki, U., Mazzocchi, M. G., Montresor, M., Ribera d'Alcalá, M., Vaqué, D., & Zingone, A. (2010). Plankton in the open Mediterranean Sea: A review. *Biogeosciences, 7*(5), 1543–1586. https://doi.org/10.5194/bg-7-1543-2010

Skejić, S., Arapov, J., Kovačević, V., Bužančić, M., Bensi, M., Giani, M., Bakrač, A., Mihanović, H., Gladan, Ž. N., Urbini, L., & Grbec, B. (2018). Coccolithophore diversity

in open waters of the middle Adriatic Sea in pre- and post-winter periods. *Marine Micropaleontology*, *143*, 30–45. https://doi.org/10.1016/j.marmicro.2018.07.006

Socal, G., Boldrin, A., Bianchi, F., Civitarese, G., De Lazzari, A., Rabitti, S., Totti, C., & Turchetto, M. M. (1999). Nutrient, particulate matter and phytoplankton variability in the photic layer of the Otranto strait. *Journal of Marine Systems*, *20*(1), 381–398. https://doi.org/10.1016/S0924-7963(98)00075-X

Spilling, K., Arellano San Martín, M., Granlund, M., Schulz, K. G., Spisla, C., Vanharanta, M., Goldenberg, S. U., & Riebesell, U. (2023). Microzooplankton communities and their grazing of phytoplankton under artificial upwelling in the oligotrophic ocean. *Frontiers in Marine Science*, *10*, 1286899. https://doi.org/10.3389/fmars.2023.1286899

Stefanni, S., Stanković, D., Borme, D., de Olazabal, A., Juretić, T., Pallavicini, A., & Tirelli, V. (2018). Multi-marker metabarcoding approach to study mesozooplankton at basin scale. *Scientific Reports*, *8*(1), 12085. https://doi.org/10.1038/s41598-018-30157-7

Sverdrup, H. U., Johnson, M. W., & Fleming, R. H. (1942). *The Oceans: Their Physics, Chemistry, and General Biology* (Vol. 1087, No. 8). New York: Prentice-Hall.

Sverdrup, H. U. (1953). On conditions for the vernal blooming of phytoplankton. *Journal du Conseil International pour l'Exploration de la Mer*, *18*(3), 287–295. https://doi.org/10.1093/icesjms/18.3.287

Talaber, I., Francé, J., Flander-Putrle, V., & Mozetič, P. (2018). Primary production and community structure of coastal phytoplankton in the Adriatic Sea: Insights on taxon-specific productivity. *Marine Ecology Progress Series*, *604*, 65–81. https://doi.org/10.3354/meps12721

Talaber, I., France, J., & Mozetič, P. (2014). How phytoplankton physiology and community structure adjust to physical forcing in a coastal ecosystem (northern Adriatic Sea). *Phycologia*, *53*(1), 74–85. https://doi.org/10.2216/13-196.1

Thingstad, T. F., & Sakshaug, E. (1990). Control of phytoplankton growth in nutrient recycling ecosystems: Theory and terminology. *Marine Ecology Progress Series*, *63*, 261–272.

Tuerena, R. E., Williams, R. G., Mahaffey, C., Vic, C., Green, J. A. M., Naveira-Garabato, A., Forryan, A., & Sharples, J. (2019). Internal tides drive nutrient fluxes into the deep chlorophyll maximum over mid-ocean ridges. *Global Biogeochemical Cycles*, *33*(8), 995–1009. https://doi.org/10.1029/2019GB006214

Turchetto, M., Bianchi, F., Boldrin, A., Malaguti, A., Rabitti, S., Socal, G., & Strada, L. (2000). Nutrients, phytoplankton and primary production processes in oligotrophic areas (Southern Adriatic and Northern Ionian). *Atti dell'Associazione Italiana Di Oceanologia e Limnologia (Proceedings of the Italian Association of Oceanology and Limnology)*, *13*(2), 269–278.

Turk, V., Njire, J., Terzić, S., Tinta, T., Benović, A., & Malej, A. (2012). The epiplankton community in the southern Adriatic: Multiple trophic levels along the south–north and inshore–offshore gradients. *Acta Adriatica*, *53*(1), 5–20.

Turley, C. M. (1999). The changing Mediterranean Sea: A sensitive ecosystem? *Progress in Oceanography*, *44*(1), 387–400. https://doi.org/10.1016/S0079-6611(99)00033-6

Ujević, I., Ninčević-Gladan, Z., Roje, R., Skejić, S., Arapov, J., & Marasović, I. (2010). Domoic acid: A new toxin in the Croatian Adriatic shellfish toxin profile. *Molecules, 15*(10), 6835–6849. https://doi.org/10.3390/molecules15106835

Umer, B., & Malačič, V. (2022). Biexponential decrease of PAR in coastal waters (Northern Adriatic). *Geofizika, 39*(1), 121–148. https://doi.org/10.15233/gfz.2022.39.2

Vadrucci, M. R., Basset, A., & Decembrini, F. (2002). Quantitative relationships among phytoplankton body size classes and production processes in the North Adriatic frontal region. *Chemistry and Ecology*, *18*(1–2), 53–60. https://doi.org/10.1080/02757540212694

Vadrucci, M. R., Catalano, G., & Basset, A. (2005). Spatial and seasonal variability of fractionated phytoplankton biomass and primary production in the frontal region of the northern Adriatic Sea. *Mediterranean Marine Science*, *6*(1), 5–16. https://doi.org/10.12681/mms.189

Vandermeulen, R. A., & Chaves, J. E. (Eds.). (2022). *IOCCG Ocean Optics and Biogeochemistry Protocols for Satellite Ocean Colour Sensor Validation, Volume 7.0: Aquatic Primary Productivity Field Protocols for Satellite Validation and Model Synthesis* (IOCCG Protocol Series). International Ocean Colour Coordinating Group (IOCCG). https://repository.oceanbestpractices.org/handle/11329/2059

Verri, G., Furnari, L., Gunduz, M., Senatore, A., Santos da Costa, V., De Lorenzis, A., Fedele, G., Manco, I., Mentaschi, L., Clementi, E., Coppini, G., Mercogliano, P., Mendicino, G., & Pinardi, N. (2024). Climate projections of the Adriatic Sea: Role of river release. *Frontiers in Climate, 6*, 1368413. https://doi.org/10.3389/fclim.2024.1368413

Vidussi, F., Claustre, H., Manca, B. B., Luchetta, A., & Marty, J.-C. (2001). Phytoplankton pigment distribution in relation to upper thermocline circulation in the eastern Mediterranean Sea during winter. *Journal of Geophysical Research: Oceans*, *106*(C9), 19939–19956. https://doi.org/10.1029/1999JC000308

Viličić, D. (1984). Phytoplankton communities of the South Adriatic in the greater vicinity of Dubrovnik. *Acta Botanica Croatica*, *43*(1), 175–189.

Viličić, D. (1985). A phytoplankton study of Southern Adriatic waters near Dubrovnik for the period from June 1979 to July 1980. *CENTRO : An International Journal of Environmental Studies in the Mediterranean, 1*(2), 35–36.

Viličić, D. (1991). A study of phytoplankton in the Adriatic Sea after the July 1984 bloom. *International Review of Hydrobiology*, *76*(2), 197–211.

Viličić, D. (1998). Phytoplankton taxonomy and distribution in the offshore southern Adriatic. *Natura Croatica, 7*(2), 127–141.

Viličić, D., Jasprica, N., Carić, M., & Burić, Z. (1998). Taxonomic composition and seasonal distribution of microphytoplankton in Mali Ston Bay (eastern Adriatic). *Acta Botanica Croatica, 57*(1), 29–48.

Viličić, D., Leder, N., Gržetić, Z., & Jasprica, N. (1995). Microphytoplankton in the Strait of Otranto (eastern Mediterranean). *Marine Biology, 123*(3), 619–630. https://doi.org/10.1007/BF00349240

Viličić, D., Marasović, I., & Mioković, D. (2002). Checklist of phytoplankton in the eastern Adriatic Sea. *Acta Botanica Croatica*, *61*(1), 57–91.

Viličić, D., & Stojanoski, L. (1987). Phytoplankton response to concentration of nutrients in the central and southern Adriatic Sea. *Acta Adriatica*, *28*(1/2), 73–84.

Viličić, D., Terzić, S., Ahel, M., Burić, Z., Jasprica, N., Carić, M., Caput Mihalić, K., & Olujić, G. (2008). Phytoplankton abundance and pigment biomarkers in the oligotrophic, eastern Adriatic estuary. *Environmental Monitoring and Assessment*, *142*(1), 199–218. https://doi.org/10.1007/s10661-007-9920-y

Viličić, D., Vučak, Z., Škrivanić, A., & Gržetić, Z. (1989). Phytoplankton blooms in the oligotrophic open south Adriatic Waters. *Marine Chemistry*, *28*(1–3), 89–107. https://doi.org/10.1016/0304-4203(89)90189-8

Villamaña, M., Mouriño-Carballido, B., Marañón, E., Cermeño, P., Chouciño, P., da Silva, J. C. B., Díaz, P. A., Fernández-Castro, B., Gilcoto, M., Graña, R., Latasa, M., Magalhaes, J. M., Luis Otero-Ferrer, J., Reguera, B., & Scharek, R. (2017). Role of internal waves on mixing, nutrient supply and phytoplankton community structure during spring and neap tides in the upwelling ecosystem of Ría de Vigo (NW Iberian Peninsula). *Limnology and Oceanography*, *62*(3), 1014–1030. https://doi.org/10.1002/lno.10482

Volpe, G., Colella, S., Brando, V. E., Forneris, V., La Padula, F., Di Cicco, A., Sammartino, M., Bracaglia, M., Artuso, F., & Santoleri, R. (2019). Mediterranean ocean colour Level 3 operational multi-sensor processing. *Ocean Science*, *15*(1), 127–146. https://doi.org/10.5194/os-15-127-2019

Volpe, G., Nardelli, B. B., Colella, S., Pisano, A., & Santoleri, R. (2018). Operational interpolated ocean colour product in the Mediterranean Sea. In E. P. Chassignet, A. Pascual, J. Tintorè, & J. Verron (Eds.), *New Frontiers in Operational Oceanography* (pp. 227–244). Springer. https://doi.org/10.17125/gov2018.ch09

Wallen, D. G., & Geen, G. H. (1971). The nature of the photosynthate in natural populations in relation to light quality. *Marine Biology*, *10*, 157–168.

Wang, F., Huang, B., Xie, Y., Cai, S., Wang, X., & Mu, J. (2021). Diversity, composition, and activities of nano- and picoeukaryotes in the northern South China Sea with influences of Kuroshio intrusion. *Frontiers in Marine Science*, *8*, 658233.

Wang, Y.-H., Dai, C.-F., & Chen, Y.-Y. (2007). Physical and ecological processes of internal waves on an isolated reef ecosystem in the South China Sea. *Geophysical Research Letters*, *34*(18), L18609. https://doi.org/10.1029/2007GL030658

Werdell, P. J., Franz, B., Poulin, C., Allen, J., Cairns, B., Caplan, S., Cetinić, I., Craig, S., Gao, M., Hasekamp, O., Ibrahim, A., Knobelspiesse, K., Mannino, A., Martins, J. V., McKinna, L., Meister, G., Patt, F., Proctor, C., Rajapakshe, C., … Sirk, E. (2024). Life after launch: A snapshot of the first six months of NASA's Plankton, Aerosol, Cloud, Ocean Ecosystem (PACE) mission. In *Sensors, Systems, and Next-Generation Satellites XXVIII* (Vol. 13192, pp. 70–84). SPIE - The International Society for Optics and Photonics. https://doi.org/10.1117/12.3033830

Whalen, C. B., de Lavergne, C., Naveira Garabato, A. C., Klymak, J. M., MacKinnon, J. A., & Sheen, K. L. (2020). Internal wave-driven mixing: Governing processes and consequences for climate. *Nature Reviews Earth & Environment*, *1*(11), 606–621. https://doi.org/10.1038/s43017-020-0097-z

Williams, R. G., & Follows, M. J. (2003). Physical transport of nutrients and the maintenance of biological production. In M. J. R. Fasham (Ed.), *Ocean Biogeochemistry: The Role of the Ocean Carbon Cycle in Global Change* (pp. 19–51). Springer. https://doi.org/10.1007/978-3-642-55844-3_3

Yahia-Kefi, D. O., Souissi, S., Gomez, F., & Daly Yahia, M. N. (2005). Spatio-temporal distribution of the dominant diatom and dinoflagellate species in the Bay of Tunis (SW Mediterranean Sea). *Mediterranean Marine Science*, *6*(1), 17–30. https://doi.org/10.12681/mms.190

Zheng, Q., Viljoen, J. J., Sun, X., Kovač, Ž., Sathyendranath, S., & Brewin, R. J. W. (2025). Simulating vertical phytoplankton dynamics in a stratified ocean using a two-layered ecosystem model. *Biogeosciences*, *22*(13), 3253–3278. https://doi.org/10.5194/bg-22-3253-2025

Zhong, Y., Bai, X., Laws, E. A., Lu, W., Huang, Z., Xiao, W., Chen, J., Ma, L., Liu, X., & Huang, B. (2024). Phytoplankton community responses to the combined effects of internal waves and anticyclonic eddies shed from the Kuroshio intrusion. *Ocean Dynamics*, *74*(6), 539–554. https://doi.org/10.1007/s10236-024-01618-7

Zore-Armanda, M. (1969). Water exchange between the Adriatic and the Eastern Mediterranean. *Deep Sea Research*, *16*, 171–178.

Zore-Armanda, M. (1984). Hydrographic and productivity conditions of the Palagruža region in the Middle Adriatic. *Acta Adriatica*, *25*(1/2), 119–138.

Zwirglmaier, K., Jardillier, L., Ostrowski, M., Mazard, S., Garczarek, L., Vaulot, D., Not, F., Massana, R., Ulloa, O., & Scanlan, D. J. (2008). Global phylogeography of marine *Synechococcus* and *Prochlorococcus* reveals a distinct partitioning of lineages among oceanic biomes. *Environmental Microbiology*, *10*(1), 147–161. https://doi.org/10.1111/j.1462-2920.2007.01440.x

8 SUPPLEMENTARY MATERIALS

Supplement 1. List of groups/taxa determined by the Utermöhl method from samples taken at station S1 at the Lastovo Island during the July field campaigns in 2021 and 2022. Shown are corresponding maximum and minimum abundances [cells L^{-1}] and frequency of appearance in samples [%] for the total number of samples (N = 156). Abbreviations: Min (minimum abundances), Max (maximum abundances), Fr (frequency of appearance), N.D (not determined).

List of taxa/groups	Max	Fr [%]
Diatoms		
Asterionellopsis glacialis (Castracane) Round	1995	0.64
Bacteriastrum jadranum Godrijan, Maric & Pfannkuchen	380	0.64
Bacteriastrum delicatulum Cleve	1135	1.28
Bacteriastrum sp.	945	5.77
Cerataulina pelagica (Cleve) Hendey	1325	21.15
Chaetoceros affinis Lauder	1515	1.28
Chaetoceros anastomosans Grunow	100	1.28
Chaetoceros atlanticus Cleve	20	0.64
Chaetoceros brevis F.Schütt	80	1.92
Chaetoceros cf. *constrictus* Gran	140	0.64
Chaetoceros convolutus Castracane	40	0.64
Chaetoceros compressus Lauder	1700	5.77
Chaetoceros curvisetus Cleve	1325	3.85
Chaetoceros dadayi Pavillard	190	1.92
Chaetoceros danicus Cleve	190	3.85
Chaetoceros decipiens Cleve	1510	4.49
Chaetoceros diversus Cleve	570	2.56
Chaetoceros laciniosus F.Schütt	200	0.64
Chaetoceros messanensis Castracane	1700	1.92
Chaetoceros rostratus Ralfs	1135	4.49
Chaetoceros simplex Ostenfeld	190	8.97
Chaetoceros sp.	2460	20.51
Chaetoceros socialis H.S.Lauder	1130	1.92
Chaetoceros tenuissimus Meunier	380	3.21
Chaetoceros wighamii Brightwell	1325	0.64
Chaetoceros vixvisibilis Schiller	2270	1.92
Cocconeis sp.	140	0.64
Cyclotella choctawhatcheeana	1515	1.92
Cylindrotheca closterium (Ehrenberg) Reimann & J.C.Lewin	1325	32.69
Dactyliosolen fragilissimus (Bergon) Hasle	755	17.95
Diploneis bombus (Ehrenberg) Ehrenberg	570	3.21
Diploneis sp.	755	6.41
Entomoneis sp.	190	5.13

Guinardia flaccida (Castracane) Peragallo	755	33.97
Guinardia striata (Stolterfoth) Hasle	2270	28.85
Haslea wawrikae (Husedt) Simonsen	190	0.64
Hemiaulus chinensis Greville	1135	19.87
Hemiaulus hauckii Grunow ex Van Heurck	755	10.26
Leptocylindrus danicus Cleve	3220	28.21
Leptocylindrus mediterraneus (H.Peragallo) Hasle	1700	7.69
Licmophora sp.	380	5.77
Lioloma pacificum (Cupp) Hasle	190	1.28
Melosira sp. C.Agardh	80	0.64
Neocalyptrella robusta Hernández-Becerril & Meave	20	0.64
Nevidinia sp.	570	2.56
Nitzschia longissima (Brébisson) Ralfs	1515	20.51
N.D. penatae (micro)	2650	78.21
N.D. penatae (< 10 µm)	710	1.28
cf. *Plagiotropis* Pfitzer	190	0.64
Pleurosigma sp.	190	7.69
Proboscia alata (Brightwell) Sundström	1325	69.23
Proboscia indica (H.Peragallo) Hernández-Becerril	570	2.56
Pseudo-nitzschia delicatissima (Cleve) Heiden	14060	46.15
Pseudo-nitzschia pseudodelicatissima (Hasle) Hasle	2280	6.41
Pseudo-nitzschia seriata (Cleve) H.Peragallo	480	1.92
Pseudo-nitzschia sp.	60	2.56
Rhizosolenia imbricata Brightwell	755	47.44
Rhizosolenia hyalina Ostenfeld	40	0.64
Rhizosolenia sp.	190	0.64
Skeletonema marinoi Sarno & Zingone	1515	3.21
Striatella unipunctata (Lyngbye) C.Agardh	120	1.92
Thalassionema frauenfeldii (Grunow) Tempère & Peragallo	1515	26.92
Thalassionema nitzschioides (Grunow) Mereschkowsky	1325	10.26
Thalassiosira sp.	755	8.33
Dinoflagellates		
Akashiwo sanguinea (K.Hirasaka) Gert Hansen & Moestrup	95	0.64
Brachidinium capitatum F.J.R.Taylor	190	1.28
Ceratium tripos (Ostenfeld) Graham & Bronikovsky	40	1.92
Dinophysis acuminata Claparède & Lachmann	190	1.92
Dinophysis caudata Kent	95	2.56
Dinophysis sp.	190	1.28
Diplopsalis complex	20	3.20
Dissodinium elegans (Pavillard) Matzenauer	95	0.64

Gonyaulax sp.	1700	1.28
Gymnodinium sanguineum K. Hirasaka	380	5.13
Gymnodinium simplex (Lohmann) Kofoid & Swezy	190	0.64
Gymnodinium spp.	190	1.28
Gyrodinium fusiforme Kofoid & Swezy	570	45.51
Gyrodinium spp.	380	2.56
Noctiluca scintillans (Macartney) Kofoid & Swezy	20	0.64
Oxytoxum sp.	570	23.08
Phalacroma rotundatum (Claparéde & Lachmann) Kofoid & J.R.Michener	40	1.28
Podolampas sp.	95	1.92
Prorocentrum micans Ehrenberg	190	3.21
Prorocentrum minimum (Pavillard) J.Schiller	190	4.49
Prorocentrum triestinum J.Schiller	20	0.64
Protoperidinuim sp.	190	5.13
*Protoperidinium steinii (*Jørgensen) Balech	95	5.13
Pyrophacus sp.	95	1.28
Scrippsiella sp.	760	42.95
Tripos furca (Ehrenberg) F.Gómez	190	10.26
Tripos fusus (Ehrenberg) F.Gómez	190	7.69
Tripos massiliensis (Gourret) F.Gómez	190	1.92
Tripos pentagonum (Gourret) F.Gómez	190	0.64
Tripos sp.	380	3.21
Tripos teres (Kofoid) F.Gómez	190	3.21
N.D. dinoflagellates (micro)	2840	39.74
N.D. dinoflagellates (<20 µm)	23430	82.69
Coccolithophorids		
Calciosolenia brasiliensis (Lohmann) J.R.Young	190	8.97
Calciosolenia murrayi Gran	190	1.92
Calyptrosphaera oblonga Lohmann	2460	19.87
Ophiaster formosus Gran	190	1.92
Ophiaster hydroideus Lohmann	380	1.92
Ophiaster sp.	40	1.92
Rhabdosphaera stylifera Lohman	945	7.69
Rhabdosphaera tignifera J. Schiller	755	8.33
Syracosphaera pulchra Lohman	190	7.05
N.D. coccolithophorids (micro)	12770	55.13
N.D. coccolithophorids (<10 µm)	5680	21.15
Others		
Chlorophyceae	3550	41.67
Chrysophyceae	3550	0.64

Cryptophyta	8510	52.56
Dictyocha fibula Ehrenberg	380	3.21

Supplement 2. Mean abundances of micro-, nano- and picophytoplankton groups during the July 2021 and 2022 field campaigns. Average abundances of total micro-, nano- and picophytoplankton, as well as heterotrophic bacteria, are also shown. Abbreviations: PPEs (photosynthetic picoeukaryotes).

	Microphytoplankton [cells L^{-1}]	**Nanophytoplankton [cells L^{-1}]**	**Picophytoplankton [cells mL^{-1}]**	**Heterotrophic bacteria [cells mL^{-1}]**
Diatoms	2354	3		
Dinoflagelates	268	2544		
Coccolithophores	156	1243		
Others	8			
Cryptophyta		754		
Chlorophyceae		460		
Chrysophyceae		24		
Synechococcus sp.			9755	
Prochlorococcus sp.			8877	
PPEs			748	
Total	2786	5029	19379	451472

Supplement 3. Canonical correspondence analysis (CCA) scores for nano- and microphytoplankton [cells L^{-1}] and picoplankton [cells mL^{-1}] data obtained in 2021 and 2022. Shown are biplot scores of environmental variables, weighted average scores of species, eigenvalues and proportion of variability explained by each constrained axis (CCA1 and CCA2). Environmental variables include nutrients [µmol L^{-1}] (phosphate (PO_4), nitrate (NO_3), nitrite (NO_2), silicic acid (SiO_4)), temperature [°C] and Chl *a* [mg m^{-3}]. Abbreviations: Chl *a* (Chlorophyll *a*), Dino (dinoflagellates), Cocco (coccolithophores), Micro (microphytoplankton), Nano (nanophytoplankton), PPEs (photosynthetic picoeukaryotes), HB (heterotrophic bacteria).

	2021				**2022**			
	Nano- and microphytoplankton		**Picoplankton**		**Nano- and microphytoplankton**		**Picoplankton**	
	CCA1	**CCA2**	**CCA1**	**CCA2**	**CCA1**	**CCA2**	**CCA1**	**CCA2**
NO_2	0.466	0.330	0.124	-0.034	0.843	0.212	0.71	-0.591
NO_3	0.927	0.019	0.852	0.433	0.889	-0.156	0.537	-0.777
PO_4	-0.223	-0.114	0.143	-0.548	-0.212	-0.098	-0.021	-0.038
SiO_4	0.920	-0.017	0.777	0.328	0.83	-0.34	0.681	-0.547
Temperature	-0.436	0.790	-0.609	-0.268	-0.772	-0.416	-0.994	-0.099
Chl *a*	0.792	-0.270	0.936	-0.181	0.6	-0.149	0.432	0.107
Diatoms (micro)	0.178	-0.034			0.216	0.015		
Dino (micro)	-0.076	0.105			-0.219	0.013		
Dino (nano)	-0.017	0.008			-0.02	-0.02		
Cocco (micro)	0.617	0.331			-0.137	-0.163		
Cocco (nano)	-0.258	0.213			0.012	-0.059		
Cryptophyta	-0.301	0.039			-0.093	0.229		
Chlorophyceae	-0.267	-0.329			-0.169	-0.012		
Micro	0.183	-0.033			0.116	-0.007		
Nano	0.021	-0.034			0.015	0.012		
PPEs			-0.043	0.013			-0.031	-0.016
Synechococcus			-0.136	-0.022			-0.054	0.018
Prochlorococcus			0.375	-0.006			0.138	0.002
HB			-0.063	0.011			-0.035	-0.007
Eigenvalues	0.034	0.014	0.031	0.000	0.016	0.007	0.006	0.000
Variability explained [%]	10.30	04.23	44.48	02.87	47.75	20.09	86.41	02.27

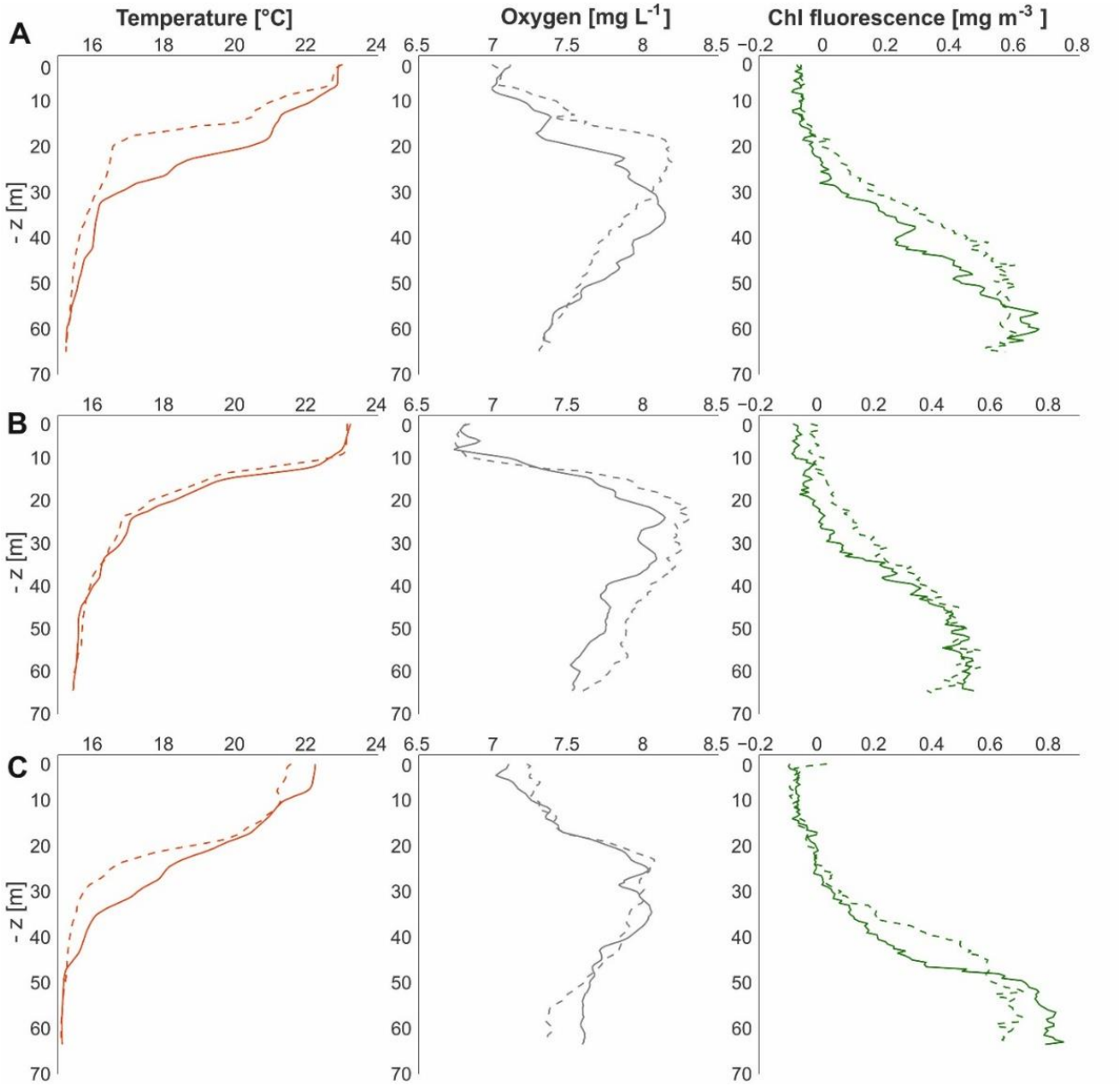

Supplement 4. Physico-chemical parameters of the incubated water column in June 2022 before (dashed line) and after (solid line) *in situ* ^{14}C incubations at stations **(A)** M1, **(B)** S0 and **(C)** P4. Shown are vertical profiles of temperature [°C], oxygen [mg L^{-1}] and Chl F [mg m^{-3}] measured using CTD.

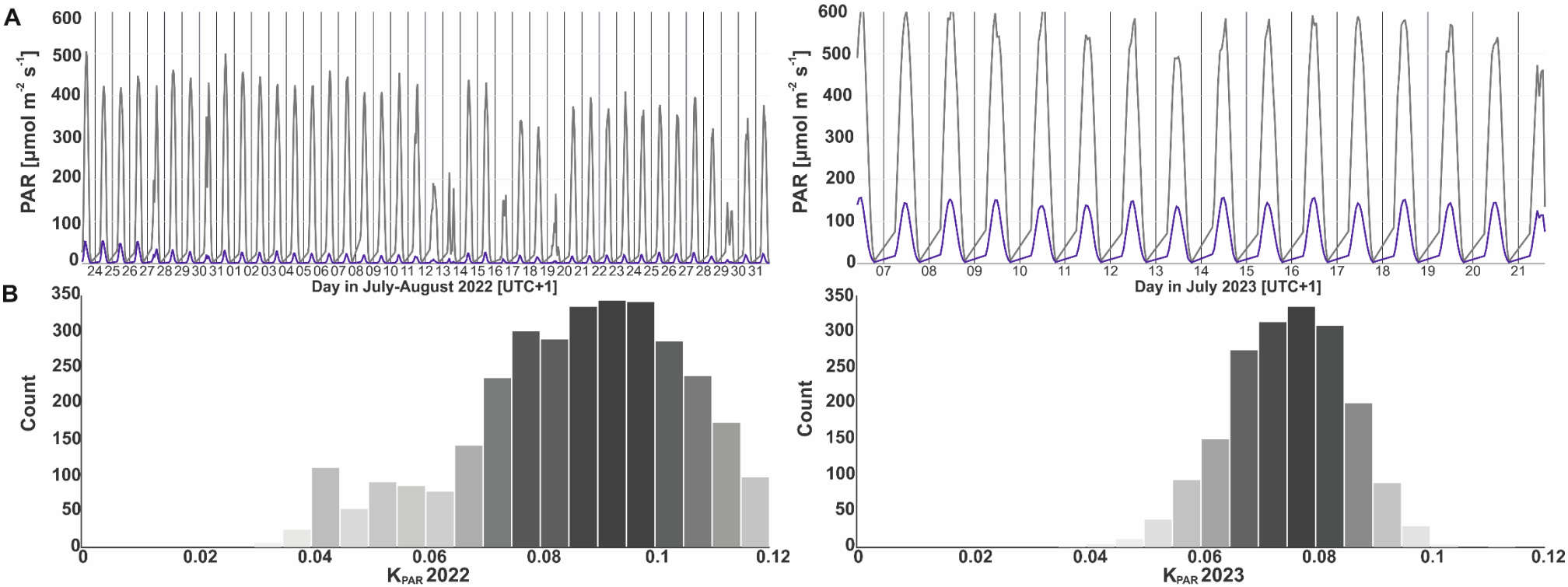

Supplement 5. PAR 1-hour interval time-series (upper panel) and attenuation coefficient of PAR (K_{PAR}) (bottom panel) applied to the underwater light field model and inverse model. Shown are data for: **(A)** 23 July–31 August 2022 at 10 m (gray line) and 40 m (blue line), and **(B)** 6–21 July 2023 at 10 m (gray line) and 30 m (blue line).

Supplement 6. Principal component analysis (PCA) results for 2022 and 2023 data. For PC1 and PC2 axis, shown are weighted-average scores for daily net primary production ($P_T(z)$), Chl *a*, temperature and oxygen, as well as eigenvalues and the proportion of variability explained by each axis.

	PC1	**PC2**
$P_T(z)$ [mg C m $^{-3}$]	0.953	-0.748
Chl *a* [mg m^{-3}]	-1.118	-1.210
Temperature [°C]	1.574	0.228
Oxygen [mg L^{-1}]	-0.883	1.130
Eigenvalue	1.80	1.18
Variability explained [%]	45.10	27.95

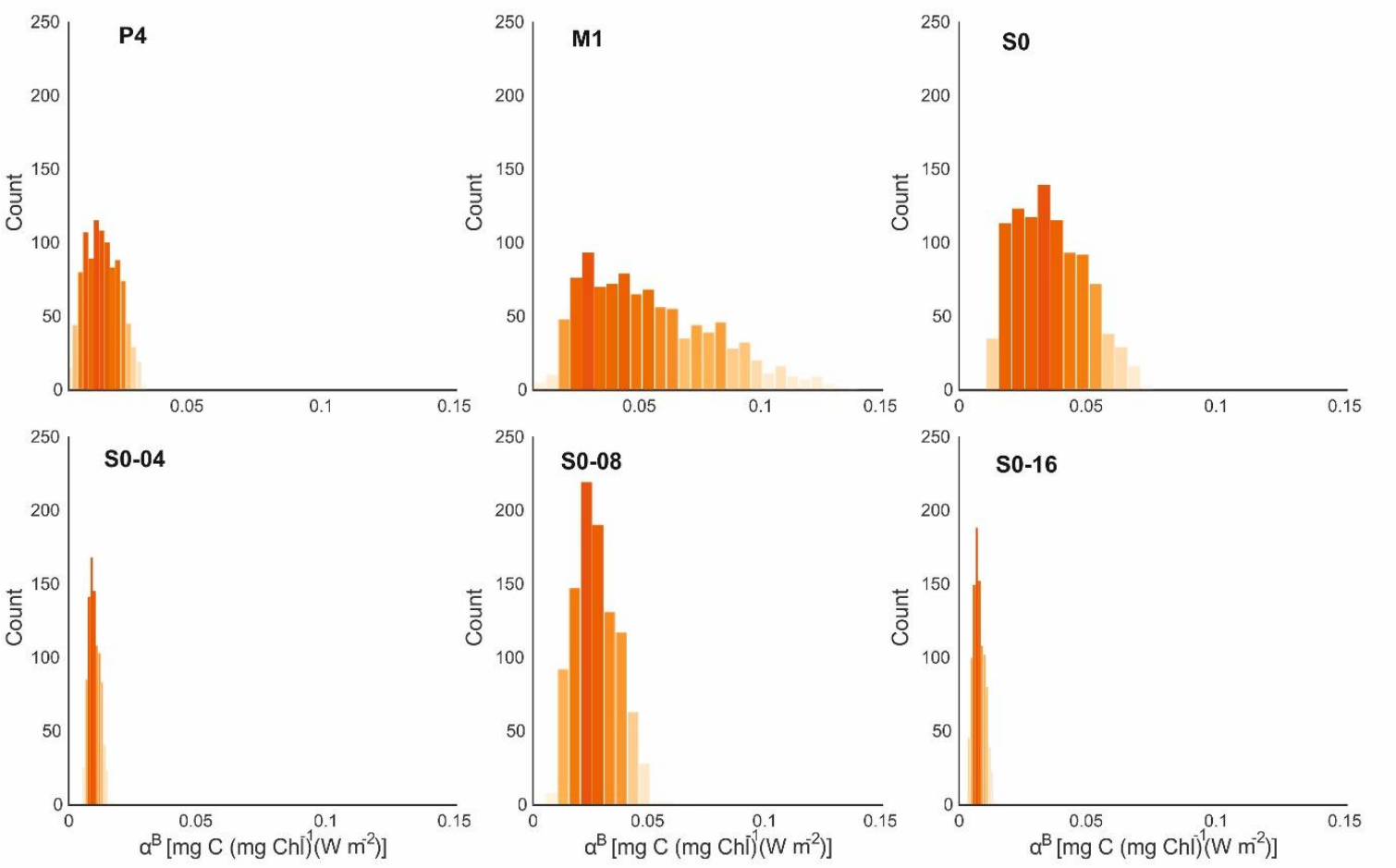

Supplement 7. The distributions of optimal photosynthesis parameter, initial slope (α_B), retrieved for *in situ* ^{14}C primary production experiments in June 2022 at stations P4, M1 and S0, and in July 2023 at station S0 (S0-04, S0-08 and S0-16). Shown are values across bootstrap steps of fitting *in situ* daily net primary production ($P_T(z)$) and Chl *a* profiles (**Figure 12**), surface irradiance at noon (I_0^m) and attenuation coefficients (K_{PAR}) (**Supplement 5B**) to the inverse model.

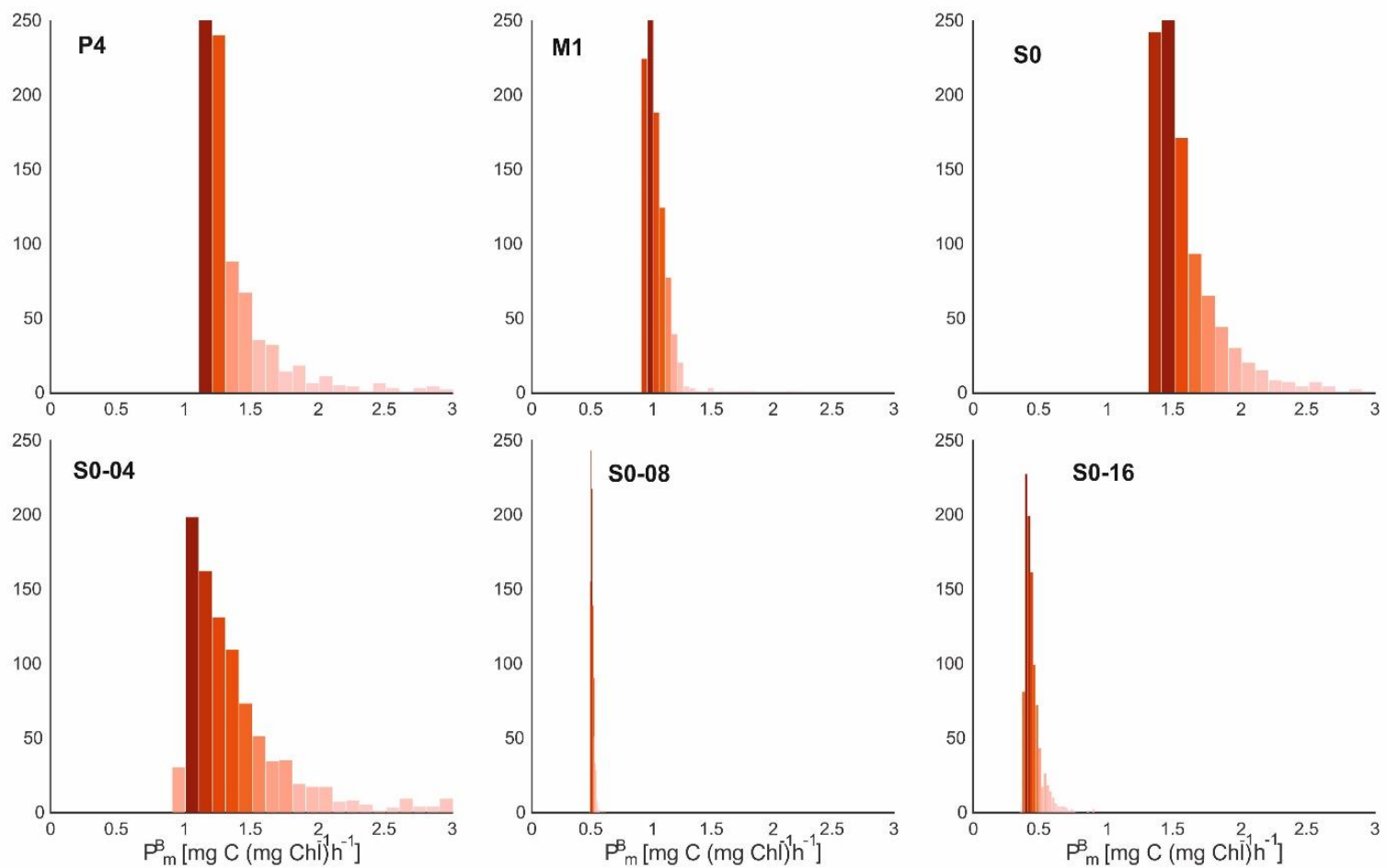

Supplement 8. The distributions of optimal photosynthesis parameter, assimilation number (P^B_m), retrieved for *in situ* ^{14}C primary production experiments in June 2022 at stations P4, M1 and S0, and in July 2023 at station S0 (S0-04, S0-08 and S0-16). Shown are values across bootstrap steps of fitting *in situ* daily net primary production ($P_T(z)$) and Chl *a* profiles (**Figure 12**), surface irradiance at noon (I_0^m) and attenuation coefficients (K_{PAR}) (**Supplement 5B**) to the inverse model.

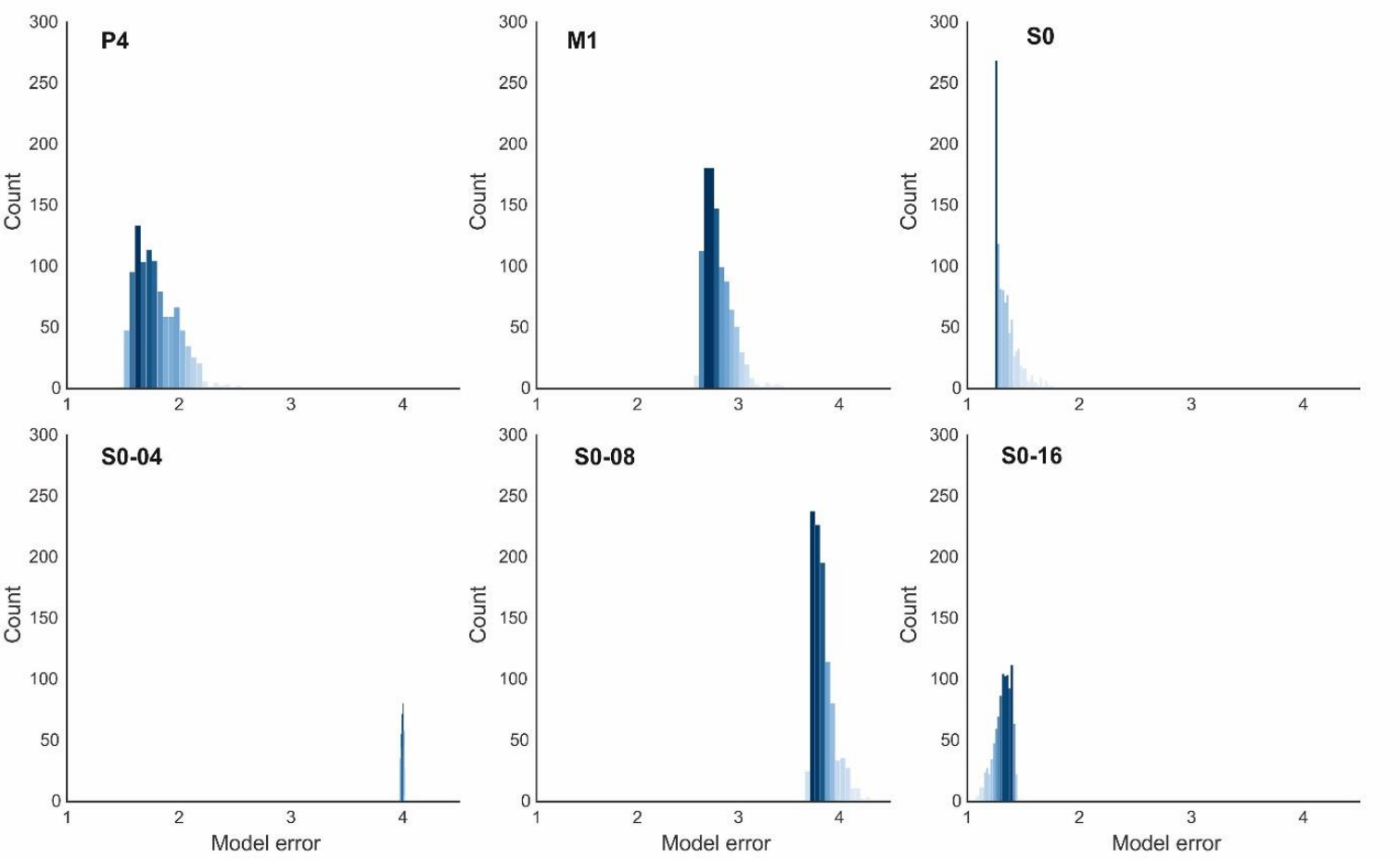

Supplement 9. Distributions of the minimal error values that are the result of optimization between *in situ* $P_T(z)$ and model ~$P_T(z)$ profiles across bootstrap steps for which optimal photosynthesis parameters were estimated (**Supplement 7**, **Supplement 8**). Shown are results for *in situ* ^{14}C primary production experiments in June 2022 at stations P4, M1 and S0, and in July 2023 at station S0 (S0-04, S0-08 and S0-16).

Supplement 10. Annual primary production (2021–2023) derived using trapezoidal integration of Copernicus 4-km monthly L4 primary production, with ITW-related primary production and its contribution to annual estimates.

Year	**Annual $P_{Z,T}$ ± SD [g C m^{-2}]**	**ITWs $P_{Z,T}$ [g C m^{-2}]**	**ITW contribution [%]**
2021	122.9 ± 8.38	2.01	1.63
2022	114.8 ± 8.24	4.37	3.80
2023	118.0 ± 8.03	1.79	1.52

9 CURRICULUM VITAE

Antonija Matek was born on 1 January 1996 in Rijeka, Croatia, where she completed her elementary education at Milan Brozović School in Kastav and her secondary education at Gymnasium Andrija Mohorovičić in Rijeka. During this period, she became deeply interested in the natural sciences, especially biology and ecology. In 2014, she began studying Biology at the Faculty of Science, University of Zagreb, and earned her bachelor's degree in 2017. That same year, she started her graduate studies in Ecology and Nature Preservation at the same faculty and received her master's degree in March 2020 with a thesis entitled "Optimization of artificial light in the cultivation of laboratory diatom cultures *Achnanthes elongata* and *Poulinea lepidochelicola*." In December 2021, she joined a PhD program under the Croatian Science Foundation project "Island trapped waves as driver of primary production - ISLAND." Key achievements include authoring 7 scientific publications (4 as first author), contributing to 23 conference proceedings, and actively participating in 10 presentations (4 posters and 6 oral presentations). She played a leading role in organizing the 8th PhD Student Symposium and led a workshop on time-series analysis for students and faculty. She developed advanced competencies in optical oceanography through specialized training in radiometry and ocean color at CNR-ISMAR in Italy and the NASA Summer Ocean Optics School in the United States, gaining both theoretical and hands-on experience. Furthermore, Antonija actively communicated science by delivering popular science lectures and participating in public events, including "Science in Passing" in Zagreb.